UNIVERSITÀ DEGLI STUDI DI PADOVA

DIPARTIMENTO DI INGEGNERIA INDUSTRIALE

CORSO DI LAUREA MAGISTRALE IN INGEGNERIA CHIMICA E DEI PROCESSI INDUSTRIALI

Tesi di Laurea Magistrale in

Ingegneria Chimica e dei Processi Industriali

ECONOMIC OPTIMISATION OF A EUROPEAN SUPPLY CHAIN FOR CO_2 UTILISATION AND SEQUESTRATION

Relatore: Prof. Fabrizio Bezzo

Correlatore: Ing. Federico d'Amore

Laureando: Victor Baldo

ANNO ACCADEMICO 2017-2018

Abstract

In the next few years carbon capture and storage technology will be strategic for the reduction of greenhouse gases. While geological sequestration techniques are struggling to start due to high costs and poor government incentives, the prospect of being able to chemically convert CO_2 can be a cost-effective solution to reduce greenhouse gases. In this Master Thesis a model based on mixed integer linear programming techniques has been developed. The goal is to minimise the total cost of the entire European supply chains for CO_2 capture, transport, sequestration and utilisation, reducing emissions of 43% from large combustion plants as a target of the European Community before 2030. After a general screening of CO_2 conversion processes, two were chosen: polyols and methanol. Several scenarios were analysed, including the overproduction of polyols and methanol, the possibility of producing also dimethylcarbonate, and the exclusion of some sequestration regions due to country legislation. Among the results obtained, it is highlighted that the total cost of the European supply chain for carbon capture, utilisation and storage is equal to 31.39 €/ton of CO_2 and that only about 0.6% of the CO_2 emitted from large combustion plants can be chemically sequestrated.

Riassunto

Nei prossimi anni la tecnologia di cattura e sequestro della CO_2 sarà strategica per la riduzione dei gas ad effetto serra. Se da un lato le tecniche di sequestro geologico stentano a partire a causa degli alti costi e scarsi incentivi governativi, la prospettiva di poter convertire chimicamente la CO_2 può essere una soluzione economicamente vantaggiosa per ridurre i gas serra.

Nell'ottemperanza del quadro per il clima e l'energia 2030, i settori interessati dal sistema di scambio di quote di emissione dell'Unione Europea devono ridurre le emissioni dei gas serra del 43% entro il 2030; risulta necessario perciò andare a determinare la configurazione ottimale della filiera produttiva per la minimizzazione dei costi dell'intera infrastruttura di cattura, trasporto, sequestro ed utilizzo della CO_2, che riesca a soddisfare sia i vincoli sulle emissioni sia i principi di sostenibilità economica.

Il lavoro di tesi magistrale si concentra perciò sulla pianificazione Europea della filiera produttiva della cattura, sequestro ed utilizzo della CO_2, analizzando quanto la conversione della CO_2 possa influenzare l'intera filiera in termini sia economici che ambientali. L'obiettivo è raggiunto attraverso lo sviluppo di modelli basati su tecniche di programmazione lineare mista a variabili intere.

Attraverso una discretizzazione del territorio Europeo si è consentita una definizione spazialmente esplicita delle fonti di emissione di CO_2 da grandi impianti di combustione, con l'obiettivo di determinare la configurazione esatta dei luoghi di cattura, trasporto, stoccaggio ed utilizzo. In particolare, la soluzione del problema di ottimizzazione economica permette di determinare le tecniche di cattura (decidendo tra tecnologie di cattura pre-combustione, post-combustione e ossi-combustione), i mezzi per il trasporto (via nave o via condutture *inshore* o *offshore*) e infine l'utilizzo finale, scegliendo tra sequestro e la conversione chimica che porta a polioli o a metanolo.

Per ciò che riguarda i processi che portano alla trasformazione chimica della CO_2, questi sono stati scelti dopo un accurato screening delle tecnologie che attualmente sono in grado di soddisfare requisiti sia economici sia ambientali in termini di riduzione dei gas ad effetto serra.

Selezionate le tecnologie attualmente più promettenti, si è svolta un'analisi dello storico dei prezzi delle materie prime, del costo dell'energia, gas naturale e manodopera e dell'attuale tassazione aziendale con l'obiettivo di determinare con la maggiore precisone possibile i parametri economici in ingresso al modello. Il modello di ottimizzazione finale è stato ottenuto dopo aver analizzato criticamente gli effetti di linearizzazione sul modello non-lineare che considera i processi di conversione della CO_2.

I risultati ottenuti dall'ottimizzazione evidenziano che il costo totale della filiera europea di cattura sequestro ed utilizzo del carbonio è uguale a 31.40 €/ton di CO2 e che grazie all'utilizzo si sequestra chimicamente circa lo 0.6% della CO_2 emessa dai grandi impianti di combustione.

Infine, con l'obiettivo di valutare meglio l'effetto di alcune variabili decisionali, si sono analizzati quattro scenari che prendono in considerazione: *i)* l'effetto dell'attuale legislazione in termini di

permesso al sequestro geologico *inshore* (ovvero il fatto che alcune nazioni attualmente non consentono il sequestro geologico della CO_2); *ii)* l'impatto della capacità produttiva di metanolo e polioli; *iii)* la possibilità di poter convertire la CO_2 in anche dimetilcarbonato per sostituire il metil-ter-butil etere come additivo per i carburanti e il fosgene nella produzione di policarbonato: *iv)* l'effetto del fattore di scala per gli impianti di utilizzo della CO_2 (assumendo che non ci sia un effetto di scala che riduca il costo di capitale per unità prodotta). I risultati non portano a sostanziali cambiamenti e indicano che le stime ottenute con il modello base sono sostanzialmente robuste.

Table of contents

Nomenclature

Acronyms

BFW	Boiled Feed Water
CAPEX	Capital Expenditure
CCS	Carbon Capture and Storage
CCUS	Carbon Capture, Utilisation and Storage
CPBR	Closed Photobioreactor
CPU	Central Processing Unit
DMC	Dimethylcarbonate
DME	Dimethyl Ether
ECBM	Enhanced Coal Bed Methane
EDGAR	Emission Database for Global Atmospheric Research
EG	Ethylene Glycol
EO	Ethylene Oxide
EOR	Enhanced Oil Recovery
eq	Equivalent
ETS	Emissions Trading System
FCI	Fixed Capital Investment
FT	Fischer-Tropsch
G	Glycerol
GGE	Gasoline Gallon Equivalent
GHG	Greenhouse Gases
HDPE	High-Density Polyethylene
LP	Linear Programming
MEG	Mono-Ethylene Glycol
MIBK	Methyl Isobutyl Ketone
MILP	Mixed Integer Linear Programming
MINLP	Mixed Integer Non Linear Programming
MIP	Mixed Integer Programming
MPG	Mono-Propylene Glycol
MTBE	Methyl Tert-Buthyl Ether
NG	Natural Gas
NLP	Non Linear Programming
OPEX	Operative Expenditure
OPS	Opend Pond System

PPP	Polyether Carbonate Polyols
PC	Polycarbonate
PEM	Proton Exchange Membrane
PO	Propylene Oxide
POM	Polyoxymethylene
PU	Polyurethane
RCP	Representative Concentration Pathways
RWGS	Reverse Water Gas Shift
S	Stoichiometric number
SC	Supply Chain
SMR	Steam Methane Reforming
SOEC	Solide Oxide Electrolyser Cell
TCI	Total Capital Investment
UK	United Kingdom
USA	United State of America

Sets

c	Chemicals {*PPP, MeOH*}
G	European region {*1, 2, …, 123, 124*}
k	Capture technology {$post_{coal}^{comb}$ $post_{gas}^{comb}$, oxy_{coal}^{fuel}, pre^{comb}}
l	Transport modality {*inshore pipeline, offshore pipeline, ship*}
p	Transport capacity {*1, 2, 3, 4, 5, 6, 7*}

Parameters

α	European Union CO_2 reduction target [%]
$acom$	manufacturing cost coefficient
$bcom$	manufacturing FCI cost coefficient
$ccom$	manufacturing labour cost coefficient
CCR^{seq}	Capital cost rate for injection well [€]
dg	Average injection well depth in region g [km]
η_k	Capture efficiency for technology k [%]
f^{ship}	Scaling factor for ship transport [€/ton of CO_2/km]
FC	Sixth-rule scalar
$FCIangular_c$	Fixed capital investment angular coefficient [€/tons of c]
$FCIquote_c$	Fixed capital investment quote coefficient [€/tons of c]

$\gamma_{k,g}$	Technology *k* utilised in region *g* according to fuels contribution to emission [tons of $CO_2^{coal/gas}$/tons of CO_2^{tot}]
int^{cost}	Intra-connection cost [€/ton of CO_2/km]
int_g^{dist}	Maximum size of region *g* [km]
$LD_{g,g'}$,	Matrix of distances between region *g* and a neighbouring region *g'* [km]
lob_c	Productivity lower bound for each chemical *c* [tons of *c*]
m_1	Cost parameter for well [€]
m_2	Cost parameter for well [€]
$maxp_c$	European productivity [tons of *c*]
$nred_c^{CO2}$	net reduction of CO_2 due to its chemical conversion according to literature [tons of CO_2/tons of *c*]
OM^{seq}	Maintenance rate for injection well
$Pmax_g$	Maximum carbon capture in region *g* [tons of CO_2]
$Ptot_g$	total yearly emission in region *g* [tons of CO_2/year]
Q_p	Transport capacity according to set *p* [tons of CO2]
$raw_{c,g}$	Raw material cost for each chemical *c* in each region *g* [€/tons of *c*]
$react_c^{CO2}$	Amount of CO_2 converted into chemical *c* [tons of CO_2/tons of *c*]
$rev_{c,g}$	Revenue for each chemical *c* in each region *g* [€]
sl	Ten year straight line depreciation factor
$Stot_g$	Total sequestration potential in region g [tons of CO_2]
$Stot^{max}$	Maximum inshore sequestration capacity in each region *g* in region g [tons of CO_2]
tax_g	corporate tax in each region *g* [%]
$Tprod_c$	Productivity parameter [tons of *c*]
$Tscal_c$	Reference fixed capital investment [€]
Qp	Transported capacity discretisation according to set *p*[tons of CO_2]
UCC_k	Unitary capture cost for technology *k* [€/ton of CO_2]
$upb_{c,g}$	Productivity upper bound for each chemical *c* in each region *g* [tons of *c*]
$UTC_{p,l}$	Unitary transport cost for size *p* through transport modality *l* [€/ton of CO_2/km]
$util_{c,g}$	Utility cost in each region *g* for each chemical *c*

Continuous Variables

$Ctot_{k,g}^{CO2}$	Carbon captured in region *g* with technology *k* [tons of CO_2]
$CF_{c,g}$	Cash flow generated for each chemical *c* [€]
$COM_{c,g}$	Manufacturing cost fro each chemical *c* [€]
$Ctot_{k,g}^{CO2}$	CO_2 capture through *k* in region *g* [tons of CO_2]

$d_{c,g}$	Depreciation for each chemical *c* [€]
$FCI_{c,g}$	Fixed capital investment for each chemical *c* [€]
L_l^{trans}	Total transport distance through *l* [km]
N_g^{seq}	Total number of injection wells in region *g* [tons of CO_2]
$profit$	Total profit generated from all chemical *c*[€]
$Ptot_{k,g}^{CO2}$	Gross quantity of CO_2 captured with technology *k* in region *g* [tons CO_2]
$Qtrans_{a.l.a'}^{CO2}$	CO_2 flowrate transported from *g* through *l* to *g'* [tons of CO_2]
$R_{c,g}$	Revenue for all chemical *c* [€]
S_g^{ratio}	CO_2sequestered in region *g* with respect to local sequestration potential [%]
$Stot_g^{CO2}$	CO_2 sequestered in region *g* [tons of CO_2]
TC	Total SC cost [€]
TCC	Total capture cost [€]
TCC_g	Total capture cost in region *g* [€]
TSC	Total sequestration cost [€]
TTC	Total transport cost [€]
TTC^{fsize}	Cost related to the shipment size and transport length [€]
TTC^{fdist}	Expense due to the length of the transport facility for ship only [€]
TTC^{int}	Expenditure connected with the intra-grid network [€]
U_g	Gross amount of CO_2reduction due to usage in each region *g* [tons of CO_2]
$Unet$	Net amount of CO_2 reduction due to usage [tons of CO_2]

Binary variables

$delta_{c,g}$	1 if chemical *c* is produced in region *g*, zero otherwise
$\lambda_{p,g,l,g'}$	1 if CO_2 transport of size *p* from *g* through *l* to *g'* , zero otherwise

Semi continuous variable

$uchem_{c,g}$	Quantity of chemical c produced in region g **[**tons of *c***]**

Integer variable

$Ichem_{c,g}$	Number of chemical plants *c* built in region *g*

List of Figure

List of Table

Introduction

In 2015 the XXI Conference of the Parties of the United Nations Climate Change Conference negotiated the Paris Agreement and as for 2018 February 195 countries have signed it. This Agreement aims at reducing the emissions caused by the anthropogenic GHG effect in order to avert the predicted global temperature increase of over 2°C before 2050 (United Nations, 2015). Currently, the efforts made to cut GHG are insufficient, since the emissions are still growing compared to previous years, mainly due to the economic growth in China and India (Il sole 24 ore, 2018). As highlighted by the International Energy Agency (IEA) CCS plants will contribute to the reduction of GHG emissions by 20% before 2050. To achieve this goal the number of plants will have to increase from the current 15 to about 3500. One alternative to the geological sequestration is represented by the possibilities of chemical conversion of CO_2 into fuels, chemicals and polymers. This should allow the costs of the entire carbon capture SC to be reduced. The objective of this Master Thesis is to develop a model that will determine the economic effects of including the possibility of using CO_2 instead of sequestering it, within the framework of a comprehensive optimisation of CCS supply chain for Europe. In particular, the model seeks to minimise the costs deriving from the entire CCUS infrastructure

This Master Thesis is structured as follows. The first Chapter, after an introduction in which the situation linked to global warming is discussed, contextualizes and carries out a screening of the literature concerning the CO_2 conversion processes. The second Chapter describes the methods used to select the prices chosen for raw materials and electricity, as well as for labour costs and corporate tax rate, and to derive the economic data that were missing from the reference articles. The third Chapter describes the original CCS model with the relative results; then the mathematical features, related to the equations of the chemical conversion of CO_2 are shown. A critical assessment on the nonlinearity of the model and the simplifications used to linearise it is eventually carried out. The fourth Chapter reports and discuss the results obtained from the simulations of the CCUS base case and four scenarios. showing the final spatially explicit configuration of the SC and the total cost of the entire infrastructure. Some final remarks conclude the Thesis.

Chapter 1

Current situation

This Chapter summarises the problem caused by the anthropogenic effect of greenhouse gases (GHG) and describes how the European Union is addressing this issue, with particular reference to large fossil fuel combustion plants (Section 1.1). Section 1.2 deals with the state of the art of all those chemical processes that convert CO_2, and whose technical and economic details are available. Finally Section 1.3 summarises the technologies chosen.

1.1 Greenhouse gas issue and legislation

The natural effect of GHG allows the earth to maintain acceptable climatic condition for human life:if its contribution would not be considered in the energy balance the temperature of the Earth's surface would be -19 ° C, against a current average value of 14 ° C (IPCC, 2014). In fact, among the energy of all the electromagnetic radiations that are received from the Sum by the atmosphere of our planet, 30% is absorbed and reflected, while the remaining 70% reaches the Earth surface. In

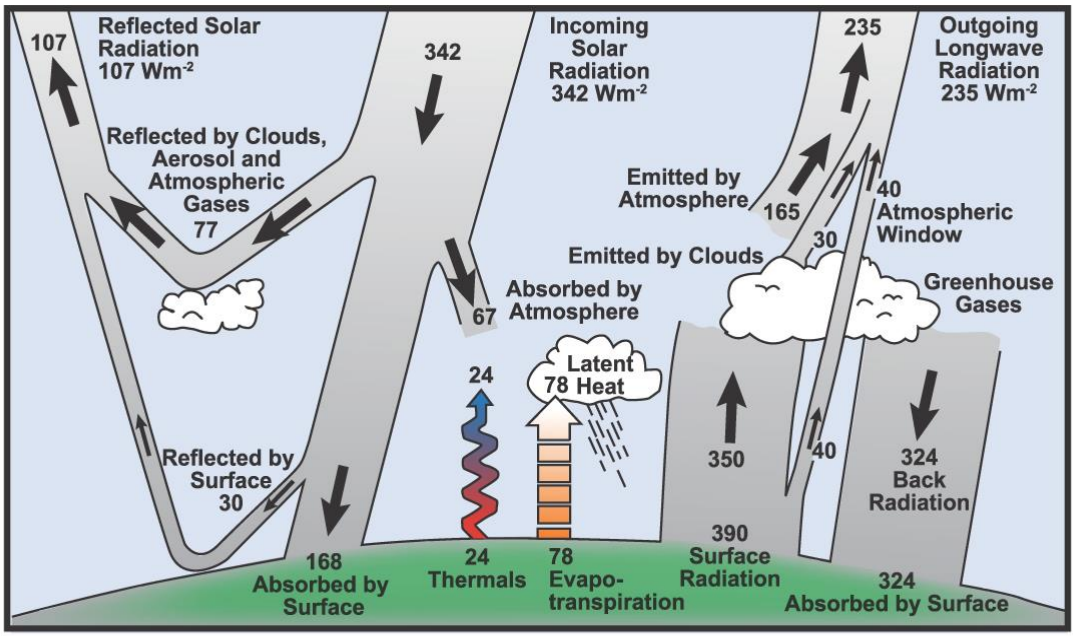

Figure 1.1. *Energy balance of the incoming solar radiation (source:Kiehl et al., 1997).*

particular, as regards the radiation that manage to reach the surface, one part of this is absorbed by the surface, while the other is reflected as radiation with a longer wavelength: the latter, thanks to the presence of GHG that act as a partial blanket, remains trapped causing the temperature to rise (Treut et al., 2007). This mechanism is shown in Figure 1.1.

However, if on the one hand the natural effect of greenhouse gases is positive for the thermal equilibrium of the athmosphere, on the other hand those produced by humans are damaging and affecting the energy balance between the Sun and the Earth.

The emissions of anthropogenic GHG are constituted of methane, nitrogen oxides, chlorofluorocarbons, hydrofluorocarbons and CO_2. These began to augment significantly since the first industrial revolution, since when it is estimated that about 2040 Gtons of anthropogenic CO_2 have been emitted, half of them from 1970 to now. In the last 50 years, about 78% of the increase of greenhouse emissions with respect to initial level has been constituted by CO_2 generated by combustion, industrial processes and the use of land and forests (IPCC, 2014). There are three main causes related to this:

- population growth;
- the increase in wealth;
- the loss of efficiency of the natural systems to absorb, reflect and emit CO_2, caused both by the deforestation processes and the increase in the temperature of the oceans.

From a quantitative point of view the atmospheric CO_2 concentration has risen from 280ppm from 1860 to 400 ppm today. This has led to (IPCC, 2007) :

- a temperature increment of about 0.85 ° C between 1880 and 2012;
- a 26% increase in acidification of the oceans, which corresponds to a decrease in the pH of 0.1;
- a reduction in the extension of the Arctic glacier by 4% compared to 1979 and an increase in sea level of 0.19m.

If no action were taken, as shown in Figure 1.2, it is estimated that by 2100 the temperature will rise by 1.9-4.6 ° C (IPCC ,2014), with potentially dramatic consequences.

As regards energy suppliers, the IPCC (2014) suggests that, in order to achieve this goal, it is necessary to promote decarbonisation by favouring the utilisation of energy from renewable and nuclear sources, and the CCS technology for fossil fuel power plants.

In the European Union, GHG emissions have been reduced by 23% compared to 1996, while for the imminent future it is proposed to reduce them by 40% by 2030, in order to be able to comply with the Paris agreement.

In particular, dividing in six sectors the main responsible sources for European GHG emissions (i.e. power sector, residential and tertiary, industry, transport, agriculture and all the others), the combustion plants together with the industrial sector result to be the main sources and also the one

with the greatest emission reduction potential since it can be zeroed (Figure 1.3) (2050 Low-carbon economy).

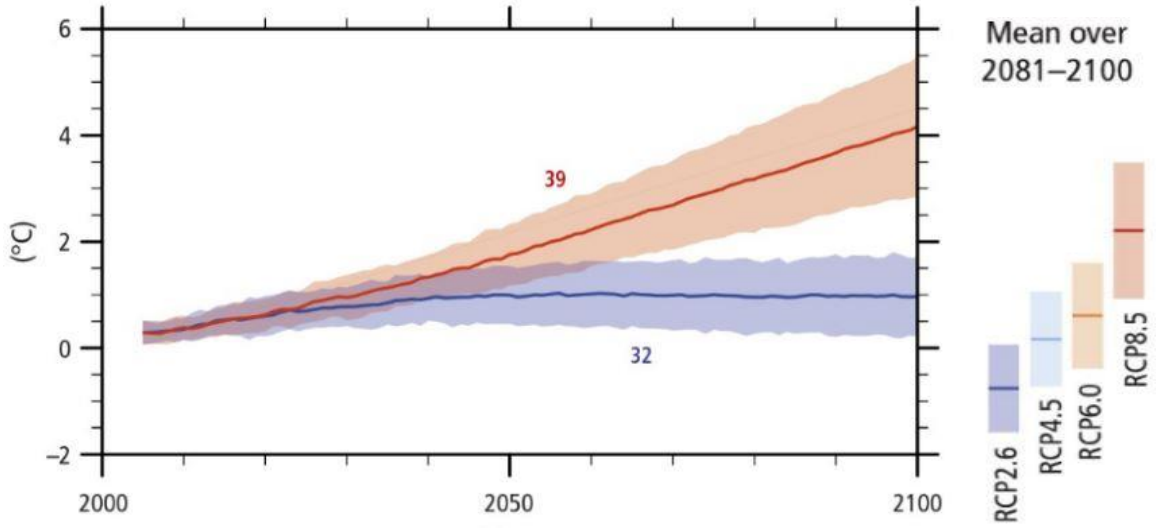

Figure 1.2. *Global average temperature change, considering four scenarios: the two depicted here are the RCP2.6, that considers all the best possible mitigations, and the RCP 8.5, that contemplates the highest GHG emissions. The two intermediates are not shown, but they have to be imagined to be in the middle* (source:IPCC, 2014).

Moreover Figure 1.3 shows the trend of GHG reduction, and it can be noticed that without changing or at least modifying the current policies, it will be difficult to reach the desired target (2050 low-carbon economy).

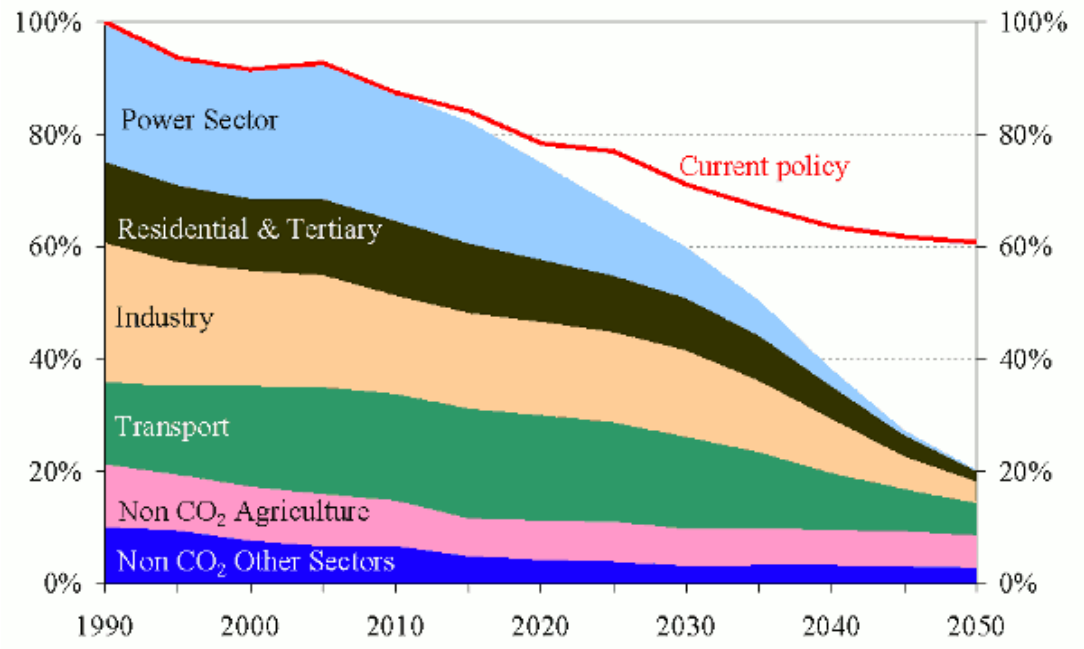

Figura 1.3. *The amount in percenatge terms of GHG impact and the respective potential of reduction (Source : (2050 low-carbon economy)*

As for large stationary plants, these aim at cutting emissions by 43%, since they are one of the sectors affected by the Emissions Trading System (ETS) (2030 climate and energy framework), which include, in addition to the aforementioned, the majority of the industrial sector (i.e. oil refineries, coke ovens, iron and steel plants, cement clinker, glass, lime, bricks, ceramics, pulp, paper and board) (European Commission, 2015). With respect to these, the legislation has moved mainly towards relaunching emission trading policies; however, despite having allocated 38 G€ to facilitate this goal (of which around 10 G€ are for research and 23 G€ are instead for the transition to renewable sources, efficient urban transport with low emissions and smart grids), no precise financial support has been dedicated to those sectors affected by ETS.

Nonetheless the European Commission has declared that large combustion plants will have to be equipped with CCS plants by 2030, since the theoretical energy efficiency has reached its maximum, and therefore this is the only way to reduce the emissions of GHG from them (European Commission, 2014). However without appropriate research that has the purpose of developing new technologies and optimizing the current ones, the cost for CO_2 reduction could be excessive for the community (Arnette, 2017; European Commission, 2015).

In relation to this need, the European community, thanks to the allocation of the research funds (e.g. Horizion 2020, NER 300, LIFE climate action,..), aimed at both the development of techniques that allow a reduction of GHG and the determination of costs of the various stages of the process of capture, transport, storage and use, which led to the establishment of a large number of data and information (European CCS Demonstration Project Network, 2015; Geske et al., 2014; Global CCS Institute, 2017; Samantha McCulloch, Simon Keeling, Raimund Malischek, Tristan Stanley, IEA, 2016; Tzimas and Georgakaki, 2005; Vangkilde-Pedersen et al., 2008; ZEP, 2011). This huge amount of material has laid the foundations for the definition of economic parameters, but these must be integrated with each other in order to provide a valid tool: without the integration to a European-scale implementation of storage, transport, capture and utilisation such studies are likely to be ends in themselves (Hasan et al., 2015a).

On the basis of this, considering the vastness and complexity of the European scale, the mixed integer linear programming (MILP) provides a powerful tool on one hand for the optimisation of the economic parameters of the entire SC, defined by capture, storage transport and utilisation; on the other hand, for preliminary information both quantitative and qualitative on the strategic planning of the entire network (Beamon and Beamon, 1998)

Currently most of the studies that use these mathematical techniques aiming at optimising the whole SC are limited to a specific region and whether they considered the utilisation of CO_2, this is limited to Enhanced oil recovery (EOR). Some of these studies are listed below in Table 1.1

As it is shown from Table 1.1, in the first place the MILP formulation with a multi-period approach is the most frequently employed technique.

For what concerns the geographical contextualization, only the models by d'Amore and Bezzo (2017) and Hasan et al. (2015) contemplate the development of the SC on a geographically vast level.

Table 1.1. *Selected literature on CCS and CCUS models.*

Reference	Utilisation	Location	Mathematical techniques	Features
(Tapia et al., 2016)	EOR	Not specified	MILP	Static deterministic
(Elahi et al., 2014)	No	UK	MILP	Multi-period deterministic
(Bakken and von Streng Velken, 2008)	No	Norway	LP	Static deterministic
(Han and Lee, 2012)	Many	Region of South Korea	MILP	Multi-period stochastic
(d'Amore and Bezzo, 2017)	No	Europe	MILP	Multi-period deterministic
(Hasan et al., 2015a)	EOR	USA	MILP	Static deterministic
(Kalyanarengan Ravi et al., 2017)	No	Netherland	MILP	Multi-period deterministic
(Middleton et al., 2012)	No	Texas	MIP	Multi-period deterministic
(Kwak and Kim, 2017a)	EOR	Texas	NLP	Multi-period stochastic

If the literature considers also the utilisation, it is mainly focused on the EOR, except for the article by Han and Lee (2012) which in addition to the EOR also considers the Enhanced Coal Bed Methane (ECMB), the production of a green polymer, biobutanol and mineral carbonates, and the usage for the growth of algae: however it does not present techno-economic evidence to support the choice of these types of use.

To date, no CCUS SC optimisation project contextualized in Europe contemplates the chemical conversion of CO_2. The objective of this thesis is therefore to tackle this issue.

The model in this Thesis starts from the one by d'Amore and Bezzo (2017), which will be modified by adding the utilisation part and by limiting the resolution to just one year. The possibility of using CO_2 as EOR will not be contemplated because it is not economically feasible (Geske et al., 2014; Tzimas and Georgakaki, 2005).

The goal is to study from an economic point of view the entire CCUS SC, implementing the option of chemical conversion within the original model (d'Amore and Bezzo, 2017).

In particular Figure 1.4 shows the main steps through which the model has been developed.

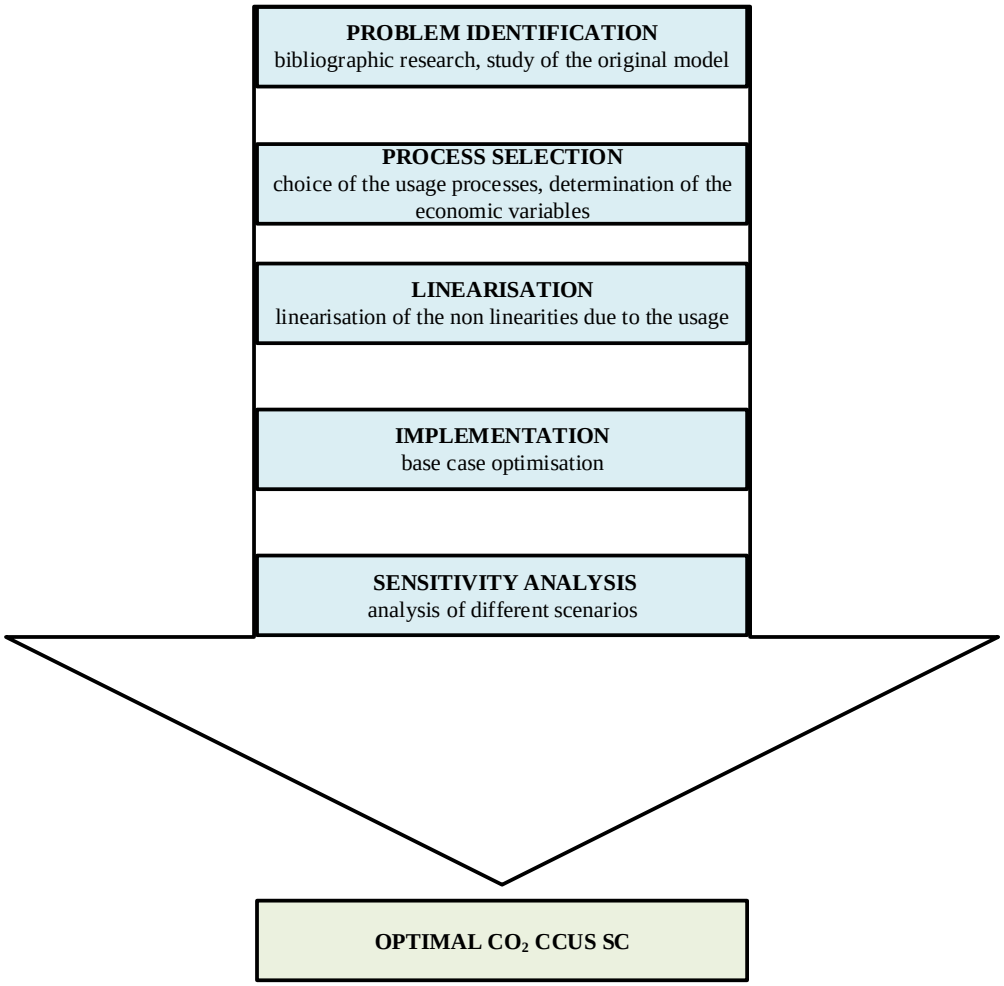

Figure 1.4. *Simplified methodology*

1.2 Usage processes

Since in the near future the large combustion plants will have to install infrastructures for the capture, transport and sequestration of CO_2, it would be interesting to study if and how these carbon network could be integrated with the chemical conversion. Therefore, given the large amount of reaction mechanism in CO_2 conversion, as reported by Aresta et al. (2015), a first screening of the processes reported by literature has to be carried out, following two principles: (*i*) the process must have a large market (i.e. at least higher than 1 Mton/y), (*ii*) the current state of the research and/or industrial application provides both the technical and economic information on the specific process (Table 1.2).

Therefore, the amount of possible production processes have been reduced according to this first screening and only promising processes will be analysed in Section 1.2.1, i.e. those characterised by the availability of techno-economic data.

Table 1.2. *Summary on the current knowledge in terms of production capacity, CO_2 utilisation and techno-economic information for the processes capable to convert carbon dioxide.*

Chemical/ Fuel	Unit	Production	Reference	CO_2 utilised (Aresta et al., 2013)	Techno-economic data
Urea	Mtons/y	208	(Heffer and Prud'homme, 2016)	153	Yes
PU	Mtons/y	18	(Covestro, 2017)	1.07	Yes
Inorganic carbonates	Mtons/y	200	(Aresta et al., 2013)	50	Yes
Syngas	kMW_{TH}	600	(Cairns, 2016)	0	Yes
Methanol	Mtons/y	80	(IHS, 2016)	20	Yes
Formaldehyde	Mtons/y	52	(MC group, 2014)	10	No
Formic acid	ktons/y	700	(Aresta et al., 2013)	0	Yes
Ethylene	Mtons/y	143	(statista, 2013)	0	No
MEG	Mtons/y	22.8	(Aresta, 2010)	0	No
Acetic acid	Mtons/y	14.2	(Aresta, 2010)	0	Yes
Acrylic acid	Mtons/y	4.7	(Aresta, 2010)	0	No
DMC	Mtons/y	-		0	Yes
Salicylic acid	ktons/y	70	(Aresta, 2010)	30	No
POM	Mtons/y	1.7	(PIE, 2016)	0	No
PC	Mtons/y	4.2	(Covestro, 2017)	0.01	No
Kerosene	Btons/y	2	(CNN, 2014)	0	Yes
Methane	Mtons/y	236	(IGU, 2014)	0	Yes
Biodiesel	Mtons/y	28	(S&P global platts, n.d.)	0.01	Yes
DME	Mtons/y	5	(Methanol Institute, 2016)	1.32	No
MTBE	Mtons/y	20	(Argus DeWitt, 2015)	1	No

1.2.1 Promising processes

This section will describe the processes of conversion of CO_2, which are divided into two categories: promising under both an environmental and an economic point of view (Section 1.2.1), and not promising because they do not respect at least one of the two characteristics mentioned above (Section 1.2.2). Moreover, for each of these processes, the chemical reaction, the maturity of technology, the profitability and the net CO_2 impact will be discussed.

1.2.1.1 Polyether carbonate polyols (PPP)

Polyols are bulk chemicals generally employed in the production of polyurethanes and are one of the most commonly produced polymers. In particular, the world annual production of polyols is 9.4 Mtons, of which 2.4 Mtons are produced in Europe (Covestro, 2017).

Figure 1.5 shows the reaction through which PPP is produced: in presence of a double metal cyanide catalyst, the addition of alkylene oxide and CO_2 takes place through one or more H-functional starter (like polyols, alkoxylated oligomers of glycols) (Müller et al.).

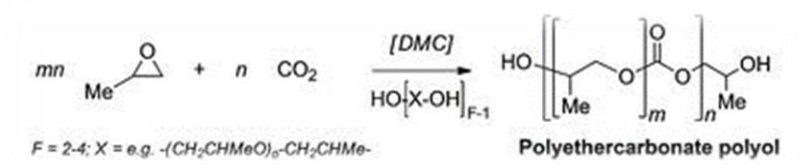

Figure 1.5. *catalytic reaction of alkylene oxide and CO_2 (Source: Langanke et al., (2014)).*

This process was started by Covestro in Dormagen (Germany) in 2016, being the world leader in the production of polyurethanes and polycarbonates and the tenth largest chemical company, with a plant with a capacity of 5 ktons/year of polyether carbonate polyol (Covestro, 2016)

In the European Union, polyether polyol prices were fluctuating from 1275 €/ton and 2200 €/ton during the previous 10 years (Lee, 2014). The production cost in the case studied by Fernández-Dacosta et al. (2017) is estimated to be 1200 €/ton: specifically it is considered that 90% of the CO_2 is captured and stored from a naphtha steam reformer unit that produces hydrogen, while the remaining 10% is employed as feedstock. The other feedstock utilized are Propylene oxide (PO), mono-propylene glycol (MPG) and Glycerol (G). In Table 1.3 the economic features the economic the economic features are summarised.

Table 1.3. Economic indexes of PPP production.

Opex [M€]	Capex [M€]	Productivity [kt/y]	Electricity [€/MWh]	Naphtha [€/t]	PO [€/t]	MPG [€/t]	G [€/t]	Interest rate [%]	Plant life [y]
1.3	21	250	100	480	1400	1550	730	7.5	25

To estimate whether the process is profitable or not, Fernández-Dacosta et al. (2017) provide only a value of the break-even CO_2 that is at 47€/ton. Therefore, since this thesis considers the CO_2 price at zero, this process results to be economically attractive: however, it is necessary to carry out a more detailed analysis.

Regarding the environmental performance, PPP production with 20 weight percentage of CO_2 generates 2.65-2.86 kg $CO_{2\text{-eq}}$ /kg_{PPP}, but compared with standard production methods, it is possible to achieve an overall reduction of 11-19% (von der Assen and Bardow, 2014a): taking into consideration the carbon dioxide employed, for the case of Fernández-Dacosta et al. (2017) $CO_{2\text{-eq}}$ it should reduce by 23% .

1.2.1.2 Methanol

Methanol is one of the most versatile and produced chemicals in the world, and its demand is increasing year by year: today the world methanol plant capacity is equal to 125 Mton/year and the European demand is 12 Mtons/year (IHS, 2016).

Methanol is conventionally produced from synthesis gas by the following reactions, which take place at 200 – 300 °C , 50 – 100 bars (Ullmann's Encyclopedia of Industrial Chemistry, 2000):

$CO+2H_2 \rightarrow CH_3OH$ $\Delta H_{300K} = -90.77$ kJ/mol (1.1)
$CO_2+3H_2 \rightarrow CH_3OH+H_2O$ $\Delta H_{300K} = -49.16$kJ/mol (1.2)
$CO_2+H_2 \rightarrow CO+H_2O$ $\Delta H_{300K} = +41.21$ kJ/mol (1.3)

In order to use CO_2 as feedstock, there are three main technologies: catalytic hydrogenation, dry reforming, and injection of CO_2 into the methanol reactor.
The catalytic hydrogenation process takes place through two different process configurations (Van-Dal and Bouallou, 2013):

- one step mechanism, where CO_2 is directly catalytically hydrogenated in a single reactor via reaction (1.2), while (1.1) and (1.3) arise parallel (Van-Dal and Bouallou, 2013); optimal condition occurs at 200°C and standard pressure (50-100 bars), by the usage of $Cu/ZnO/Al_2O_3$ catalyst (Vanden Bussche and Froment, 1996);
- two step mechanism, in which CO is produced from CO_2 via Reverse Water Gas Shift (RWGS) (1.3) and then converted into methanol by hydrogenation; according to CAMERE process, the first step takes place at 600°C, 20 bars and it converts 61% of CO_2 into CO, the second step comes about through $Cu/ZnO/ZrO_2/Ga_2O_3$ catalyst at 240°C and at 30 bars with a carbon conversion to methanol of 89 % (Joo et al., 1999).

The Dry reforming process transforms CO_2 into a mixture of syngas, which is then utilised to produce methanol in a standard manner, and the reactions are described as:

$CO_2 + CH_4 \rightarrow 2CO + 2H_2$ $\Delta H_{298} = +247$ kJ/mol (1.4)
$CO_2 + H_2 \rightarrow H_2O + CO$ $\Delta H_{298} = +41$ kJ/mol (1.5)
$2CO \rightarrow CO_2 + C$ $\Delta H_{298} = -172$ kJ/mol (1.6)
$CH_4 \rightarrow C + 2H_2$ $\Delta H_{298} = +75$ kJ/mol (1.7)

Reaction (1.4) is the desired, (1.5) is the RWGS, (1.6) is the Boudouard and (1.7) is methane cracking: (1.6) and (1.7) are responsible for carbon deposition above the catalyst: in order to minimize this effect the optimal temperature and pressure have to be between 870-1040 °C and 1 bar, for a ratio between CO_2/CH_4 equal to 1 (if higher, it will cause CH_4 conversion to slightly increase, but CO_2 dramatically increases) (Wang et al., 1996).
Finally, the third process is based on the fact that the optimal stoichiometry number for synthesis gas, defined as $S = ([H_2]-[CO_2])/([H_2]-[CO_2])$, for methanol production is 2 (Ullmann's Encyclopedia of Industrial Chemistry, 2000), but for the standard steam methane reforming (SMR) condition, that number is higher (de Freitas Silva et al., 2013): through the addition of CO_2 to the SMR reactor or afterwards, which has been previously separated from the flue gas of the burner, it is possible to increase by 20% the methanol production rate (Reddy et al., 2014).
The only plant that converts CO_2 through hydrogenation that has a consistent capacity (about 4 ktons/year) is located in Svartsengi, Iceland, and it is owned by the Carbon Recycling International Inc., which is planning to expand up to 80 kton/year: the one step mechanism is employed. Dry reforming technology is only at demonstration plant level (Alper and Yuksel Orhan, 2017). CO_2

injection has been performing since 1997 in a plant located in Rio de Janeiro, Brazil and owned by Prosint.

Regarding the price, the one of Methanol during the previous 15 years has been fluctuating from 125 €/ton of January 2002, to 525 €/t of March 2008: today the price is 330 €/ton (Methanex, 2017). Depending on the technique employed, the cost varies a lot. Beginning with catalytic hydrogenation, the aspect that mostly weighs on production cost is the way H_2 is produced.

Table 1.4. *Economic indexes of methanol production for different scenarios.*

	Units	A	B	C	D	E	F
H_2	[€/ton]	3090	-	-	-	-	-
Electricity	[€/MWh]	95.1	50	50	30	30	30
Water	[€/ton]	0.03	3	3	-	-	-
CO_2	[€/ton]	0	3-10	3-10	0	0	0
CAPEX	[M€]	220	14.39	117.4	75	21.7	10.1
OPEX	[€/year]	295	-	-	-	-	-
Plant life	[year]	20	20	20	15	15	15
Discount rate	[%]	8	10	10	5	5	5
Productivity	[kton/year]	440	16.3	19.2	50	10	4
Production	[€/ton]	-	891	5459	-	-	-

Table 1.4 shows a review of simulated plant:

- Case A is readapted from Pérez-Fortes et al. (2016): H_2 is not produced, but bought outside of the plant, which is produced via renewable sources, and its price and electricity price vary according to future hypothesis;
- Case B and C are readapted from Rivera-Tinoco et al. (2016): H_2 is directly produced in the plant through water hydrolysis, and both Proton Exchange Membranes (PEM) and Solid Oxide Electrolyser cells (SOEC) are employed in order to understand the differences;
- Case D, is readapted from (Bellotti et al., 2017): H_2 is produced via a PEM, three plant sizes are considered with a CO_2 system and it is assumed to either sell O_2 at 100€/ton or not;

Regarding the other two technologies analysed in table3, Mondal et al. (2016) (E) state that it is possible to produce methanol via dry reforming at 123 €/t (which is even lower than the production cost via steam reforming) in a plant that has a total production of 1.667 Mtons/year of methanol (they did not considered the CO_2 price), while regarding production cost of CO_2 injection (F) no information has been found.

Concerning the scenario of plant A, methanol production via hydrogenation is able to use 1.234 tons of CO_2 per ton of methanol: this data is in line with the article of (Roh et al., 2016a) who report that it is possible to reduce by 1.2 and 2.17 kg of CO_2 per kg of methanol, with respect to steam

reforming of natural gas. Other plant configurations have no detailed data about a net amount of CO_2 emission. Lastly, the dry-reforming option consumes 0.022 tons of CO_2 per ton of methanol.

1.2.1.3 dimethylcarbonate (DMC)

DMC is a green reagent, since it is biodegradable, non-toxic, nor irritating, nor mutagenic (Tundo and Selva, 2002); it has an extensively industrial application because it can be used as a methylation agent, solvent, fuel additive and a substitute for phosgene in the production of aromatic polycarbonate and isocyanate (Keller et al., 2010).
Regarding the annual production there are conflicting opinions. Garcia-Herrero et al. (2016) report that the annual production of DMC is equal to 98 kton/year, while Alper and Yuksel Orhan (2017) indicate 10Mtons/year. Not more is reported in literature except that the 50% of the world DMC production is involved in PC production, which is produced at a current rate of 4.2 Mtons/y: this implies that no more than 2 Mtons/y of DMC can be produced (IHS Markit, 2017). Moreover most of PC world production is currently made via phosgene (Covestro, 2017).The data by Garcia-Herrero et al. (2016) may not be correct since in 2013 in China a DMC plant with capacity of 100ktons/y was started up (CEN ACS, 2012).

However if it is considered that:

- DMC can replace MTBE as a fuel additive, which in Europe has a demand of 2.85 Mtons/y (IEA AMF.) and has 3 times less the amount of oxygen with respect to DMC expressed as mass, this will have a demand in Europe of 0.9Mton/y (De Groot et al., 2014; Haba et al., 1999; IEA AMF);
- DMC can fully replace phosgene in Europe in the production of PC, which in Europe accounts for a total production of 1Mton/y, it may reach a production of 0.5Mtony (Covestro, 2017; IHS Markit, 2017; statista, 2016).

Therefore DMC can achieve a total production of 1.4 Mton/y in Europe.

The reaction for the direct synthesis of DMC from CO_2 is shown in Figure 1.6: it is characterized by stability of CO_2 and by the fact that, as soon as the product is formed, the DMC tends to hydrolyse, strongly shifting the equilibrium to the right. In order to solve this issue it is necessary to pressurize CO_2, find an efficient catalyst and a proper dehydrating agent. The dehydrating agent can be:

- recyclable, i.e. acetals and molecular sieve;
- non-recyclable, i.e. dicyclohexyl carbodiimide and orthoesters.

Depending on the dehydrating agent, different catalysts can be employed: the most common are tin (IV) based alkoxides and dialkoxides, which are toxic metals, and titanium and zirconium based catalyst, which are less toxic; some additives can be used in order to speed up the reaction and make

it more efficient (like an acid catalyst) (Sakakura and Kohno, 2009). The reaction is carried out between 100-200°C, at 30-300 bars for several hours (Sakakura and Kohno, 2009).

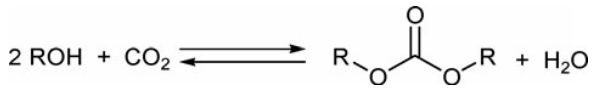

Figure 1.6. *DMC reaction via direct synthesis (Source: Sakakura and Kohno (2009)).*

Another way to produce DMC via CO_2 is the indirect route: CO_2 and ethylene oxide (EO) react to form ethylene carbonate, which then reacts with methanol to produce DMC: this reaction is catalysed by zirconium or titanium, that takes place at 100-150°C and at about 80 bars. Again, the reaction has unfavourable equilibrium, which can be shifted to the product by removing the above reactants through azeotropic distillation. Figure 1.7 shows the process, which is commercialized by Asahy Kazei Chemicals Corporation.

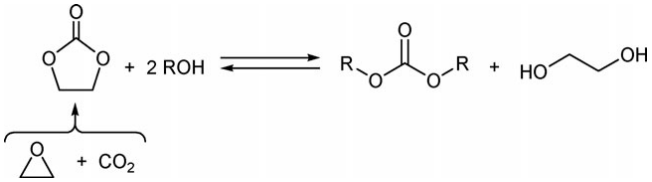

Figure 1.7. *DMC reaction via EO (Source: Sakakura and Kohno (2009)).*

DMC can also be produced via transesterification of urea as shown by Sakakura and Kohno (2009) in Figure 1.8.

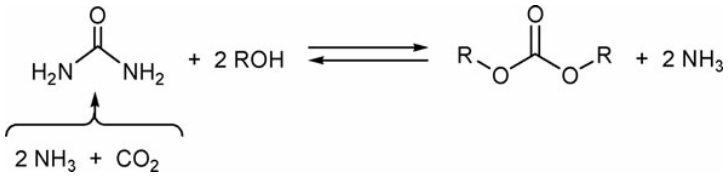

Figure 1.8. *DMC via transesterification (Source: Sakakura and Kohno (2009)).*

Urea reacts with an alcohol (generally methanol), the reaction is generally catalised by ZnO, at 170-190°C, for 6-12 h, to a yield of DMC over methanol of 30% in a batch process (Wang et al., 2005) and of 60-70% with a catalytic distillation (Wang et al., 2007): during the reaction some intermediates are formed like methyl carbamate.

Finally, the other ways to produce DMC are transesterification of acyclic carbonates and alkylation of carbonate salts.

Currently the only commercial technology is based on the indirect route process of Asahi Kazei Chemicals Corporation (Fukuoka et al., 2010).It has been possible to retrieve price information only from Alibaba, which report a range between 800-1000 €/ton.

Table 1.5. *Economic indexes of DMC for different methods of production*

	Unit	Via urea	Indirect with MIBK	Indirect with EG	direct
Methanol	[€/ton]	-	569	569	378
Electricity	[€/MWh]	-	30	30	51
Water	[€/ton]	-	0.022	0.022	0.0042
CO_2	[€/ton]	-	3.6	2.6	0
CAPEX	[M€]	110	-	-	45.4
OPEX	[M€/year]	-	-	-	23.82
Plant life	[year]	-	13	13	-
Discount rate	[%]	.	8	8	5
Productivity	[kton/year]	86	134.4	130.6	20
DMC	[€/ton]	935	807	807	850

Each of the four cases found in literature do not report a direct price but simply the price that should have DMC in order to make the process economically profitable (Table 1.5):

- Via urea process is described by De Groot et al. (2014), in which article many assumptions are missing: anyway they state that for a selling price of 935 €/ton it would be possible to have a payback period of 3 years;
- The two indirect processes are reported by Souza et al. (2014): the one that uses Methyl isobutyl ketone (MIBK) to break methanol/DMC azeotrope looks more eco-friendly but it has a lower economic performance compared to the one with ethylene glycol (EG); in fact the estimated payback time is respectively 5.5 and 4.5 years;
- The direct process is shown by Kuenen et al. (2016), who employ a membrane reactor in the simulation: it achieves its break-even point at a price of 1033 €/ton.

Regarding the environmental impact, Souza et al. (2014) report that in the indirect process the CO_2 equivalent emitted is negative in both cases, particularly -15.9 kton/year for MIBK and −8.1kton/year for EG extraction. Kuenen et al. (2016) show that the direct process emits more CO_2 then that consumed. Kongpanna et al. (2015) have calculated that the indirect route produce 0.452 kg CO_2/kg_{DMC} and the urea route 2.38 kg_{CO2}/kg_{DMC}, considering burning methane as fuel.

1.2.2 NON-PROMISING PROCESSES

Here those processes that are incompatible in economic and environmental terms are shown.

1.2.2.1 Urea

Urea is one of the most commonly produced chemicals, it is mainly used as fertiliser, and since the population is growing, its demand is expected to grow.

The current industrial mechanism can be described by the Basaroff reaction (Ullmann's Encyclopedia of Industrial Chemistry,2000):

$$2NH_3 + CO_2 \rightarrow NH_2COONH_4 \qquad \Delta H = -117 \text{ kJ/mol} \qquad (1.8)$$

$$NH_2COONH_4 \rightarrow NH_2CONH_2 + H_2O \qquad \Delta H = +15.5 \text{ kJ/mol} \qquad (1.9)$$

Reactions (1.8) and (1.9) take place at high temperature T=190-220 °C and pressure P=140-210 bar, and at a ratio of NH3:CO2 between 4.2-3 moles, depending on the technology employed (Ullmann's Encyclopedia of Industrial Chemistry, 2000).
Currently the production of urea occurs exclusively from NH_3 and CO_2 (Ullmann's Encyclopedia of Industrial Chemistry, 2000), and the annual production is about 208 Mtons (Heffer and Prud'homme, 2016), 10% of which is produced in the European Union (Fertilizers Europe).
About the Urea price, it can be noticed that in the last five years it has fluctuated between 159 and 308 €/ton (Index mundi), while in Italy it has moved between 297 €/ton and 463 €/ton over the last three years (clal). Table 1.7 shows the economic performance of different production technique.

Table 1.7. *Economic indexes of Urea production.*

	Unit	(Kempka et al., 2011)	(Edrisi et al., 2016)	(Dobrée, 2016)
Electricity	[€/MWh]	-	65,9	-
NH_3	[€/ton]	190		-
CO_2	[€/ton]	12.5	43.3	-
CAPEX	[M€]	-	320.8	-
OPEX	[M€/year]	-	224.9	-
H_2	[€/ton]	721	-	-
N_2	[€/ton]	-	247.3	-
Plant lifetime	[year]		25	-
Production	[€/ton]	262-318	180	1400

Considering the current market prices of urea the only processes that look promising are those that utilise fossil raw materials to make hydrogen (i.e. those described by Kempka et al. (2011) and Edrisi et al. (2016), that respectively study the scenario when urea is produced from coal and NG). In fact, as reported by Dobrée (2016),the urea production costs when ammonia is produced through water electrolysis is too high to be commercialised.
With respect to environmental consideration, if on the one hand Urea production consumes 1 mole of CO_2 every mole of urea, on the other hand CO_2 comes from the previous ammonia plant, which

needs N_2 and H_2, that is produced by steam reforming or coal gasification: therefore no further CO_2 can be utilized. Actually, 0.91 $kg_{CO2\text{-}eq}/kg_{urea}$ is produced (which becomes 5.15 considering the usage of urea as fertilizer) (Brentrup and Pallière). For this reason, no further investigation on it will be taken into account.

1.2.2.2 Mineral carbonate

Production of mineral carbonate is a way of storing CO_2 through geologic formation, by the exothermic reaction between minerals containing calcium of magnesium and gaseous CO_2. The product thus formed can be reused, for example for mine reclamation or disposed in dedicated places. The annual production of mineral carbonate can be estimated between 200-250 Mtons per year (Aresta et al., 2013).
A generic carbonation reaction (1.10) can be described by the following:

$$(Ca,Mg)SiO_3 + CO_2 \rightarrow (Ca,Mg)CO_3 + SiO_2 \qquad \Delta Hr = \ <0 \quad (1.10)$$

The feedstock that can be used are natural silicate (i.e. olivine, wollastonite, serpentine,..) and industrial residues like slags and ashes. The pros of this process are that the reaction is exothermic, the chemical compounds that are formed are stable. The cons are essentially based on the kinetic, since the reaction is slow. There are two possible routes: direct carbonation at high temperature and aqueous process, which can take place directly or indirectly. In the case of direct carbonation the kinetic is unfavourable: the reaction almost does not proceed at ambient conditions and the Gibbs free energy remains negative for temperatures less than 888 °C for calcium oxide, 281 °C for wollastonite, 242 °C for olivine (Lackner et al., 1995). Therefore, in order to make CO_2 carbonation possible, high pressure needs to be employed. However. the process is currently industrially unfeasible (Mazzotti et al., 2005).
The aqueous process can be summarizes in three phases (Huijgen and Comans, 2003):

$$CO_2 + H_2O \rightarrow H2CO_3 \rightarrow H^+ + HCO_3^- \quad (1.11)$$
$$Ca/Mg\text{-silicate} + 2H^+ \rightarrow (Ca/Mg)^{2+} + SiO_2 + H_2O \quad (1.12)$$
$$(Ca/Mg)^{2+} + HCO3^- \rightarrow (Ca/Mg)CO_3 + H^+ \quad (1.13)$$

Reaction (1.11) represents the CO_2 dissolution in water, (1.12) is the dissolution of Ca/Mg from the mineral and (1.13) Mg or Ca precipitates as carbonate. The rate limiting step is represented by (1.12), so, in order to make the process industrially attractive, the dissolution of the metal needs to be sped up by increasing the surface area through the removal of SiO_2 layer and the reduction of $(Ca/Mg)^{2+}$ activity: this can be achieved by adding catalysts (like strong, weak acids or base), additives (i.e. chelating agents), through heat treatment or ultrafine grinding (Mazzotti et al., 2005). Depending on the feedstock the reaction takes place at 10-175 bars and at 155-200 °C.

As reported by Aresta et al. (2013) the total utilization of CO_2 in inorganic carbonation is 50 Mtons per year. The commercial technology is the Solvay. However, the CO_2 comes from the same process (calcination). The high temperature method and the aqueous method are still at development/demonstration stage.
The main part of the production cost is due to the grinding both on the investment and operating points of view. In Table 1.8 the following are summarised.

Table 1.8. *Cost of different carbonation technique*.

Process	Feedstock	Cost [€/ton CO_2 avoided]	Reference
Direct-water	Wollanstonite	93	(O'Connor et al., 2005)
-	Wollanstonite	102	(Huijgen and Comans, 2003)
-	Steel slag	77	(Huijgen and Comans, 2003)
-	Olivine	65	(O'Connor et al., 2005)
-	Serpentite	258	(O'Connor et al., 2005)
Direct molten	Mg-silicate	95	(Newall et al., 2000)
Indirect-water	Waste cement	25	(Iizuka et al., 2004)
-	Concrete/Steel slag	8	(Stolaroff et al., 2005)
Indirect-acetic acid	Wollansonite	57	(Yanagisawa, 2001)
Indirect-Hcl	Mg-silicate	>150	(Newall et al., 2000)

Bodénan et al. (2014), with respect to the case of no CCS, show that the aqueous carbonation with olivine leads to an increase of CO_2 emission, since the increase of the energy consumption leads to an overall environmental worsening. Chang et al. (2011) report that, depending on the mixture of steelmaking slags, the net CO_2 emission range between 0,019 – 0,037 kg_{CO2}/kg_{slags}.

1.2.2.3 Formic acid

Formic acid is an important commodity and its main usage are in animal feed, dyeing, textile and leather industries and as intermediate in the chemical and pharmaceutical industry; the current production takes place through four processes: methyl formate hydrolysis, oxidation of hydrocarbons, hydrolysis of formamide and preparation from formamates (Ullmann's Encyclopedia of Industrial Chemistry, 2000). The CO_2 conversion into formic acid may occur via two different routes: electrochemical and catalytic hydrogenation.
The catalytic hydrogenation process is described by Thomas et al. (2014):

$$CO_2 + H_2 + C_{18}H_{39}N_4 \rightarrow C_{18}H_{39}N\text{--}HCOOH \quad (1.14)$$
$$C_{18}H_{39}N + HCOOH_4C_{18}H_{39}N + HCOOH \quad (1.15)$$

Reaction (1.14), which is the hydrogenation with homogenous catalyst (ruthenium based), occurs between 50-100 °C at 85-120 bars, while step (1.15), which is the dissociation of the ammine-formic acid adduct previously formed in the reactor to formic acid and an ammine, arises at 150-185 °C and at 100-250 mbar.
Another way to produce formic acid from CO_2 is through electrochemical reduction: CO_2 is electrolysed by running the cell in reverse mode through the following reactions:

Cathode:	$2CO_2 + 4H^+ + 4e^- \rightarrow 2\ HCOOH$	(1.16)
Anode:	$2H_2O \rightarrow O_2 + 4e^- + 4\ H^+$	(1.17)

The mechanism is described by Peterson et al. (2010): a pair of protons and electrons are adsorbed together with CO_2 as formate (Eq. 1.16), and then another proton is added so as to form formic acid (Eq. 1.17).
One of the main advantages is that it can utilise wasted electricity from intermittent renewable sources, but two aspects need to be overcome: energy efficiency, high faradaic efficiency and low overpotential, and high current density, which gives the indication of the reaction rate. Another limiting factor is due to the fact that CO_2 has a low diffusivity coefficient, that implies a slow mass transfer: gas diffusion electrodes, on which the catalyst is deposited seems to be promising, since they set up three phases (Lu et al., 2014; Whipple and Kenis, 2010).
Regarding the current price of formic acid, ICIS (2014) reports that the annual production of formic acid is at 697 ktons/year, of which 310 ktons/year in Western Europe, at a price between 0,5-0,6 €/kg for formic acid of 85% purity. No industrial plants that utilises CO_2 as feedstock exist, but only lab or demonstration plants exist (Lu et al., 2014; Pérez-Fortes et al., 2016a).
For the homogeneous catalytic hydrogenation, the production cost has been estimated at 1524 €/ton (Pérez-Fortes et al., 2016a): no information on the electrochemical reduction process has been found.
About the environmental performance, Pérez-Fortes et al., (2016a) report that 0,166 tons of CO_2 per tonnes of formic acid are formed, comparing to 2.18 of a conventional process. No information on the electrochemical reduction process has been found.

1.2.2.4 Jet fuel

Jet fuel is based on kerosene or on naphtha/kerosene mixture, and its current demand is about 184 Mtons/year (Cha, 2014).
The technology to produce jet fuel from CO_2 is based on its reduction to synthesis gas (previously described), which is further transformed through the Fischer-Tropsch (FT) process to synthetic fuel, after hydrocarbon upgrading. Taking into consideration the kind of feedstock and the desired product, a good choice for the FT is the cobalt based catalyst (König et al., 2014); the reactions take place at 220-250 °C , 10-40 bars, and can be summarised in (Modesti, 2011):

Paraffins	$(2n+1)H_2 + nCO \rightarrow C_nH_{2n+2} + nH_2O$	(1.18)
Olefins	$2nH_2+nCO \rightarrow C_nH_{2n} + nH_2O$	(1.19)
Water gas shift (WGS)	$CO + H_2O \rightarrow CO_2 + H_2$	(1.20)
Alcohols	$2nH_2 +nCO \rightarrow C_nH_{2n+2}O + (n-1)H_2O$	(1.21)
Boudouard	$2CO \rightarrow C+CO_2$	(1.22)

The upgrade phase is carried out by an hydrocracking unit, which generally employs a platinum based catalyst, at 350-380°C and at 35-70 bars (Leckel and Liwanga-Ehumbu, 2006).
Currently there are no existing plants on CO_2 conversion to synthetic fuel for aviation. The price for the jet fuel in Europe is estimated to be 1,43 €/GGE (IATA, 2017).

Table 1.9. *Economic indexes of jet fuel production.*

	Unit	(König et al., 2015)	(Becker et al., 2012)	(Dietrich et al., 2017)	(Schmidt et al., 2016)	(Tremel et al., 2015)	(Li et al., 2016)
Technology		PEM	SOEC	PEM	-	PEM	PEM
Productivity	[kton/y]	490	23	90	-	15.4	490
Electricity	[€/MWh]	115-190	17-120	105	134	93	26-51
TCI	[M€]	8690	81	660	-	31	-
H_2	[€/kg]	-	-	-	-	3	4.25
CO_2	[€/ton]	-	13	-	0	50	-
Interest Rate	[%]	7	10	-	-	-	10
Plant life	[y]	30	40	-	-	-	-
Production	[€/GGE]	4.25-18.14	3.74-12.75	-	20	-	3.23-7.82
	[€/kg]	-	-	3.76	-	2.01	-

Table 1.9 summarises the data on jet fuel production. From an economic standpoint the main limitation of this process, whatever the price or the source of electricity, is the way H_2 is produced: if it is not produced via fossil raw materials, the process cannot currently be economically viable.
With respect to environmental considerations, Schmidt et al. (2016) estimate that 1 g of CO_2/MJ is emitted, considering production, transportation and distribution.

1.2.2.5 Methane

Methane is the finale reduction step of carbon, it is substantially of natural origin, it is the main component of natural gas and it is mainly employed for energy purpose.
The chemical reaction that converts CO_2 into methane is the CO_2 methanation (or Sabatier):

$$CO_2 + 4H_2 \rightarrow CH_4 + 2H_2O \qquad \Delta H_{298\,K} = -252{,}9\ kJ\ mol^{-1} \quad (1.23)$$

This reaction (Eq. 1.23) usually employs Ni, Ru, Rh, Pt and CO based catalysts, upon which a specific temperature and pressure are chosen: 300-450 °C, 1-100 atm (Chiang and Hopper, 1983; Fujita et al., 1991; Weatherbee and Bartholomew, 1982). A generic scheme for the mechanism is shown in Figure 1.11 (Park and McFarland, 2009).

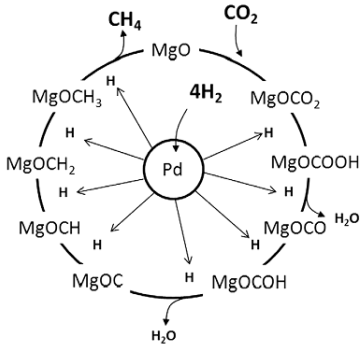

Figure 1.11. *Sabatier mechanism (Source: Park and McFarland, 2009).*

Another possible route to produce methane from CO_2 is to catalyse the reaction by Archaea microorganism: the reaction occurs at 8 bar, 62 °C (Forstmeier, 2017). Cheng et al. (2009) discovered that is possible to produce methane in a microbial electrolysis cells.

Table 1.10. *Economic indexes of methane production.*

	Unit	(Buchholz et al., 2014)	(Vandewalle et al., 2015)	(Parra et al., 2017; Parra and Patel, 2016)	(Breyer et al., 2015)	(Schiebahn et al., 2015)
Capex	[M€]	107	0.8·MW	1.6·MW	17.9-15.5	76000
Opex	[M€/y]	26-28	14% Capex	7% Capex	(0.4-0.3)·MW	3% Capex
Electricity	[€/MWh]	41	0-50	34-38	40	60
Water	[€/m^3]	-	0.7	-	0.25	-
O_2	[€/m^3]	-	70-10	85	-	-
Interest	[%]	-	7	8	4	8
CO_2	[€/ton]	-	-	120	10	-
Incentives	[€/ton]	-	-	51	50	-
Production	[€/MWh]	-	60	230-100		230

Currently, the amount of proven reserves of natural gas is equal to 186,6 trillion m^3 (BP, 2017), and the market price in Europe is 0.03-0.04 €/kWh (Eurostat, 2017a), while the technology that convert CO_2 into methane is under a demonstration level since there are different power to gas plant, both based on Sabatier and Archaea: the biggest is the Audi e-gas plant, which has electrolysers with a total power of 6 MW (Götz et al., 2016).

The capital and operational cost has been estimated by 2000-1000 €/kW_{el} and 60-30 €/(kW_{el}a) depending on the plant size, which has an average life of 15-20 years (Sterner, 2009).The production cost is summarised in Table 1.10
The other production costs have been taken from Götz et al. (2016) , and are summarised in Table 1.11, where each letter is a different scenario.

Table 1.11. *Economic results from Götz et al. (2016).*

	Unit	A	B	C	D	E	F	G
Production	[€/MWh]	190-500	270-300	135-170	630-210	165-392	72-102	218

As for urea, jet fuel and formic acid, the main reason why this process is economically unfeasible is the way in which H_2 is produced: until the costs for the production of H_2 via electrolysis are lowered, these processes are unlikely to be profitable.
Regarding the impact on the carbon balance, from Meylan et al. (2017) it depends on one hand on the renewable energy source, and on the other, on the source of CO_2: not taking into account one of their cases, which state that energy surplus emits 0 gCO_2-eq/MJ, the technology that emits more GHG is the photovoltaic (12.5), while the one that emits less is the hydro (1.9).

1.2.2.6 Biodiesel from microalgae

Biodiesel production using microalgae is the third generation of biofuel production and here the photoautotrophic production is described, since it is considered the only feasible method to produce microalgae (Borowitzka, 1997).
The overall process is schematically described by the Figure 1.9.

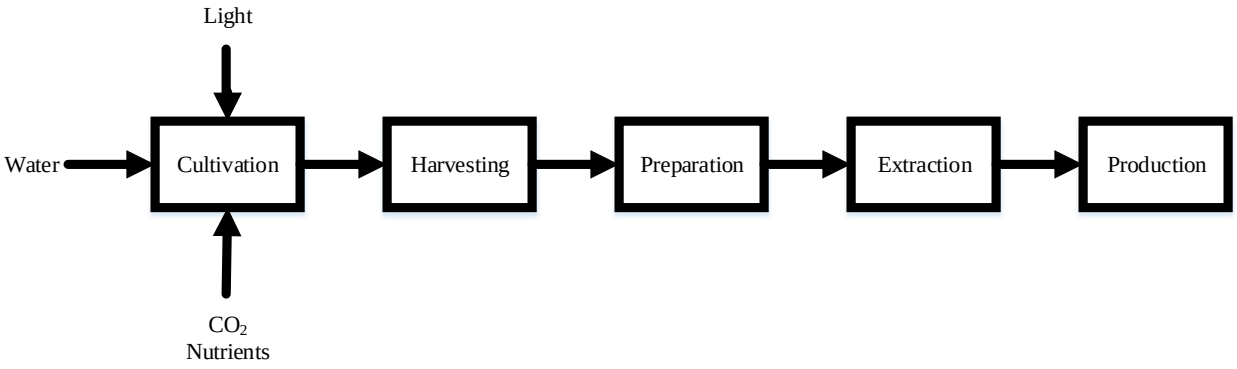

Figure 1.9. *biofuel production process.*

The production of microalgae is connected to the photosynthesis, i.e. to the conversion of CO_2 into glucose, which depends on light efficiency: the maximum theoretical efficiency (ψmax) is only about 12.3.However, other factors need to be taken into account to determine the overall efficiency; the efficiency due to the configuration of the microalgae plant (85-95 %), the efficiency represented

by the factors like temperature, light etc.. (30-80 %) and the efficiency related to the energy needed for the cellular life (10-90 %): this leads to a total efficiency of 0.5-10 %, depending on the cultivation process employed (Bezzo, 2017).

The production technique can be either the open pond system (OPS), whose efficiency is estimated to be 0.5-1 %, or the closed photobioreactor (CPBR) which is 2-5 %. The OPS is the cheapest and easiest method to produce microalgae (Brennan and Owende, 2010), but it has several drawbacks compared to the photobioreactor: less accurate control over process parameters (like temperature fluctuations between night/day and seasons), contamination of other microorganisms (not suitable for food or pharmaceutical purposes), mass transfer limitation of CO_2 into the ponds (since it comes from the atmosphere) and less production (Brennan and Owende, 2010; Mata et al., 2010).

After the algae are produced, the have to be dried, lipids and fatty acids extracted: then the transesterification reaction takes place in order to produce biodiesel. A schematic representation of the reaction is shown in Figure 1.10. Depending on the catalyst employed (i.e. base or acid) alcohol excess varies from 6:1 to 50:1 and temperature from 50 to 120 °C (Bezzo, 2017).

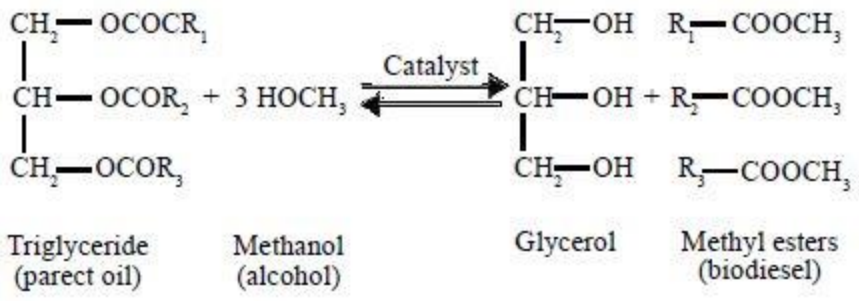

Figure 1.10. *transesterification reaction (Source: Dixit (2016)).*

Chisti and Yan (2011) describe the situation that consists of different demonstration plants. However, with no industrial plants currently in Italy, Eni signed a partnership with Sun Algae Technology to produce biodiesel in Ragusa (adnkronos, 2017).

The annual production of diesel is estimated to be roughly 1.3 billion tonnes per year (Indexmundi, 2012), of which about 28 million of biodiesel (Glystra and Bartlett, 2016). Table 1.6 shows the production cost for OPS and CPBR technique. The only processes that look economically attractive are the following reported by : *i)* R. Davis et al. (2014) who analyse the situation where the dried biomass is already available at 365€/t; in particular the biomass is fermented and then extracted to give fatty acid methyl ester which is then hydrogenised, and as by-product ethanol and electrical energy are produced. *ii)* Gong and You (2015) who make a superstructure analysis, in which they consider the possibility of upgrading the G into valuable products in order to optimise the production cost;

Table 1.6. *Economic indexes for different production technique of algae biodiesel.*

	Units	(Domenicali, 2013)	(R Davis et al., 2014)	(Davis et al., 2011)	(Davis et al., 2011)	(Gong and You, 2015)	(Slade and Bauen, 2013)	(Slade and Bauen, 2013)	(Sun et al., 2011)
Technique		CPBR	OPS	OPS	CPBR	OPS	OPS	CPBR	OPS
Plant size	[kt/y]	4.14	147.47	31.1	31.1	158.47	-	-	-
Capex	[M€]	38.83	390.68	331.4	841.2	-	-	-	-
Opex	[M€/y]	10.81	177.52	31.44	46.73	-	-	-	-
Electricity	[€/MWh]	50.91	57.78	67.97	67.97	-	-	-	-
Plant life	[y]	20	30	20	20	-	-	-	-
Interest	[%]	-	10	-	-	-	-	-	-
Production	[€/GGE]	18.98	3.7	7.9	16.48	2.52	5.69	31.77	11.3

In order to determine the greenhouse gas impact, Campbell et al. (2011) analyse the scenario depending on the productivity of the plant (30-15 g $m^{-2}d^{-1}$ in OPS) and on the CO_2 source (from ammonia plant, as a flue gas at 15% concentration or delivered by a truck, which does approximately 200 km): the result is that a negative impact only occurs when CO_2 is supplied by the ammonia plant or the flue gases; the productivity weighs only in one order of magnitude of the emission. Passell et al. (2013) study the case of Seambiotic, Inc. in Ashkelon, Israel, there the CO_2 is delivered by the flue gases, where the cultivated area is 1 $km^2$and the future is 101 km^2, while the algae are still cultivated in OPS and the productivity is 3 g $m^{-2}d^{-1}$, and for the optimised case up to 25: the outcome is worse compared with a conventional diesel if the energy does not come from renewable sources. Barlow et al. (2016) consider algae production through a biofilm reactor: for the optimised scenario a net CO_2 reduction is achievable (i.e. - 44 g $CO_{2\text{-}e}$ MJ). Soratana and Landis (2011) show that the material of which the photobioreactor is made contributes for about half of the global warming potential, and the balance is due by the CO_2 and the nutrients: the best situation is the one when the reactor is made HDPE, the nutrients, CO_2 and cultivation synthetic resources come from waste resources, which lead to a reduction of $9{,}7 \cdot 10^3$ $kgCO_{2\ eq}$.
However, the algae conversion into biodiesel has not been chosen since the two articles that report that the technology is profitable is that by R Davis et al. (2014),, who deal with a technology that is not yet implemented, and by Gong and You (2015) who consider that actually the main profit is generated not by biodiesel, but by the by-product which are upgraded into highly valuable products.

1.3 Final remarks

Table 1.12 summarises the results obtained from the analysis of the different technologies for CO_2 conversion.

As it is shown, most of the technologies are not capable to reduce CO2, because of poor economic or/and environmental performance. For what concerns those that are able, not all are selected for the integration in the model by d'Amore and Bezzo (2017). Then with respect to DMC, since its demand is not yet well known in contrary as its potential of utilisation, it has been considered to not implement this chemical in the base case model, but it will be considered in a scenario.
Therefore the two chemicals that are selected are PPP and MeOH.

Table 1.12. *Summary on feasibility*

	Utilisation	Cost feasible	Carbon emission
Urea	Coal	No	No
	Natural gas	Yes	No
	Water electrolysis	No	No
PPP		Yes	Yes
Methanol	Hydrogenation (one step)	No	Yes
	Hydrogenation (two step)	No	Yes
	Dry reforming	Yes	Yes
	CO_2 injection	Yes	Yes
DMC	Urea	No	No
	Indirect MIBK	Yes	Yes
	Indirect EG	Yes	Yes
	Direct	No	No
Mineral carbonate	direct	No	No
	Indirect	Yes	No
Formic acid		No	Yes
Jet fuel		No	No
Methane		No	No
Algae	OPS	Yes	Yes
	CPBR	No	Yes

Chapter 2

Methods and Economic Analysis

As regards to the processes selected in the previous Chapter, it is necessary to obtain the prices of natural gas, electricity, corporate tax, labour costs and raw materials in order to have available all the data necessary for the mathematical model that will be explained in Chapter 3.Therefore, this Chapter describes the methodology that was applied to evaluate the prices for the four conversion processes selected (Section 2.1). Then a mass and an energy balance has been carried out for each of these processes, with the purpose of both recovering the missing data from the reference papers, and homogenising them with the aim of obtaining all the economic data which will be necessary for the model described in Chapter 3 (Section 2.2). Finally Section 2.3 summarises the results.

2.1 The choice of economic data

Here, the price data that are common to all four processes will be analysed, and in particular the cost of utilities, labour and corporate tax (Section 2.1.1). Then the prices that have been obtained for each of the four processes on raw materials, products and by-products will be shown, as well as the decision criteria to choose the implemented value of selected parameter(Section 2.1.2).

2.1.1 Labour, tax and utilities data

The price of natural gas and electricity rely on the data provided by Eurostat (2017a, 2017b), whereas the taxation data are taken from KPMG (2018) and the labour cost data are again provided by Eurostat (2017c) except for Moldova and Ukraine, which are available from the Italian Foreign Ministry (Farnesina) website (Table 2.1) .

Data reported in Table 2.1 has been compared with the historic ones. In particular, in certain cases, the most recent value was taken (i.e. the trend had clearly been bearish or bullish); on the other hand the average value was chosen to describe a cyclic trend. Given that the corporate tax rate is linked to geo-political issues, it has been decided to select the value of 2018. The labour cost data was referred to one year only, hence the choice of this value.

Table 2.2 *Prices of natural gas and electricity, labour cost and corporate tax for the countries dealt with in this master thesis.*

Country	Natural gas price [€/kWh]	Electricity price [€/kWh]	Labour cost [k€/y]	Corporate tax [%]
Belgium	0.0244	0.113	55.691	0.3399
Czech Republic	0.0238	0.069	17.48	0.19
Denmark	0.0327	0.082	62.756	0.22
Germany	0.0317	0.152	51.825	0.2979
Ireland	0.0332	0.124	49.66	0.125
Greece	0.0283	0.107	28.179	0.29
Spain	0.0310	0.106	36.388	0.25
France	0.0326	0.099	53.384	0.3333
Croatia	0.0246	0.087	16.659	0.2
Italy	0.0271	0.148	43.822	0.24
Lithuania	0.0246	0.084	10.263	0.15
Hungary	0.0261	0.074	13.136	0.09
Netherlands	0.0365	0.082	56.107	0.25
Poland	0.0273	0.086	13.227	0.19
Portugal	0.0279	0.114	22.321	0.21
Romania	0.0255	0.079	7.648	0.16
Slovakia	0.0282	0.112	15.205	0.21
Finland	0.0441	0.067	50.376	0.2
United Kingdom	0.0248	0.127	47.068	0.19
Macedonia	0.0300	0.056	6.626	0.1
Albania	0.0578	0.084	4.626	0.15
Serbia	0.0310	0.064	8.404	0.15
Turkey	0.0187	0.063	13.899	0.2
Bosnia	0.0343	0.059	9.702	0.1
Moldova	0.0263	0.083	3.6	0.12
Ukraine	0.0262	0.039	3.35224	0.19

As regards the cost of steam production, considering it is here assumed to it at 41 barg (i.e. high pressure (HP) steam), other factors besides the natural gas price must be taken into consideration (Turton et al., 2015). First, the following equation is considered:

$$Cost_g^{NG} = \frac{\text{energy required to produce HP steam} \cdot NG\ price_g}{\text{efficiency} \cdot \text{EBP}} \tag{2.1}$$

Eq. (2.1) calculates the cost of natural gas to produce steam at 41 barg ($Cost_g^{NG}$ [€]), by multiplying the price of natural gas ($NG\ price_g$ [€/kWh]), which is a function of each region g, with the energy required to produce steam. This consists in the energy that has to be spent on the reboiler, which takes into account that steam is produced at 44.3 barg and the exhausted steam at 0.7 barg. On the other hand in the denominator the efficiency, assumed at 0.9, multiplies the enthalpy balance for the product (EBP), which is calculated as follows :

$$\text{EBP} = \frac{\text{enthalpy}_{44.3\ \text{barg}} - \text{enthalpy}_{0.7\ \text{barg}}}{\text{enthalpy}_{41\ \text{barg}} - \text{enthalpy}_{0.7\ \text{barg}}} \tag{2.2}$$

In Eq. (2.2) any value of enthalpy is taken from Turton et al. (2015), while the choice in obtaining steam at 41 barg is made for conservative issues. Next, the following cost equation is added:

$$Cost_g^{BFW} = \mathrm{BFW}^{\mathrm{makeup}} \cdot (BFW_g^{energy} \cdot \mathrm{BFW}^{\mathrm{chemicals}} \cdot \mathrm{BFW}^{\mathrm{water}}) \quad (2.3)$$

Eq. (2.3) calculates the boiler feed water (BFW) cost ($Cost_g^{BFW}$ [€]) by assuming that the amount of makeup ($\mathrm{BFW}^{\mathrm{makeup}}$) is equal to 0.1 and this multiplies the cost of chemicals for treatment ($\mathrm{BFW}^{\mathrm{chemicals}}$ [€]) times the cost of water makeup ($\mathrm{BFW}^{\mathrm{water}}$[€]) the energy in the steam (BFW_g^{energy}[€]) for each region g, which is calculated as follows:

$$BFW_g^{energy} = NG\ price_g \cdot (\mathrm{C_{P,H2O}} \cdot \Delta \mathrm{T} \cdot \dot{\mathrm{m}}) \quad (2.4)$$

In Eq. (2.4), $\mathrm{C}_{P,H2O}$ [Cal/°C·kg] is the specific heat capacity of water, ΔT [°C] is the difference between the saturation temperature at 0.7 barg and the room temperature, and $\dot{m}$ [kg/s] is the mass flowrate of BFW. Therefore, the total cost equation ($Cost_g$ [€]) for high pressure steam in each region g is given by the following:

$$Cost_g = Cost_g^{NG} + Cost_g^{BFW} + \mathrm{Cost}^{\mathrm{chemical}} + Cost_g^{blower} \quad (2.5)$$

In Eq. (2.5), $\mathrm{Cost}^{\mathrm{chemical}}$ ([€]) has the same meaning and value as $\mathrm{BFW}^{\mathrm{chemicals}}$ [€] in (Eq. 2.3), while the electricity cost for usage of blowers is determined through $Cost_g^{blower}$ [€] which is calculated as follows:

$$Cost_g^{blower} = price_g^{electricity} \cdot \mathrm{usage}^{\mathrm{blower}} \quad (2.5)$$

$price_g^{electricity}$ [€/kWh] is the electricity price in each region g according to Table 2.1 and $\mathrm{usage}^{\mathrm{blower}}$ [kWh/kg] is a scalar that take into account the energy needed per kg of steam generated for blower's utilisation, whose value is given by Turton et al. (2015).

2.1.2 Raw material price

Below are the chemicals utilised for each production process for which a price analysis is mandatory for a proper profitability study :

- DMC: ethylene oxide EO, methanol MeOH, mono-ethylene glycol MEG and ethylene carbonate EC;
- PPP: mono-propylene glycol MPG, glycerol G and propylene oxide PO;
- MeOH: demi-water and natural gas.

The method for choosing prices follows similarly that outlined in Section 2.1.1. However, here the complexity linked to the price swing involves some minor changes, made for precautionary reasons:

- Generally, even if the trend leans towards an increase or decrease on the basis of linear regression, it is preferred to choose the average if it is cyclic;
- If the data are related to different countries and they present a significant difference, the European ones are selected.

The prices of chemicals involved in DMC production are shown In Figure 2.1.

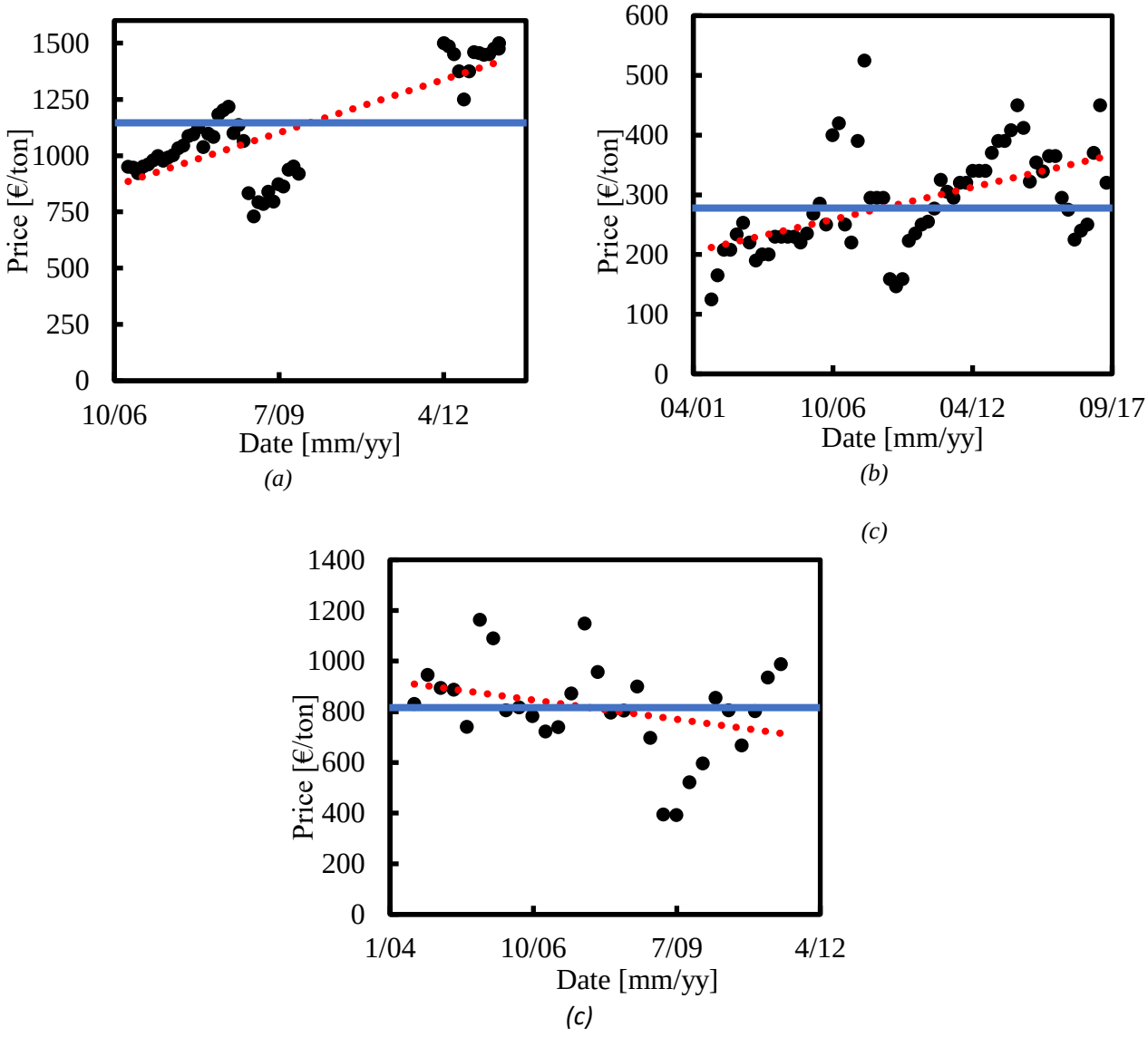

Figure 2.1.*Raw materials prices that are connected with DMC production: (a) EO, (b) MeOH, (c) MEG. The red points represent the linear regression done on the prices, while the blue line shows the price chosen.*

It can be noted that the long-term trend of EO (Intratec, 2013a; ICIS, 2013) and MeOH (Methanex, 2017) prices shows a net growth: however, in the first case the data come from both USA (2006 to

2009) and Europe (2012 to 2013) therefore it is adequate to set it at 1150 €/ton. In the other case, even though it had been more precise to fix the price at around 350€/ton, because of the strong cyclicity, it has been decided to be more conservative and take the average (i.e. 288 €/ton). Afterwards, MEG (VIF, 2014) presents a predominant cyclic behaviour with respect to the trend to decrease, therefore a reasonable price is 812 €/ton (calculated as an average).

Regarding DMC and EC, no historical data has been found, so according to literature the selected prices are correspondingly 950 €/ton (alibaba, 2018) and 1700 €/ton (IHS, 2003a; Molbase, 2017).

Then, Figure 2.2 shows the graphs related to PPP's production process.

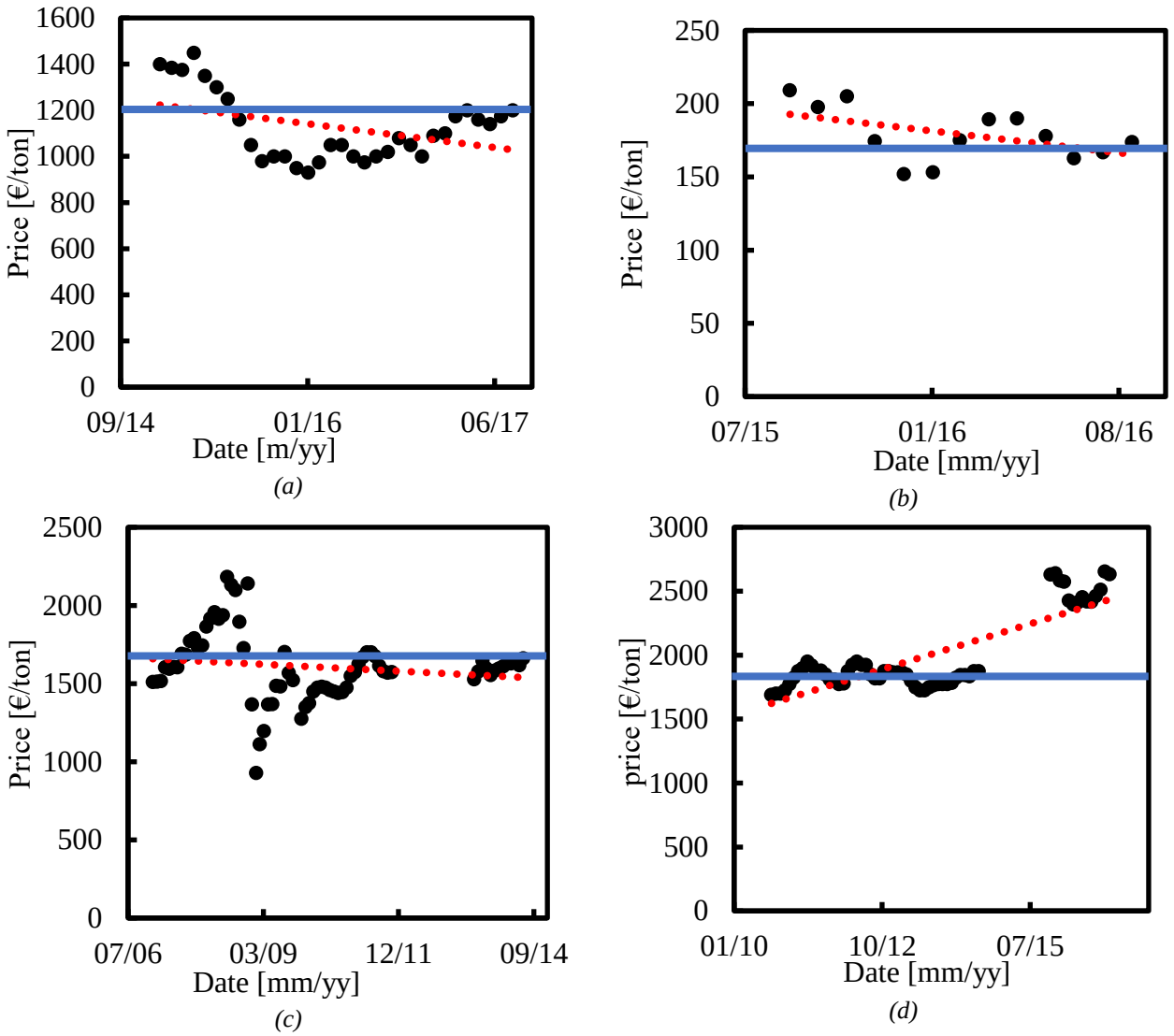

Figure 2.2.*Raw materials prices that are involved in the PPP process: (a) MPG, (b) G, (c) PO and (d) PPP. The linear regression done over the data is given by the red points, while the blue line shows the price chosen.*

Considering the trend shown in Figure 2.2, the prices selected are 1200 €/ton, 170 €/ton, 1700 €/ton and 1850 €/ton respectively for MPG (ICIS, 2007; Echemy technology, 2017), G (Ciriminna et al., 2014; ICIS, 2016), PO (ICIS, 2014, 2011a; Intratec, 2013b) and PPP (ICIS, 2017, 2012a; Mintec,

2014). Regarding the MPG and PO, an average is made, while for G, even though the data from 1995 were available (at that time the price was equal to about 3500 €/ton), it has been decided to omit them since only recently the price of G is getting stable (Ciriminna et al.,2014) . Figure 2.2 *d* displays a growing trend, but, since the data on the right are from the USA (ICIS, 2017), the ones on the left are from Europe (Mintec, 2014) , in order to be conservative, only the average of the European prices is adopted .

The prices for the chemicals involved with MeOH process are illustrated in Figure 2.3.

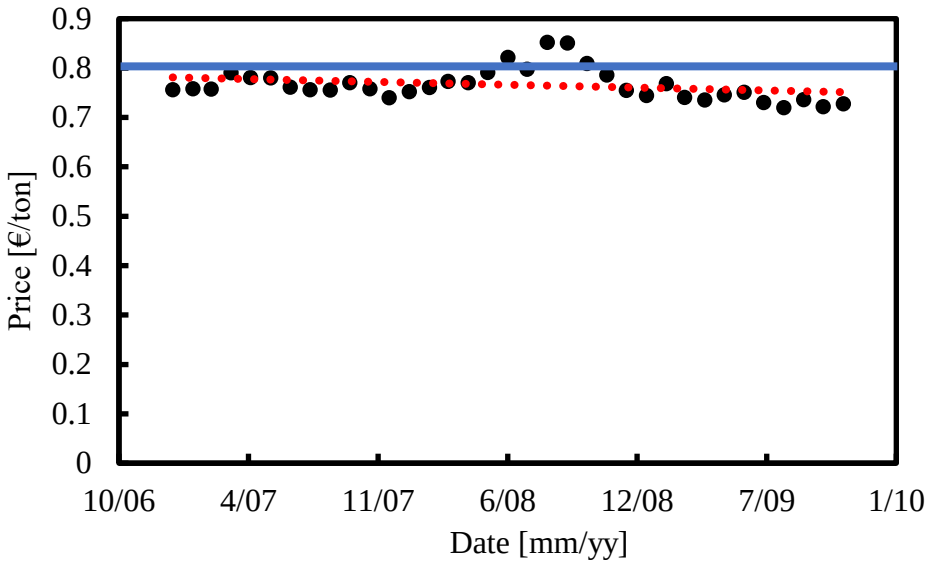

Figure 2.3. *Demineralised water price: the red points represent the linear regression, while the blue line shows the price chosen.*

Figure 2.3 shows the trend of the demineralised water price: it can be seen that it is stable, and therefore it is correct to select the average price: so the choice of 0.8 € / tons is appropriate (Intratec).

2.2 Economic analysis

This Section describes the mass and energy balances for each of the four CO_2 conversion processes, with the purpose of retrieving information that are needed to get all the economic data. In particular, through Section 2.2.1 the fixed capital investment (FCI [$]) of the DMC process is determined, while Section 2.2.2 aims both to check whether the kinetic of the PPP process is consistent with respect to literature (Langanke et al., 2014) and to calculate number of operators, whereas Section 2.2.3 determine both the quantity of NG utilised and the number of employs for MeOH process. Finally, in Section 2.2.4 will be shown how the sets, scalars, parameters and tables, which will be implemented in the model explained in the next Chapter, are calculated.

2.2.1 DMC

The reference process for the production of DMC is that described in the article by Souza et al. (2014): this article was chosen as it shows excellent performances from a technical and environmental point of view. Available data consist in net present value (NPV [€/y]), thermal and electrical consumption in kW, raw material prices, interest rate (i [%]), taxation (*t* [%]) , labour costs (C_{OL} [$/y]) and the relative distribution in terms of operating charge and plant overhead. From Souza et al. (2014) the data on the *FCI* [$] was missing, thus it has been estimated using a mass and energy balance.

The process flows are reported in Figure 2.4. The first reactor consumes 250 kmol/h of EO, with a conversion and selectivity equal to 100% in EC: to do this a 25% excess of CO_2 is utilised, which is recirculated in the first reactor.

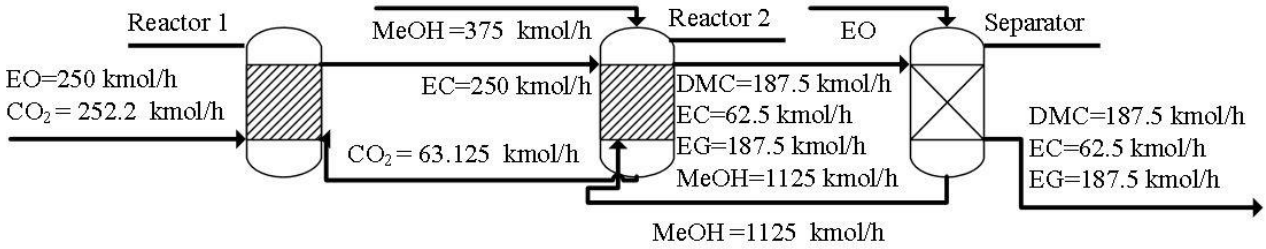

Figure 2.4. *Simplified diagram of DMC process.*

In the second reactor, EC is reacted with MeOH, which is present in a molar ratio of 6: 1. The reaction takes place with a conversion of 75% in DMC: the by-products are EG, EC. The main problem deriving from this process is the formation of an azeotrope between DMC and methanol, which involves the addition of a further unit operation: this is broken by the addition of ethylene glycol, which is subsequently separated and then completely recirculated with the consequence that it is not consumed during the whole process. Table 2.2 shows the differences between the calculated values and those reported in the article, with reference to the mass balance and the value of production.

Table 2.3. *Summary of the mass balance and the value of production, and the respective differences between the values reported in literature and the one calculated.*

	Production in the article [kton/y]	Calculated production [kton/y]	Value of production in the article [M$]	Calculated value of production [M€]
EO	-91.70	-97.32	-169.343	-111.922
MeOH	-93.30	-97.92	-65.607	-28.201
DMC	130.60	139.08	132.123	132.123
EG	94.10	95.81	153.294	74.731
EC	58.70	45.33	77.059	77.059
CO_2	-98.60	-90.66	-0.272	0

The value of the production was calculated on the basis of the prices of raw materials and utilities reported in section 2.1.2. As it can be noted in Table 2.2, the relative difference between the values of the production in the article and those calculated is always less than 5%, except for the EC for which it was considered that the reliable value was that of the article. Subsequently the labour cost was evaluated through the equation proposed by Turton et al. (2015):

$$\mathrm{LC} = \mathrm{C_{OL}} \cdot 4.5 \cdot \sqrt[2]{6.29 + 31.7 \cdot P^2 + 0.23 \cdot N_{np}} \tag{2.1}$$

In Eq. (2.1) $\mathrm{C_{OL}}$ [$ / y] represents the salary, $\mathrm{N_{np}}$the number of step of the process that does not use powders or solids as P does, while 4.5 expresses the number of operators necessary for each position. Since the process scheme is known from Souza et al. (2014), P was set equal to zero and it is possible to calculate a $\mathrm{N_{np}}$= 14. Thus it has been possible to calculate the direct manufacturing cost (DCM [€/y]), which is defined as follows:

$$\mathrm{DCM} = (\mathrm{RMC} + \mathrm{UTC} + \mathrm{LC})/0.7 \tag{2.2}$$

In Eq. (2.2), RMC [$/y] is the cost of raw materials, UTC [$/y] is the cost of utilities, while the term 0.7 is taken from Bezzo, (2016), and it accounts everything that cannot be calculated with the known data (i.e. the fixed charges and the general expenses) .
Now all the data for the calculation of the fixed capital investment (FCI [€]) are know:

$$\mathrm{CF} = \mathrm{NPV} \cdot \sum_{n=1}^{n=t} (1+i)^n \tag{2.3}$$

Through Eq. (2.3) it is possible to calculate the cash flow (CF [$ / y]), since both i [%] and the time period over which the NPV [€/y] is calculated (n [y]) are known. Therefore, it is possible to calculate FCI [$] according to the following relation:

$$\mathrm{FCI} = 10 \cdot (\mathrm{CF} - \mathrm{R} + \mathrm{DCM} + \mathrm{R} \cdot \mathrm{t} - \mathrm{DCM} \cdot \mathrm{t})/\mathrm{t} \tag{2.4}$$

In Eq. (2.4) 10 represents the number of years for the depreciation. The result is equal to 588.461 M $, which is a high value, but congruous with what shows qualitatively in Figure 4d of the reference article (Souza et al., 2014b).

2.2.2 PPP

Figure 2.5 represents the simplified process flow diagram from Fernández-Dacosta et al. (2017) for PPP production who study the case of a hydrogen production plant in which a unit that capture the 10% of CO_2 to produce PPP is incorporated .

Since R [€/y] and RMC [€/y] are already provided for the entire process, a mass balance is done with the kinetic data provided by Langanke et al. (2014) which are also utilised by Fernández-Dacosta et al. (2017). By setting the same input the overall mass balance is checked to see if it is the same: here the relative error is zero. However, the weight percentage of CO_2 that reacts in the reactor should be different with respect to the reference article since Langanke et al. (2014) report that at the pressure at which the current process is operated the weight percentage of CO_2 should be 1.2 instead of 20.

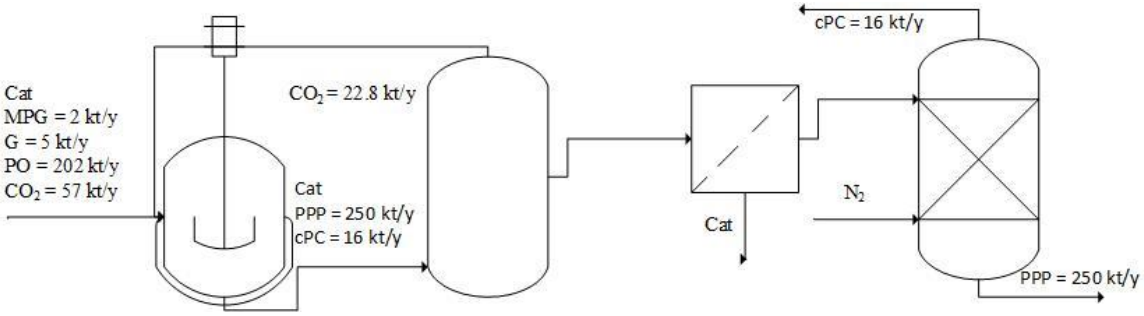

Figure 2.5 *Simplified diagram of PPP process with respect to the article of* Fernández-Dacosta et al. 2017).

Nevertheless, it has been decided to keep the value from Fernández-Dacosta et al. (2017), even if it may impact the FCI [€].

Compared to the reference article (Fernández-Dacosta et al., 2017), in order to guarantee the homogeneity of this master thesis, it has been decided to modify the number of operators required in the plant, for which this number is calculated through Eq. (2.1). Here P=3, since solids are utilised in three steps (in this particular case solids are the catalyst (Peeters et al., 2013)) the result of the number of operators is 77.

2.2.3 MeOH

Regarding the reforming processes that may be chosen, the most promising is the bi-reforming since the presence of steam reduces the coke phenomena, which is one of the main drawbacks of the dry reforming (Arora and Prasad, 2016; Wang et al., 1996). Wiesberg et al., (2016) provided the mass balance for this conversion process, which is schematised in Figure 2.6.

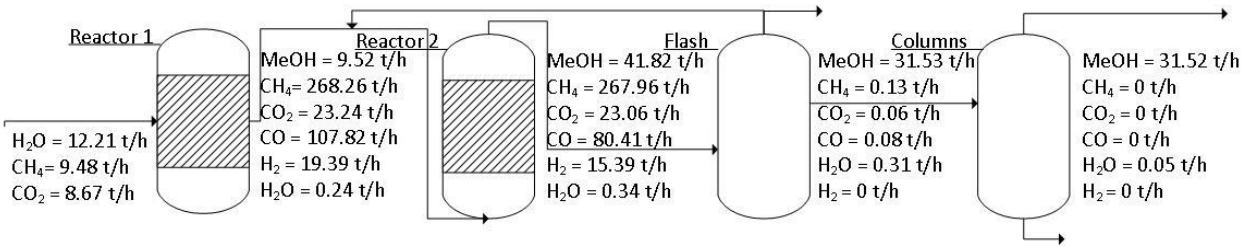

Figure 2.6. *Simplified diagram of the bi-reforming process.*

With respect to the calculations done by Wiesberg et al. (2016), the relative difference between the values of the production in the article and those calculated are always less than 2%. The amount of Methane (which is supplied as NG that, in the article, is formed by methane, ethane, propane and nitrogen, respectively at 75%, 15%, 7.5%, 2.5% in molar basis) is expressed in moles at the operating temperature and pressure of the process; however the price data are given in kWh, so it has been necessary to do a conversion. The molar flowrate of NG is converted into standard volumetric flowrate [m^3_{std}/h] through the Peng-Robinson Equation of State, which is an appropriate thermodynamic model for such system (Wankat, 2017), and then in kWh since NG has 0.095143 m^3_{std}/kWh (Turton et al., 2015).
For the same reason as the PPP process, given that the two reactors use a solid catalyst, the labour cost has been calculated thanks to Eq. (2.1), and the resulting number of workers is equal to 53.

2.2.4 Definition and calculation of the constants implemented in GAMS®

The three selected chemicals define the set *c* = {*DMC, PPP, MeOH*}, while, instead of using countries, the regions *g* are employed, which represent the same set (*g* = {*1,. .124*}), that will be detailed in Chapter 3.
The fundamental equations for the calculation of all the economic parameters in the usage model that will be presented in the next chapter are the following.

$$COM = 0.280 \cdot FCI + 2.73 \cdot LC + 1.23 \cdot (RMC + UTC) \quad (2.5)$$

Eq. (2.5) is from Turton et al. (2015) and calculates the COM [€ / y]. As it can be noticed it depends on four variables which are FCI [€], LC [€/y], RMC [€/y] and UTC [€/y] and each coefficient represent a short-cut so that this equation is capable to account also for more detailed direct cost (e.g. maintenance, patents,..), for fixed manufacturing cost and for general manufacturing expenses. The other fundamental relation is the following:

$$CF = (R - COM) \cdot (1 - t) + FCI/10 \quad (2.6)$$

Eq. (2.6) calculates the CF [€/y] according to Turton et al. (2015): the term FCI / 10 [€] represents the depreciation, since a ten years straight line approach is adopted, while t [%] is the corporate tax rate according to Table 2.1.
As for the parameters contained in Equations 2.5 and 2.6 the following apply:

- R [€] and FCI [€] are solely function of the chemical product, while t [%] is function of the country in which the chemical plant is built, therefore they will be parameters in GAMS ®;
- RMC [€], LC [€/y] and UTC [€/y] are function of the chemical product and of the country in which it is produced, so they will be tables in GAMS ® .

Here, the methodology to evaluate the parameters and tables will be explained.
The parameter of the corporate tax is determined according to Table 2.1, while the FCI [€] of each plant of chemical *c* calculated according to the reference articles (Fernández-Dacosta et al., 2017; Souza et al., 2014; Wiesberg et al., 2016) forms the parameter *Tscal*[€] (*Tscal* [M€] = {*DMC* 369.23, *PPP* 21, *MeOH* 111.2}), whereas rev_c [€/ton], that in GAMS is defined as the parameter of the revenues, is calculated in the following way:

$$\mathrm{rev_c} = \sum_p VP_{p,c} \cdot \dot{m_{p,c}} / (Tprod_c) \tag{2.7}$$

$VP_{p,c}$ [€/ton] and $\dot{m_{p,c}}$ [ton/y] are respectively the price of the raw materials chosen according to Section 2.1 and the mass flowrate of each product and by-product (*p*) related to chemical *c*, while $Tprod_c$ [ton/y] is the plant capacity according to the reference (Fernández-Dacosta et al., 2017; Souza et al., 2014; Wiesberg et al., 2016) ($Tprod_c$ [kton/y] = {*DMC* 130.6, *PPP* 250, *MeOH* 250}(Eq. 2.7). This way the parameter rev_c [€/ton], is uniquely function of the amount of chemical c that is produced.
The tables of raw material price ($\mathrm{raw}_{c,g}$ [€/ton]) , utility ($\mathrm{util}_{c,g}$ [€/ton]) and labour cost (lab [€/ton]) have been obtained through the following equations.

$$raw_{c,g} = \sum_f VM_{f,c,g} \cdot \dot{m_{f,c}} / (Tprod_c) \tag{2.8}$$

Eq. (2.8) calculates the table of raw material by multiplying the mass flowrate of the feedstock ($\dot{m_{f,c}}$ [ton/y]) by the price of the feedstock ($\mathrm{VM_{f,c,g}}$ [€/ton]) employed for each raw material utilised (*f*) related to chemical *c* in region *g*, according to Section 2.1,. So $\mathrm{raw}_{c,g}$ [€/ton] is function of the amount of chemical *c* that is produced and of the location of the plant.

$$\mathrm{util}_{c,g} = (STEAM_c \cdot \mathrm{CNG_g} + ELCONS_c \cdot \mathrm{CEL_g} + COOL_c \cdot \mathrm{CC})/ (\mathrm{Tprod_c}) \tag{2.9}$$

Through Eq. (2.9) the table of utility cost is calculated, where $STEAM_c$[ton/y], $ELCONS_c$ [kWh/y] and $COOL_c$ [ton/y] are respectively the amount of steam, electrical energy and cooling utility utilised to produce the chemical *c*, which multiply correspondingly $\mathrm{CNG_g}$ [€/ton] that is the cost for HP steam and $\mathrm{CEL_g}$ [€/kWh] that is the electricity cost, which are both function of region *g*, and CC [€/ton] that is the cooling utility cost and is set equal to 0.2 €/ton according to literature (Bezzo, 2016)).

$$\mathrm{util}_{c,g} = 4.5 \cdot \mathrm{N}_{OL} \cdot CL \tag{2.10}$$

Eq. (2.10) calculates the table of utility cost for each chemical c in each region g, by multiplying the labour cost (CL [€/y]), which is determined according to Table 2.1, by the number of operators per shift N_{OL}, which is calculated as follow according to Turton et al. (2015):

$$N_{OL} = \sqrt[2]{6.29 + 31.7 \cdot P^2 + 0.23 \cdot N_{np}} \tag{2.11}$$

In particular, it can be noticed that Eq. (2.11) is a part of Eq. (2.1) where each term inside the equation (P and N_{np}) is defined in the same manner.

2.3 Final remarks

This chapter deals with both the choice and the recovery of the data necessary for the development of the model described in the following chapter. In particular Table 2.3 shows the selected prices for raw materials, while Table 2.4 summarises the parameters that have been calculated and estimated through the energy and mass balances.

Table 2.4. *Summary on price selection of raw materials for each process .*

	Substance	Time lapse	Price selected	Rationale of choice	Source
DMC	EO	2007-2009, 2012-2013	1150 €/t	Cyclic	(Intratec, 2013a; ICIS, 2013)
	MeOH	2002-2017	288 €/t	Cyclic	(Methanex, 2017)
	MEG	2004-2011	812 €/t	Cyclic	(VIF, 2014)
	EC	2003, 2017	1700 €/t	Value of 2017	(IHS, 2003b; Molbase, 2017)
	DMC	2017	950 €/t	Value of 2017	Alibaba,2017
PPP	PG	2007, 2015-2017	1200 €/t	Cyclic	(Echemy technology, 2017; ICIS, 2007)
	G	1995-2010, 2015-2016	170 €/t	Decline trend	(Ciriminna et al., 2014; ICIS, 2016)
	PO	2007-2009, 2010-2011, 2013-2014	1700 €/t	Cyclic	(ICIS, 2014, 2011b; Intratec, 2013b)
	PPP	2010-2012, 2011-2014, 2016	1850 €/t	Cyclic	(ICIS, 2017, 2012b; Mintec, 2014)
MeOH	Demi-H_2O	2007-2009	1 €/t	Fixed	(Intratec.)

In particular Table 2.3 specifies also the time frame and the methodology with which the data were obtained, whereas in Table 2.4 are shown the cooling, heating and electrical energy consumption, the total number of operators and the total capital investment.

Table 2.5. *Summary on selected plants features.*

	Unit	DMC	PPP	MeOH
Total number of operators		14	77	53
Cooling energy	$ton_{coolin\ water}/ton_{chemical}$	0	1.69	36.21
Electrical energy	$kWh/ton_{chemical}$	40.35	10	394.77
Thermal energy	$Ton_{steam}/ton_{chemical}$	5.31	0.05	2.58
TCI	M€	369.23	21	111.2

Chapter 3

Mathematical features

Chapter 3 starts with the description of the MILP mathematical formulation that was retrieved from d'Amore and Bezzo (2017) (Section 3.1), then describes the details related to the inclusion of the CO_2 conversion-related stage (Section 3.2) and finally summarises the main features (Section 3.3. The model has been optimised by aim of GAMS® (General Algebraic Modelling System) software and then solved through CPLEX in around 10 hours on a 2.50 GHz computer with 12 GB RAM.

3.1 The CCS optimisation model

According to the current policies about climate (EU climate action, 2014), the European Commission has decided to reduce by 43% the amount of CO_2 emitted by fossil fuel power plants (i.e. those affected by the exchange of ETS) compared to the one issued in 2005. In agreement with this demand, the original model by d'Amore and Bezzo (2017) aims at minimising the total cost of a European SC for CO_2 CCS through a multi-echelon and spatially explicit MILP mathematical formulation, through which the objective is to optimise the following main variables:

- the size and location of CO_2 capture plants and the chosen capture technology;
- the size and location of CO_2 sequestration place, along with the number of injection wells;
- the size and typology of transport network between the chosen transport nodes;
- the amount of geological exploitation resulting from regional CO_2 sequestration;
- the economic performance of the entire system and, specifically, the costs that occur to install and set into motion the capture, transport and sequestration facilities.

The next subsection will describe the hypotheses and assumptions of the original formulation (Section 3.1.1), the mathematical features (Section 3.1.2) and the main results (Section 3.1.3) of this SC model.

3.1.1 Materials and method

To determine the objectives previously described, it is first necessary to determine the size and location of the CO_2 emission point sources: in relation to this the data referred to are those of Emission Database for Global Atmospheric Research (EDGAR) , as it provides information relative

to the place of emission(i.e. latitude and longitude) compared to other available sources (eg. Birol, (2008)).

This database considers 336 combustion plants producing more than 10^6 tons of CO_2, for a total of $1.375 \cdot 10^9$ tons of CO_2. This amount represents the 37% of the total CO_2 produced in EU and the 69% of that issued by the sectors affected by the ETS (i.e. cement clinkers, oil refineries, coke ovens, iron and steel plants, glass, lime, bricks, ceramics, pulp, paper and board).
These sources are shown in Figure (3.1) through a grid consisting of 124 cells, in which each cell represents a set of region g: this configuration allows both a correct description of the emission points and to keep the computational calculation at acceptable levels.

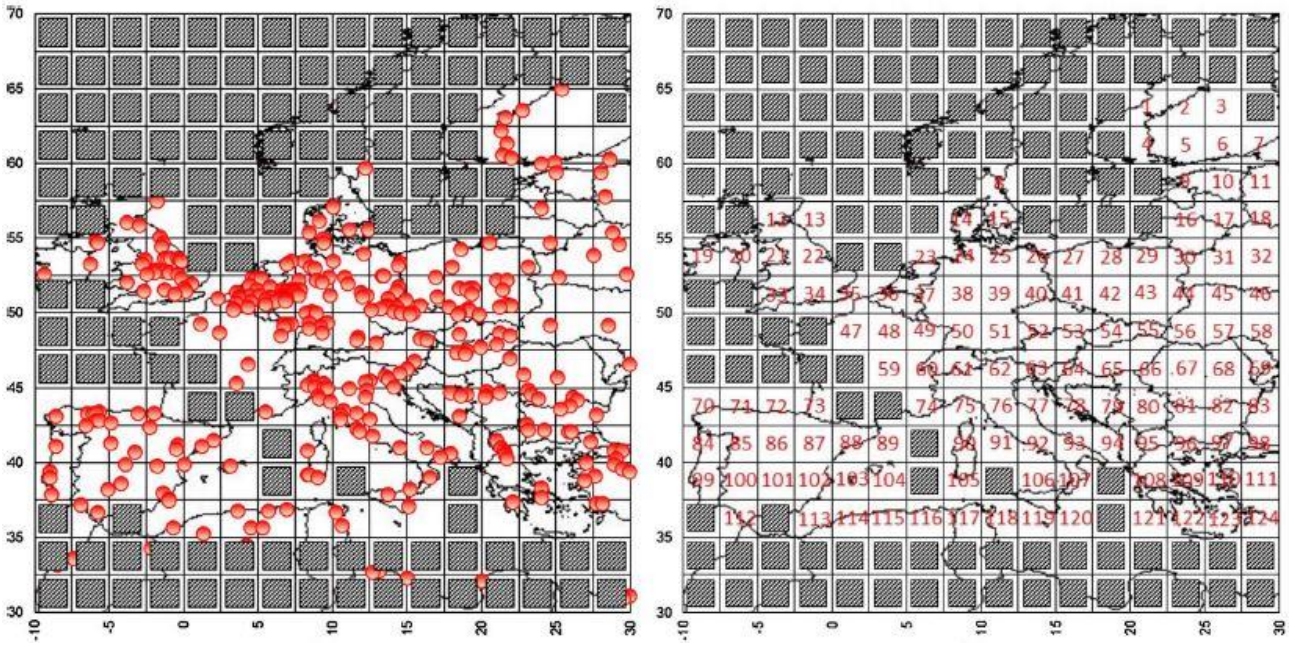

(a) *(b)*

Figure 3.1. *Spatially explicit representation of Europe. Red points stand for emission sources >10^6 of CO_2/year (a), and (b) cells enumeration (Source: (d'Amore and Bezzo, 2017)).*

From a quantitative point of view the matrix of distances ($LD_{g,g'}$,[km]) between a region g to a neighbouring region g' is calculated as follow:

$$LD_{g,g'} = cos^{-1} \cdot [\sin(lat^{g}) \cdot \sin(lat^{g'}) + \cos(lat^{g}) \cdot \cos(lat^{g'}) \cdot \cos(long^{g} - long^{g'})] \cdot R \quad (3.1)$$

In particular the table $LD_{g,g'}$,[km] is calculated taking into account the sphericity of the earth, where lat[km] and $long$ [km] are latitude and longitude, while R [km] is the average radius of the earth (Eq. 3.1).
However, this database does not consider the fuel used by these combustion plants: this aspect will be important to consider the capture technology. The only data available are of Eurostat (2016) which provide the percentage of energy produced for each nation from coal or natural gas (as they

are the only two types that constitute the major sources of CO_2 emissions), according to which are emitted respectively 1.04 and 0.383 kg of CO_2 per kWh. Therefore we proceed to the determination of the parameter $\gamma_{k,g}$ [$tons\ of\ CO_2^{coal/gas}/tons\ of\ CO_2^{tot}$], which provides the percentage of CO_2 generated from the two fuels for each country, for which there is one and only region g.

As anticipated, now, the capture techniques that are addressed in the model, are defined by the set *k*. Four types of technologies has been chosen due to their maturity and affordability based on the reference literature (Feron and Jansen, 1997; Herzog et al., 1991; Metz et al., 2005):

- $k = \{post_{coal}^{comb}\}$ represents the post-combustion capture of CO_2 by absorption from coal power plant;
- $k = \{post_{gas}^{comb}\}$ is characterised by the same technique as that previously defined, only for plants that utilise natural gas;
- $k = \{oxy_{coal}^{fuel}\}$ considers the capture of the combustion gases from coal plants, whose air has been previously cryogenically purified from nitrogen to reach an almost total concentration in oxygen (i.e. higher than 95%) so as to obtain an output of 85-90% of CO_2;
- $k = \{pre^{comb}\}$ represents the case in which the fuel is gasified to give syngas, from which the CO_2 is separated, to be subsequently burned (eventually the syngas instead of producing energy can be used to make chemicals).

The parameter of capture efficiency (η_k[%]) and of unitary capture cost (UCC_k [€/ton of CO_2]) for each technology *k* are shown in Table 3.1 according to the results reported by d'Amore and Bezzo (2017).

Table 3.6. *Data of capture efficiency ($\boldsymbol{\eta_k}$[%]) and of unitary capture cost ($\boldsymbol{UCC_k}$ [€/ton of CO_2]) from Metz et al.(2005) and Rubin et al. (2015)*

k	$post_{coal}^{comb}$	$post_{gas}^{comb}$	oxy_{coal}^{fuel}	pre^{comb}
η_k	0.87	0.88	0.92	0.86
UCC_k	33	54	36	25

It can be noticed that the highest capture efficiency is that of the oxy-fuel technology $k = (oxy_{coal}^{fuel})$, while the lowest one is for $k = \{pre^{comb}\}$. Instead, the highest cost applies to technology $k = \{post_{gas}^{comb}\}$ while the cheapest one is $k = \{pre^{comb}\}$.

Once the CO_2 has been captured, it is necessary to send it to geological storage. This can be transported in gaseous, liquid or solid form, through pipelines, tanks or ships. However, the transport of solid state CO_2 and/or tanks has not yet reached sufficient commercial maturity for both technical and economic reasons (Metz et al., 2005), and therefore has not been considered. The set l = $\{inshore\ pipeline, offshore\ pipeline, ship\}$ is therefore defined.

The first and second term of set *l* represent respectively the transport of inshore and offshore CO_2: in this case the CO_2 is compressed at pressures higher than 9.6 Mpa so that there is certainty, unless impurities (eg. nitrogen, oxygen ...), of being in the supercritical region. Since this phase has higher

density compared to the gas phase, on one hand it is 20% cheaper than the low pressure case (i.e. 4.8 Mpa), while on the other hand it is ready for inshore storage (Metz et al., 2005).

The third case ($l = \{ship\}$) is the transport by ship of CO_2 in the liquid state, which can be achieved in three ways: through low temperatures, high pressures or a middle way between the two. In general, for low-capacity carriers, high-pressure technology is preferred; otherwise, the other two types are preferred.

The transport cost varies in a non-linear way and it is inversely proportional to the amount of CO_2 transported due to the scaling factor: for this reason it is necessary to linearise the costs by discretising them. The technique consists in defining a set $p = \{1,..,7\}$ that represents seven possible capacities, apiece of which a value of the parameter Q_p [tons of CO_2/year] is linked to which corresponds a respective table of the unit cost of transport ($UTC_{p,l}$ [€/ton of CO_2/km]). Table 3.2 shows the values obtained from the discretisation (D'Amore and Bezzo, 2017)

Table 3.7. *Discretisation of transport unitary cost (UTCp,l [€/ton of CO2/km]) according to its capacity (Qp [tons of CO2/year]).*

p	Q_p	$UTC_{p,"inshore\ pipeline"}$	$UTC_{p,"offshore\ pipeline"}$	$UTC_{p,"ship"}$
	[Mtons of CO_2/year]	[€/ton of CO_2/km]	[€/ton of CO_2/km]	[€/ton of CO_2/km]
1	1	0.04009	0.07137	0.03215
2	5	0.01476	0.02215	0.03215
3	10	0.00959	0.01338	0.03215
4	15	0.00746	0.00997	0.03215
5	20	0.00624	0.00808	0.03215
6	25	0.00543	0.00687	0.03215
7	30	0.00485	0.00602	0.03215

As shown in Table 3.2, the mode of transport by ship varies linearly as function of capacity p, therefore the respective value has been set equal to the scalar f^{ship}[€/tons], which represents the angular coefficient obtained through linear regression. All data utilised to calculate transport costs are taken from Metz et al.(2005).

Finally, carbon dioxide can be only stored, being not yet implemented in the original model the utilisation option. According to d'Amore and Bezzo (2017) only onshore storage is considered as an option, since it has an estimated potential of 91 Gtons of CO_2, that is huge when compared with the offshore European sequestration potential (equal to 26 Gtons of CO_2 according to European Commission (2017)). The parameter $Stot^{max}$ [Gtons of CO_2] represents the inshore sequestration capacity in each region g.

3.1.2 Mathematical formulation

The objective function of the original model of d'Amore and Bezzo (2017) is defined in the following way:

$$obj = \min(TC) \tag{3.2}$$

Eq. (3.2) aims at the minimisation of the total cost (TC [€]) to install and operate the SC through the next relation:

$$TC = TCC + TTC + TSC \tag{3.3}$$

The variable TC [€] is obtained by the sum of the total cost of capture (TCC) [€], the total transport cost (TTC) [€] and the total sequestration cost (TSC) [€] (Eq. 3.3).
The value TCC [€] of Eq. (3.3) is given by the sum, for each region g, of the total capture cost:

$$TCC = \sum_g TCC_g \tag{3.4}$$

Where TCCg [€] is the variable of the total capture cost in each region g (Eq. 3.4), that is calculated as follows:

$$TCC_g = \sum_k UCC_k \cdot Ctot_{k,g}^{CO2} \tag{3.5}$$

In Eq. (3.5) it is summed over k the parameter UCC_k ([€/ton of CO_2]) with the net CO_2 captured in each region g by technology k, represented by the positive variable $Ctot_{k,g}^{CO2}$ [tons of CO_2], which is calculated as follow:

$$Ctot_{k,g}^{CO2} = \eta_k \cdot Ptot_{k,g}^{CO2} \tag{3.6}$$

Since each k technology has a precise efficiency defined by the parameter η_k [%], in connection with this a specific amount of carbon dioxide is lost, and therefore the positive variable $Ptot_{k,g}^{CO2}$ [tons CO_2] is the gross quantity of CO_2 captured with technology k in region g (Eq. 3.6).

$$Ptot_{k,g}^{CO2} \leq Pmax_g \cdot \gamma_{k,g} \tag{3.7}$$

Eq. (3.7) constrains $Ptot_{k,g}^{CO2}$ [tons CO_2] to be less than the total CO_2 emitted in each region g $Pmax_g$ [tons of CO_2] times the parameter $\gamma_{k,g}$ [%] that defines in each region g the percentage of coal or gas base power plant facility, and therefore the feasibility to build a capture facility with technology k.
Since it is desired to capture a specific amount of CO_2 according to EU climate action, it is added the next relation:

$$\sum_{k,g} Ctot_{k,g}^{CO2} = \alpha \cdot \sum_g Pmax_g \tag{3.8}$$

So in Eq. (3.8) it is inserted the parameter α [%] which is set in such a way as to respect the target of European Commission to capture 43% of the total CO_2 emitted from those sectors interested by ETS (EU climate action, 2014).
Then it is calculated the variable *TTC* [€] as the sum of three contributes:

$$TTC = TTC^{fsize} + TTC^{fdist} + TTC^{int} \tag{3.9}$$

- TTC^{fsize} [M€] describes the cost related to the shipment size and transport lenght;
- TTC^{fdist} [M€] defines the expense due to the length of the transport facility for ship only;
- TTC^{int} [M€] is the expenditure connected with the intra-grid network.

Each of these three variables (TTC^{fsize} [M€] , TTC^{fdist} [M€] , TTC^{int} [M€]) are calculated as follow:

$$TTC^{fsize} = \sum_{p,l} [UTC_{p,l} \cdot (\sum_{g,g'} Qtrans^{CO2}_{g,l,g'} \cdot LD_{g,g'})] \tag{3.10}$$

Through Eq. (3.10) it is calculated the positive variable TTC^{fsize} [€] by considering the discretised parameter of the unitary transport cost $UTC_{p,l}$ [€/ton of CO_2/km], which multiplies the total distance of both inshore and offshore pipelines. Similarly it is calculated TTC^{fdist} [€]:

$$TTC^{fdist} = \sum_{l} [f^{ship} \cdot (\sum_{g,g'} Qtrans^{CO2}_{g,l,g'} \cdot LD_{g,g'})] \qquad \forall\, l = \{ship\} \tag{3.11}$$

Where f^{ship} [€/ton of CO_2/km] multiplies the total distance travelled by ships (Eq. 3.11). Then the variable TTC^{int}[€] is defined by the next relation:

$$TTC^{int} = int^{cost} \cdot (\sum_{k,g} Ctot^{CO2}_{k,g} \cdot int^{dist}_{g}/2) \tag{3.12}$$

In Eq. (3.11) these two parameters *(1)* int^{cost} [€/ton of CO_2/km] and *(2)* int^{dist}_{g} [km] have the meaning of transport cost through *l* = {inshore pipeline} and the cell size of each region *g* since is considered only short-farness.
Nevertheless in order to determine the terms in Eq. (3.10) and in Eq. (3.11), it is necessary to estimate the variable $Qtrans^{CO2}_{g,l,g'}$, which depends on the discretised parameter of transport capacity Q_p[tons of CO_2] as function of $UTC_{p,l}$ [€/ton of CO_2/km], conforming to set *p*:

$$Qtrans^{CO2}_{g,l,g'} = \sum_{p} Q_p \cdot \lambda_{p,g,l,g'} \tag{3.13}$$

Eq. (3.13) is characterised by the binary decision variable $\lambda_{p,g,l,g'}$, which, according to Q_p, selects whether or not an amount *p* is transported from *g* through *l* to *g'*.
So two bounds are added:

$$\sum_k Ctot_{k,g}^{CO2} + \sum_{l,g'} Qtrans_{g',l,g}^{CO2} = Stot_g^{CO2} + \sum_{l,g'} Qtrans_{g,l,g'}^{CO2} \quad (3.14)$$

By Eq. (3.13) it is set the highest value for the infrastructure size, while through Eq. (3.14) it is represented a mass balance between the ingoing flows of CO_2 in each region g (left term), which is determined by the CO_2 that is captured in each region g ($Ctot_{k,g}^{CO2}$[tons CO_2]) and the CO_2 transported from region *g'* to region g across *l* ($Qtrans_{g',l,g}^{CO2}$[tons CO_2]), and the outgoing flows of CO_2 in each region g (right term), that is estimated through the total carbon sequestered ($Stot_g^{CO2}$[tons CO_2]) and the whole transferred CO_2 from region g' to g ($Qtrans_{g,l,g'}^{CO2}$[tons CO_2]) .
So in Eq. (3.14) $Stot_g^{CO2}$ is determined in such a way as it must be lower than $Stot_g$ [tons of CO_2]:

$$Stot_g^{CO2} \leq Stot_g \quad (3.15)$$

Where $Stot_g$ [tons CO_2] is the upper bound of the storage capacity in each region g (Eq. 3.15).
Thus, it is possible to calculate the variable TSC[€] by solving the two next equations:

$$N_g^{seq} = Stot_g^{CO2} / Stot^{max} \quad (3.16)$$

Through Eq. (3.16), N_g^{seq} [tons of CO_2] estimates the total of injection wells in each region g according to the relative utmost capacity, which is necessary to calculate TSC [€]:

$$TSC = \sum_g [(CCR^{seq} \cdot OM^{seq}) \cdot (m_1 \cdot d_g + m_2) * N_g^{seq}] \quad (3.17)$$

In Eq. (3.17) CCR^{seq}[%], OM^{seq} [%], m_1 [€/km], d_g[km] and m_2[€] are all parameters (determined in agreement with published literature (Hasan et al., 2015b; Kwak and Kim, 2017b; OGDEN, 2003)) which describe the capital charge rate, the cost due to operation and maintenance, and the expense due to construction and injection of CO_2.

3.1.3 Results

The model of d'Amore and Bezzo (2017) is optimised through the solver CPLEX, by setting the parameter α equal to 43%.
The total cost of the entire infrastructure, which considers the capture as well as the transport and the sequestration, is equal to 20.044 B€.
S_g^{ratio} [%] and L^{trans} [km] are calculated through the following relations:

$$S^{ratio} = (\sum_g Stot_g^{CO2} / Stot_g) * 100 \quad (3.18)$$

By Eq. (3.18) the value is calculated by diving the tons of CO_2 stored ($\sum_g Stot_g^{CO2}$), over the whole capacity ($\sum_g Stot_g$): this provides the ratio of the exploitation of the inshore storage.

$$L_{pipe}^{trans} = \sum_{p,g,g'} \lambda_{p,g,l,g'} \cdot LD_{g,g'} \tag{3.19}$$

Through Eq. (3.19) the total pipe length is determined multiplicand the binary variable $\lambda_{p,g,l,g'}$ which provides the information on which decision is taken regarding whether to build or not a pipe between a region g and g', times the distance between the two regions ($LD_{g,g'}$).

Considering the actual scenario, it is possible to notice that the saturation of the geological inshore storage will occur in about 144 years (since S_g^{ratio}= 0.695%) , while the total pipe length L_{pipe}^{trans} [km] is equal to 4409.64 km.

The final SC configuration is reported in Figure 3.2.

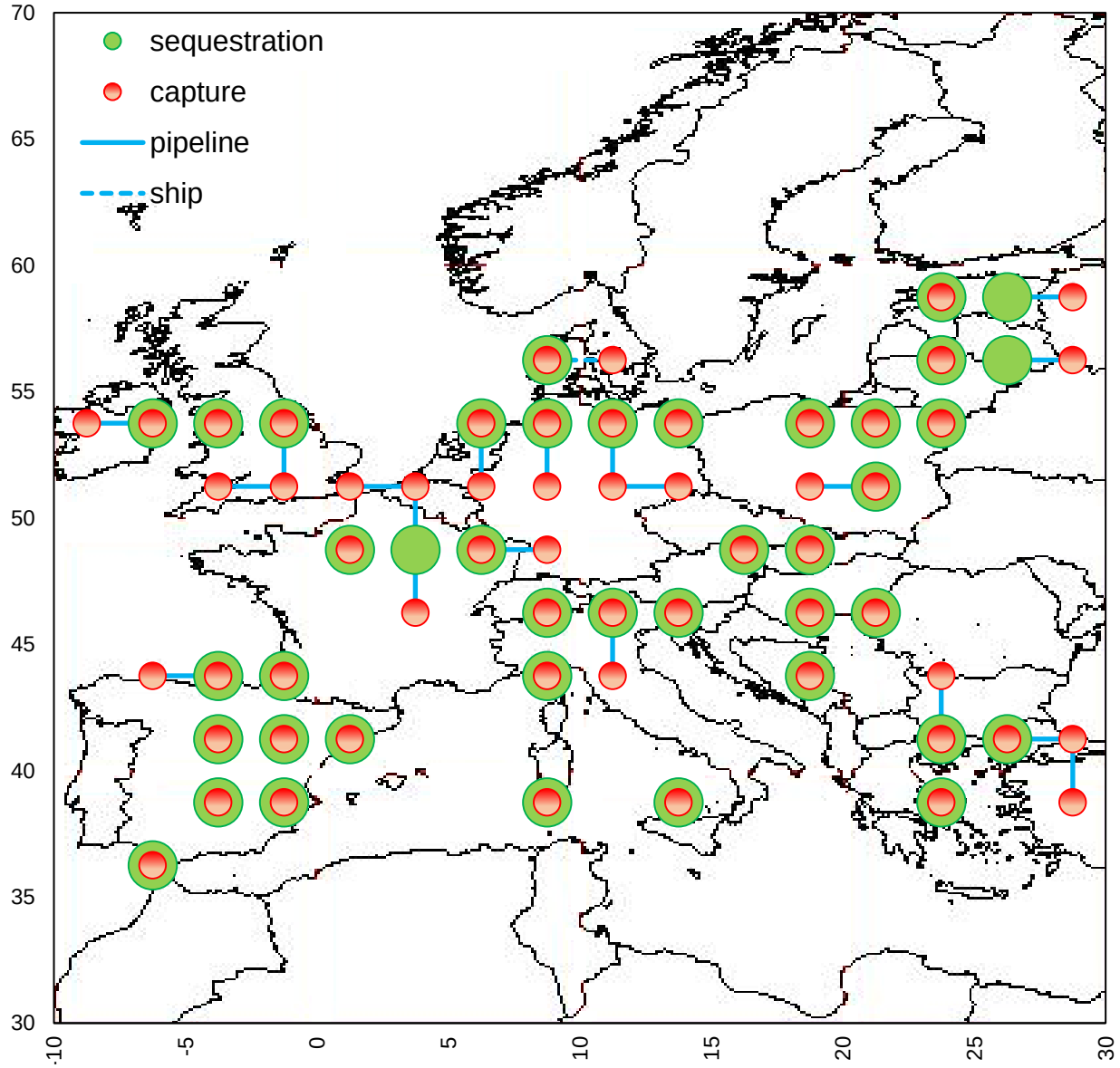

Figure 3.1. *SC final configuration for α =43%.*

3.2 Non-linear optimisation model

The aim of the usage model is to investigate whether CO_2 conversion could lead to a reduction in the total cost, in the exploitation of the geological storage and in the infrastructure related to the transport. First Section 3.2.1 shows the new rigorous CCU non-linear model that will be named USAGE^{MINLP}. Subsequently, this non-linear formulation gets linearised in Section 3.2.2 . Afterwards Section 3.2.3 demonstrates the goodness of the linearization. Then the equations related to chemical conversion and utilisation of CO_2 will be described in Section 3.2.4. Finally the mathematical formulation of the scenario where the plant size is kept constant is illustrated in Section 3.2.5, as well as the scenario where also DMC is allowed to be produced (Section 3.2.6).

3.2.1 USAGE^{MINLP} model

In order to implement the conversion of CO_2 in GAMS® it is necessary to define a set c = *{PPP, MeOH}* of the three chemicals that were described in Chapter 2 as feasible conversion alternatives.
In the USAGE^{MINLP} model the objective function is defines as follow:

$$obj = \max(profit) \tag{3.20}$$

Therefore the aim is to maximise the total *profit* [€], which is defined as follow:

$$profit = \sum_{c,g} CF_{c,g} \tag{3.21}$$

Where $CF_{c,g}$ [€] is the positive variable of the cash flow generated by each chemical c in region g, and is defined as:

$$CF_{c,g} = \left(R_{c,g} - COM_{c,g}\right) \cdot \left(1 - tax_g\right) + d_{c,g} \tag{3.22}$$

The revenue ($R_{c,g}$ [€]) is represented by a positive variable and it is calculated considering the selling of both the product and by-product for each produced chemical c in region g, as it was described in Chapter 2. On the other hand, tax_g [%] is a parameter given by the corporate tax in each region g (KPMG, 2018), while $d_{c,g}$ [€] is the positive variable that describe the depreciation of chemical c in region g. Then the positive variable $COM_{c,g}$ [€] describes the manufacturing cost (Eq. 3.22).
The revenue $R_{c,g}$ of chemical c in region g is given by:

$$R_{c,g} = \text{rev}_{c,g} \cdot uchem_{c,g} \tag{3.23}$$

Where $uchem_{c,g}$ [tons of c] is the positive variable that represents the quantity of chemical c that is produced in region g, which is than multiplied by the table of revenues $rev_{c,g}$ [€/tons] in such a way to provide the revenue $R_{c,g}$ [€] (Eq.3.23).
The positive variable $d_{c,g}$ [€] is determined as follows:

$$d_{c,g} = 0.1 * FCI_{c,g} \tag{3.24}$$

In Eq. (3.24) the depreciation ($d_{c,g}$ [€]) is calculated as 10% of the fixed capital investment ($FCI_{c,g}$ [€]) that is estimated as next:

$$FCI_{c,g} = \left(\frac{uchem_{c,g}}{T\mathrm{prod}_c}\right)^{0.6} \cdot Tscal_c \tag{3.25}$$

$FCI_{c,g}$ [€] is computed according to Sinnot and Towler (2009) through the six tenth rule (Eq.3.25). This allows to estimate the fixed capital investment ($FCI_{c,g}$ [€]) by raising to the power of 0.6 the positive variable $uchem_{c,g}$ [tons of c] which is divided by the parameter of productivity $Tprod_c$ [tons of c] referring to the plant capacity (Fernández-Dacosta et al., 2017; Wiesberg et al., 2016) and then multiplied by the parameter of the fixed capital investment $Tscal_c$ [€] previously calculated in Chapter 2.
Although there are more precise and complex methods (eg. factorial methods, Bare module cost,..), due to the lack of data this technique has been considered the best.
No location factor has been added since, as reported by Bridgewater (1979), all the possible plants of each chemical c in region g are always closer to 1000 miles from the closer industrial centre (hypothesised conservatively as a refinery) as in it shown in Fig 3.2, where each segment in abscissa and in ordinate has a length of between 246-448 km.
Then the positive variable of manufacturing cost ($COM_{c,g}$ [€]) is estimated according to Turton et al. (2015):

$$COM_{c,g} = uchem_{c,g} \cdot \left[acom \cdot \left(raw_{c,g} + util_{c,g}\right)\right] + bcom \cdot FCI_{c,g} + ccom \cdot lab_{c,g} \cdot delta_{c,g} \tag{3.26}$$

In Eq. (3.26) the tables of raw materials ($raw_{c,g}$ [€/tons of *c*]) and utilities ($util_{c,g}$ [€/tons of *c*]) cost for each chemical *c* in region *g* are multiplied by the scalar *acom* = {1.23}, as well the positive variable of the fixed capital investment ($FCI_{c,g}$ [€]) is multiplied the scalar *bcom* = {0.28}, and eventually the table of labour cost ($lab_{c,g}$[€]) is again multiplied by a scalar, that is *ccom* = {2.73}, and by the binary variable $delta_{c,g}$ that is estimated as follow:

$$uchem \leq upb_{c,g} \cdot delta_{c,g} \tag{3.27}$$

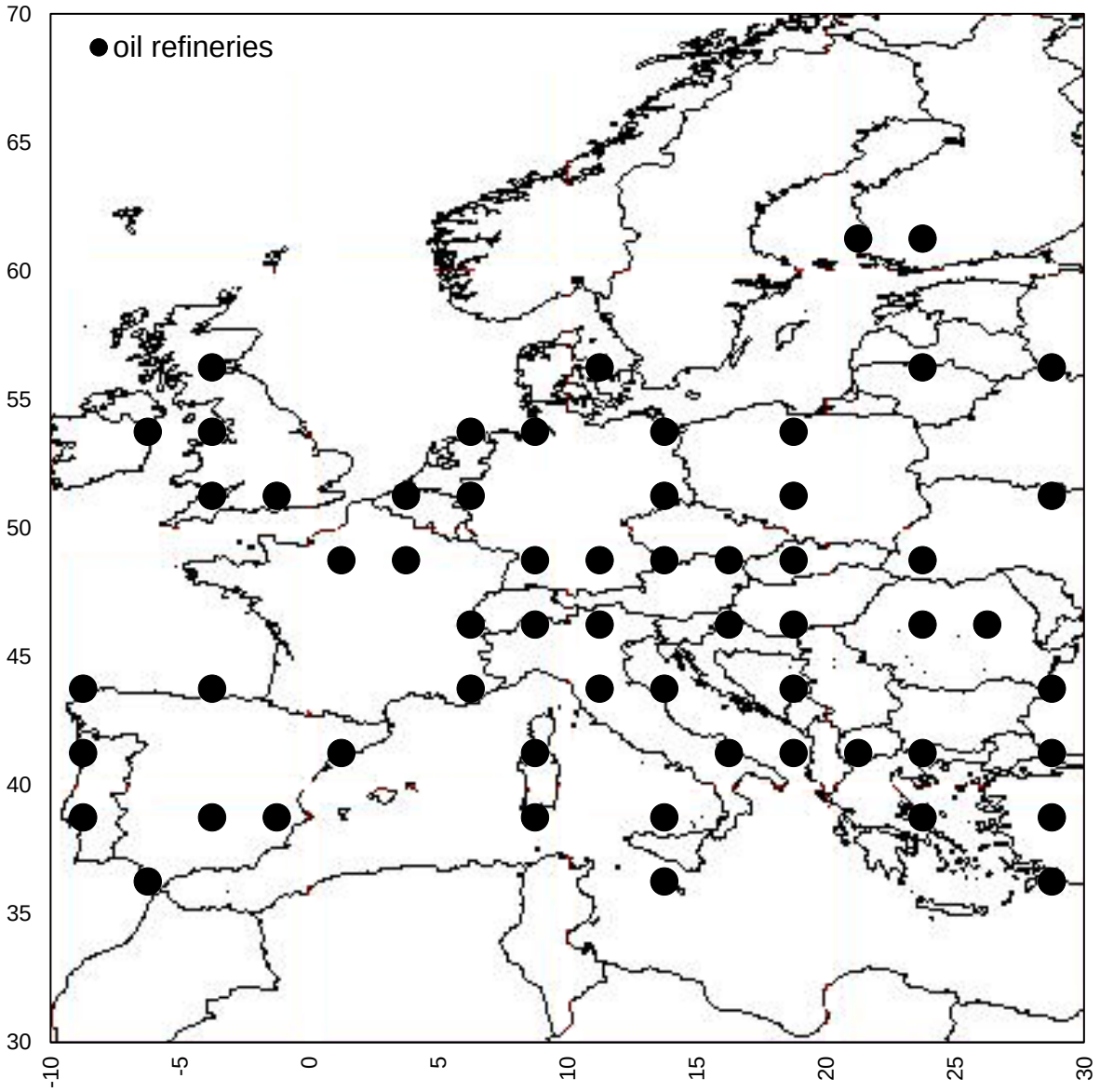

Figure 3.2. Refineries location in Europe according to "List of oil refineries" (2018).

In fact if productivity ($uchem_{c,g}$ [tons of c]) falls to a null value, even the manufacturing cost ($COM_{c,g}$ [€]) should go to zero: however, without the presence of the binary variable $delta_{c,g}$ this does not occur and therefore Eq. (3.26) would lead the objective function to wrong results. To model this logical restriction, two steps are necessary.

First through Eq. (3.27) the productivity $uchem_{c,g}$ [tons of *c*] is bounded by $upb_{c,g}$ [tons *c*] that is the table made by the productivity upper bound for each chemical c in region g, defined in such a way as it is equal to the current European demand for the chemical *c* (Covestro, 2017; IHS, 2016). Then $uchem$ [tons of *c*] is further bounded through the following relation:

$$\sum_g uchem_{c,g} \leq maxp_c \tag{3.28}$$

In Eq. (3.28) the parameter $maxp_c$ ={*PPP* 2.4, *MeOH* 12 }[tons *c*] defines the demand and it is characterised in the same manner as $upb_{c,g}$[tons *c*] (Covestro, 2017; Alvarado, 2016).
Through Eq. (3.27, 3.28) the binary variable $delta_{c,g}$ assumes the value 1 if the logical expression is verified, that is if the productivity ($uchem$ [tons of *c*]) is between 0 and $upb_{c,g}$ [tons *c*]: otherwise the positive variable $uchem$ [tons of *c*] becomes zero and therefore Eq. (3.26) becomes zero if it is not chosen to build a plant in a certain region *g* for a chemical *c*.
After that it is done the simulation of the non-linear model in GAMS®. In order to justify the goodness of the results, three global solvers were used: BARON, ANTIGONE and LINDOGLOBAL.

3.2.2 Linearisation of the USAGE^{MINLP} optimisation model

The USAGE^{MINLP} model has to be implemented in the original CCS model described in Section 3.1 and retrieved from d'Amore and Bezzo (2017), therefore it must be linear to be solved by aim of CPLEX solver. The model could in fact be formulated in MINLP mode but it would have the disadvantage of not providing proven global solutions with certainty (Sioshansi and Conejo, 2017).
The reason of non-linearity is due to the scaling factor of Eq. (3.25): therefore it has been decided to analyse how the fixed capital investment ($FCI_{c,g}$[€]) varies as function of the productivity ($uchem_{c,g}$[tons of c]) for each chemical *c* in the range of productivity of our interest (i.e. between lob_c and $maxp_c$) .
So it has been necessary to set a lower bound to the productivity $uchem_{c,g}$ [tons of c] through the parameter lob_c = {*PPP* 0.1, *MeOH* 0.2}[Mtons of *c*] according to standard size of plants that were retrieved from the literature (Haldor Topsoe, 2008; Utech, 2017) and which define the lower bound for productivity. This has allowed to build the curve by placing on the abscissa $uchem_{c,g}$ [tons of *c*] and on the ordinate the capital investment cost ($FCI_{c,g}$[€]) calculated according to Eq. (3.25), and thus to obtain the following equation:

$$FCI_{c,g} = uchem_{c,g} \cdot FCIangular_c + FCIquote_c \cdot delta_{c,g} \quad (3.29)$$

In Eq. (3.29) the parameters $FCIangular_c$= { *PPP* 37, *MeOH* 80 } [€/tons of *c*] and $FCIquote_c$ = {*PPP* 21, *MeOH* 229} [M€] are respectively the angular coefficient and the quote of the straight lines shown in Figures 3.4 and they represent the results of the linearization of Figures 3.4.
It is important to remember that in the non-linear model $uchem_{c,g}$ [tons of *c*] was a positive variable, whereas here it has been modelled as a semi-continuous variable: on one hand, in order to respect the lower bound of productivity, the parameter $FCIquote_c$ [M€] is multiplied by the binary variable $delta_{c,g}$ (defined as in Eq. (3.27, 3.28)). On the other hand, if the plant of chemical *c* is not built in region *g*, then $FCI_{c,g}$ [€] can assume a null value.

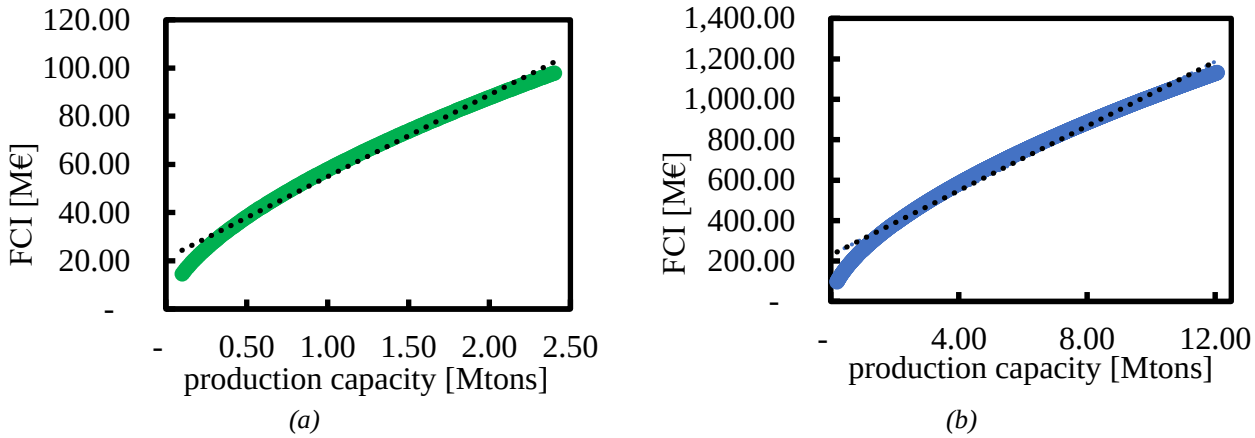

Figure 3.4. *Linearization of fixed capital investment for PPP (a) and MeOH (b) plants.*

Now the non-linearity has been linearised, so it is possible to proceed with the simulation through the solver CPLEX: this model will be named USAGE^{MILP}

3.3.3 Validation of the USAGE^{MILP} model

Here are shown the solutions of the objective function in order to prove the goodness of the linearization, and in particular these results

The USAGE^{MINLP} model has been solved using three solvers that use different resolutive approaches, since an optimal global solution is not guaranteed in the nonlinear field (Kallrath, 2012). Table 4.1 compares the result of the objective function ($profit$ [€]), the relative gap and the computational time among the chosen solvers. As a results, both BARON, ANTIGONE and LINDOGLOBAL have the same value of final $profit$ [€] and for the optimality gap (it is here chosen not to set a value for the optimality gap, since the optimisation is performed in low computational time and a global optimum is always easily reached).

Table 3.3. *Comparison of the optimisation between linear and non-linear solvers.*

Solver	*profit* [B€]	Optimality gap	No. equations	No. variables	Execution time [s]
CPLEX	1.006	0	2,857	3,846	0.920
BARON	1.016	0	2,485	3,102	2.462
ANTIGONE	1.016	0	2,485	3,102	2.917
LINDOGLOBAL	1.016	0	2,485	3,102	3602.557

On the other hand, the objective function ($profit$ [€]) present a difference of 10 M€ between the USAGE^{MILP} and the USAGE^{MINLP} models, which in relative terms is equivalent to a 0.98 % difference. According to this results, the linearization can be considered satisfactory.

It is observed that after the linearization of the USAGE^{MINLP} model, shown in Chapter 3, the number of equations and variables of the USAGE^{MILP} model increase. However, this does not correspond to a growth in computational time that is about 3 times lower than the one used by the fastest NLP solver, because inherently the resolution of a non-linear problem requires more time with respect to a linear one (Kallrath, 2012), and also since CPLEX is the most performing solver on the market in the mixed integer and linear field (Meindl and Templ, 2012). Finally, the huge difference between ANTIGONE and LINDOGLOBAL, in the time needed to find the optimal solution, is generated by the different methodologies of solving the problem. So, now it will be explained shortly and schematically how these global solvers work:

- BARON computes global optima of MINLPs problem, by utilising three combined techniques that are the constraint propagation and interval analysis, integrated branch and bound, and a duality approach in a problem reduction framework. In this case it employs CPLEX for solving MILP and MINOS for NLP problems;
- LINDOGLOBAL adopts a combination of three methodologies based on the linearization of certain functions (i.e. max(), abs()..), on researching several distinct starting point such that it is easier to find a good global optimum (i.e. multi-start), and on a general relax and branch for non-linear functions. This utilises its own library of solvers;
- ANTIGONE, whereas, solves the MINLP nonconvex model through three procedures, that are first a reformulation of the model input, then a research of special mathematical structures, and finally find feasible solution through a branch and cut global approach. It uses CPLEX for MILP and CONOPT for NLP problems.

In fact, besides the mathematical technique, another reason why these three global solvers have been chosen is because they employ different sub-solvers.

3.2.4 CCUS optimisation model

With respect to the original model of d'Amore and Bezzo (2017), three equations (Eq. (3.3, 3.8, 3.14)) have been here modified in order to insert the part related to the utilisation:

$$TC = TCC + TTC + TSC - profit \tag{3.30}$$

In Eq. (3.30) it is added the variable $profit$ ([€]) in order to take into account the earnings from CO_2 conversion. Then the capture constraint is changed as follow in order to consider the CO_2 reduction due to utilisation:

$$\sum_{k,g} Ctot_{k,g}^{CO2} + Unet = \alpha \cdot \sum_{g} Pmax_g \tag{3.31}$$

Where $Unet$ [tons of CO_2] is the net amount of CO_2 that has been converted (Eq. 3.31) and it is determined by the next equation:

$$Unet = \sum_{c,g} uchem_{c,g} \cdot nred_c^{CO2} \tag{3.32}$$

The parameter $nred_c^{CO2}$[tons of CO_2/tons of *c*] represents the net reduction of CO_2 due to its chemical conversion according to literature (Roh et al., 2016b; von der Assen and Bardow, 2014b), such that the positive variable $Unet$ [tons of CO_2] represents the whole amount of CO_2 reduction only generated by usage (Eq. 3.32).
Afterward the mass balance of the original model (Eq. 3.14) is changed as follow:

$$\sum_k Ctot_{k,g}^{CO2} + \sum_{l,g'} Qtrans_{g',l,g}^{CO2} = Stot_g^{CO2} + (\sum_{l,g'} Qtrans_{g,l,g'}^{CO2}) + U_g \tag{3.33}$$

With respect to Eq. (3.14), Eq. (3.33) has one more term, that is the positive variable U_g [tons of CO_2] which has been calculated through the following equation:

$$U_g = \sum_c uchem_{c,g} \cdot react_c^{CO2} \tag{3.34}$$

In Eq. (3.34) the parameter $react_c^{CO2}$[tons of CO_2/tons of *c*] is defined as the amount of CO_2 converted into chemical *c*, over the amount of chemical *c* that has been produced. In this way it is possible to define the mass balance of CO_2 between origin region *g* and destination *g'*. The flowrate of CO_2 that is converted in each region g (U_g [tons of CO_2]) along with the amount that is sequestered ($Stot_g^{CO2}$[tons of CO_2]) and the quantity transported from g to g'($\sum_{l,g'} Qtrans_{g,l,g'}^{CO2}$ [tons of CO_2]), is the same of the total CO_2 captured in g ($\sum_k Ctot_{k,g}^{CO2}$ [tons of CO_2]) and possibly transported from *g'* to g ($\sum_{l,g} Qtrans_{g,l,g'}^{CO2}$ [tons of CO_2]) (Eq. 3.32).
Afterwards the positive variable Net^{CO2} [%] defines the net quantity of chemically sequestrated CO_2 over the whole amount emitted, which is defined as follow:

$$Net^{CO2} = U_{net} / \sum_g Pmax_g \tag{3.35}$$

In Eq. (3.35) the net flowrate of utilised CO_2 (U_{net} [tons of CO_2]) is divided by the parameter that stands for the overall CO_2 emitted ($\sum_g Pmax_g$[tons of CO_2]).

3.2.5 CCUS^{FCI} model

Here it is described a different implementation of the CCUS model aimed at simulating a different scenario.
In particular, instead of considering the possibility that the size of the plant may vary within the ranges defined above, it was decided to consider the plant capacity constant and equal to that of the reference articles (Fernández-Dacosta et al., 2017; Wiesberg et al., 2016).
Firstly, a new variable ($Ichem$ [adim]) is added through the following relation:

$$Ichem_{c,g} = uchem_{c,g}/Tprod_c \tag{3.36}$$

$Ichem$ [adim] is a positive integer variable that defines the number of chemical plants c that are built in the several regions g, which is calculated by multiplying the parameter that expresses the amount of chemical product c produced ($Tprod_c$[tons of c]) times the variable $uchem$ [tons of c], which is defined in the same way as in the USAGE^{MILP} model (Eq. 3.36)
Then also Eq. (3.29) is different:

$$FCI_{c,g} = Ichem_{c,g} \cdot Tscal_c \tag{3.37}$$

Thanks to the fact that the scaling factor is not considered, Eq. (3.37) does not present non-linearity: in particular, the parameter $Tscal$ [€] represents the fixed capital cost for the reference plant size previously calculated in Chapter 2.
Eq. (3.26) has also changed:

$$COM_{c,g} = uchem_{c,g} \cdot Tprod_c \cdot \left[acom \cdot \left(raw_{c,g} + util_{c,g}\right)\right] + bcom \cdot FCI_{c,g} + ccom \cdot lab_{c,g} \cdot Ichem_{c,g} \tag{3.38}$$

Compared to Eq. (3.26), Eq.(3.38) has no longer any needs to use binary variables ($delta_{c,g}$): the labor cost table ($lab_{c,g}$[€]) is multiplied by the number of plants ($Ichem_{c,g}$[adim]), which may take any positive value including zero.
Other equations of the USAGE^{MILP} model have not been modified except for Eq. (3.27): this equation is in fact no longer necessary because of the binary variable $delta_{c,g}$ is no longer utilised. This model will be named USAGE^{MIP}, which is then implemented in the CCUS model in order to provide the CCUS^{FCI} scenario.

3.2.6 CCUS^{DMC} model

This section shows the mathematical features of the CCUS^{DMC} scenario, which considers that also DMC can be produced according to the hypothesis made on Chapter 1.

Conceptually the model is the same compared with the CCUS model, except that c = {*DMC, PPP, MeOH*}. Therefore, again, Eq. (3.25) has to be linearised following the same rationale as in Section 3.2.2. By setting the lower bound of productivity equal to 50 ktons/y (Tremblay, 2012) and the upper bound equal to the potential European demand (i.e. 1.4 Mtons/y), Figure 3.5 shows the linearization of the fixed capital investment of DMC.

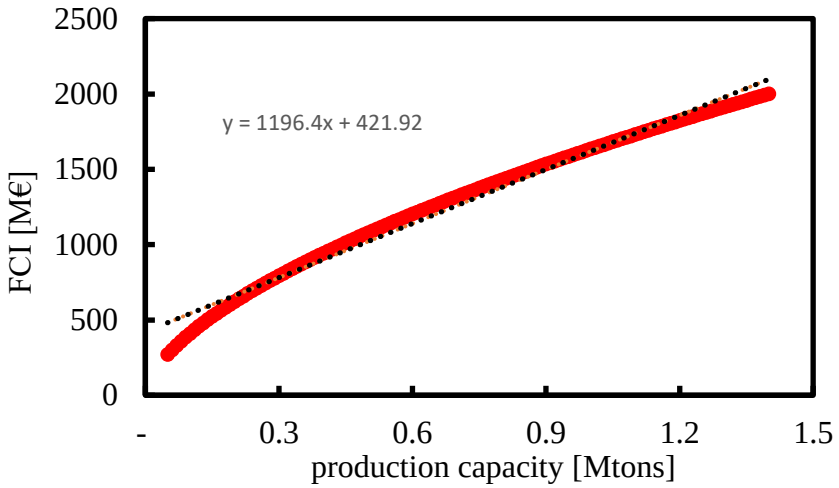

Figure 3.5. *Linearization of fixed capital investment for DMC plants.*

So, In Eq. (3.29) the parameters $FCIangular_c$ [€/tons of c] $FCIquote_c$ [€/tons of c] become respectively equal to {*DMC* 1196, *PPP* 36.232, *MeOH* 79.792 } and {*PPP* 19.156, *MeOH* 229.02 } [M€].

Then, the comparison between the solution of the linear and the nonlinear model has to be done: Table 3.4 shows that the linearization generates a relative error equal to 6%, which is larger than the one obtained for the USAGE^{MILP}, but still acceptable.

Table 3.4. *Comparison of the optimisation between linear and nonlinear solvers, when DMC is allowed to be produced*

Solver	*profit* [B€]	Optimality gap	No. equations	No. variables	Execution time [s]
CPLEX	1.555	0	2,857	3,846	0.557
BARON	1.658	0	2,485	3,102	2.349
ANTIGONE	1.658	0	2,485	3,102	2.853
LINDOGLOBAL	1.658	0	2,485	3,102	3597.429

3.3 Final remarks

In this chapter the model developed in this Thesis has been described. In particular, it has begun by describing the original model that does not contemplate the utilisation, which has been then implemented through three steps: first it has been described the USAGE^{MINLP} model, after that the linearization has been carried out which has been justified thanks to the small difference between the results of the two models, and finally the utilisation has been integrated into the original CCS model giving rise to the CCUS model, which network is schematically shown in Figure 3.6.

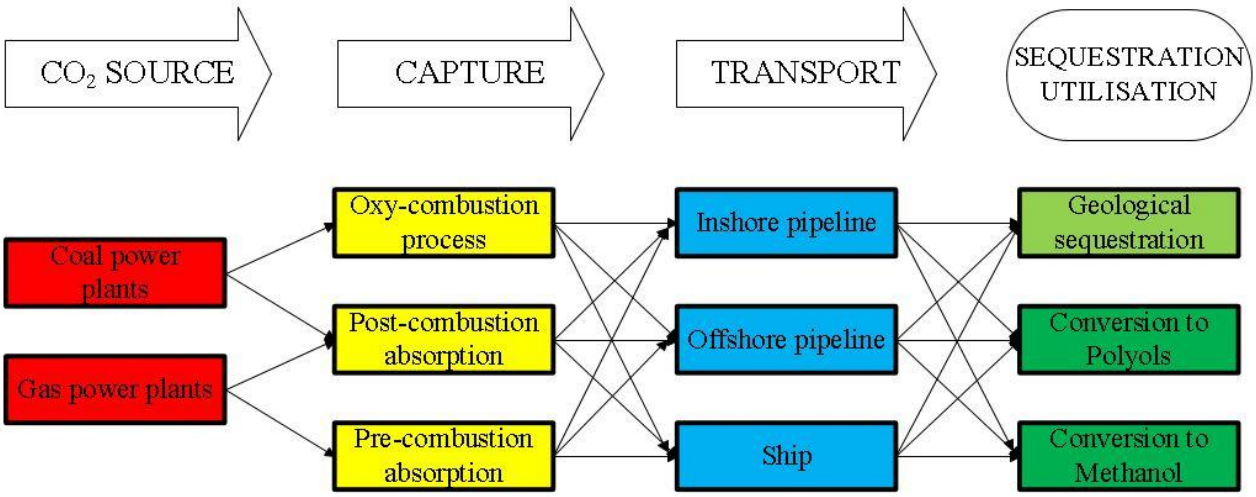

Figure 3.6. *CCUS SC network, showing the CO_2 flow direction*

It is a single-objective MILP model aiming at the total cost minimisation of a European SC by determining the optimal configuration in terms of technology for CO_2 capture, transport, sequestration and conversion, represented in a spatially explicit grid.

Besides the results of the base case, in the next Chapter two scenarios, which aim to describe on one hand the current situation regarding the storage potential, and on the other a possible limitation due to the CO_2 chemical conversion, will be considered.

Chapter 4

Results and sensitivity analysis

Chapter 4 shows the results obtained by optimising the model described in Chapter 3 by aim of the solver CPLEX for MILP mathematical frameworks. First the solutions of the objective function are compared with those from the original model of d'Amore and Bezzo (2017) (Section 4.1). Then, a sensitivity analysis is performed on the scalar α , which represents the minimum European carbon reduction target, considering both: (*i*) the case in which the countries that currently do not allow inshore exploitation are excluded from the storage stage, (*ii*) the case in which the plant size is kept constant in reference to those reported in the scientific literature (Section 4.2.). Section 4.3 summarises with some final remarks.

4.1 Results of the optimisation

The economic results and the SC configurations will be here presented, both as regards the differences with respect to the original CCS model (section 4.1.1) and for what concerns the reasons why a specific region *g* is chosen rather than another for the construction of plants of chemical *c* (section 4.1.2).

4.1.1 Final SC configuration

The implementation of the original CCS model with the USAGE^{MILP} involves an almost zero increase in both equation and variables. In computational terms, this should mean that the time spent on solving the CCUS model is almost the same as CCS: however, this is not the case. In fact, due to a necessary formulation of the problem, which involves the management of numbers that have very different orders of magnitude (for example the variables related to the capture and those related to the chemical conversion) the scaling problem is generated, which causes an exponential increase of the time necessary to reach the solution (Table (4.1)).

Table 4.1. *Results in terms of problem size and computational performance.*

Model	Solver	No. Equations	No. Variables	Execution time [s]	Optimality gap
CCS	CPLEX	416 377	1 019 818	15.711	0.0 %
CCUS	CLPEX	418 862	1 020 192	97 144	0.761 %

In fact the value of the objective function of the CCUS model is larger of one order of magnitude with respect to the USAGE^{MILP} model: this is because the profit generated by the chemical production of *c* is much smaller compared to the total cost of the whole SC

When comparing the results of CCS and CCUS models, it is possible to analyse how much the implementation of the CO_2 conversion affects the total cost of the whole SC and on the level of exploitation of the geological storage.

Table 4.2 *Result summary over CCS and CCUS model.*

	TCC [B€]	TTC [B€]	TSC [B€]	$TC/Ctot^{CO2}$ [€/ton of CO_2]	S^{ratio} [%]	L^{trans}[km]
CCS	18.586	1.177	0.281	33.36	0.695	4409.64
CCUS	18.402	1.162	0.277	31.39	0.686	4843.34

It is possible to notice that in Table 4.2, the variable TC ([€]) of the CCUS model is reduced by 7% with respect to the original model, this involves that the ratio $TC/Ctot^{CO2}$ [€/ton of CO_2], which represents the total cost for carbon capture, transport and storage (physically and/or chemically), decreases to 2.49 €. Meanwhile the exploitation of inshore storage has diminished by 1.44%, which leads to an increase of 2 years compared to the saturation time of the original model. Then the total length of the transport infrastructure defined by the variable L^{trans} [km] is increased by 10%.

Therefore the main impact of the implementation of the usage model regards the total cost while the lowest impact is about the storage capacity.

Furthermore, the positive variable Net^{CO2} [%], that is calculated through Eq. (3.34), is equal to 0.584%: therefore the impact on CO_2 reduction of the profitable technologies of chemical conversion is minimal compared to the one related to the geological sequestration.

For both CCS and CCUS model the total capture cost (TCC [€]) weighs in a decisive way on the total cost (TC [€]) of the entire SC: for the first case the capture cost accounts for 92.73% ,while for the other case for 92.66 %. Moreover the total cost the entire transport infrastructure (TTC [€]) contributes for 5.87% (CCS model) and for 5.94% (CCUS model) compared to TC [€]: therefore the cost for the geological sequestration (TSC [€]) is almost irrelevant.

Moreover, following the implementation of the utilisation in the CCS model the variables TSC ([€]) and TTC ([€]) decrease by about 1% which implies that the chemical conversion of CO_2 does not lead to a reduction of the construction costs of the overall infrastructure (TC [€]) but rather the moderate reduction is mainly caused by the sale of the chemicals produced.

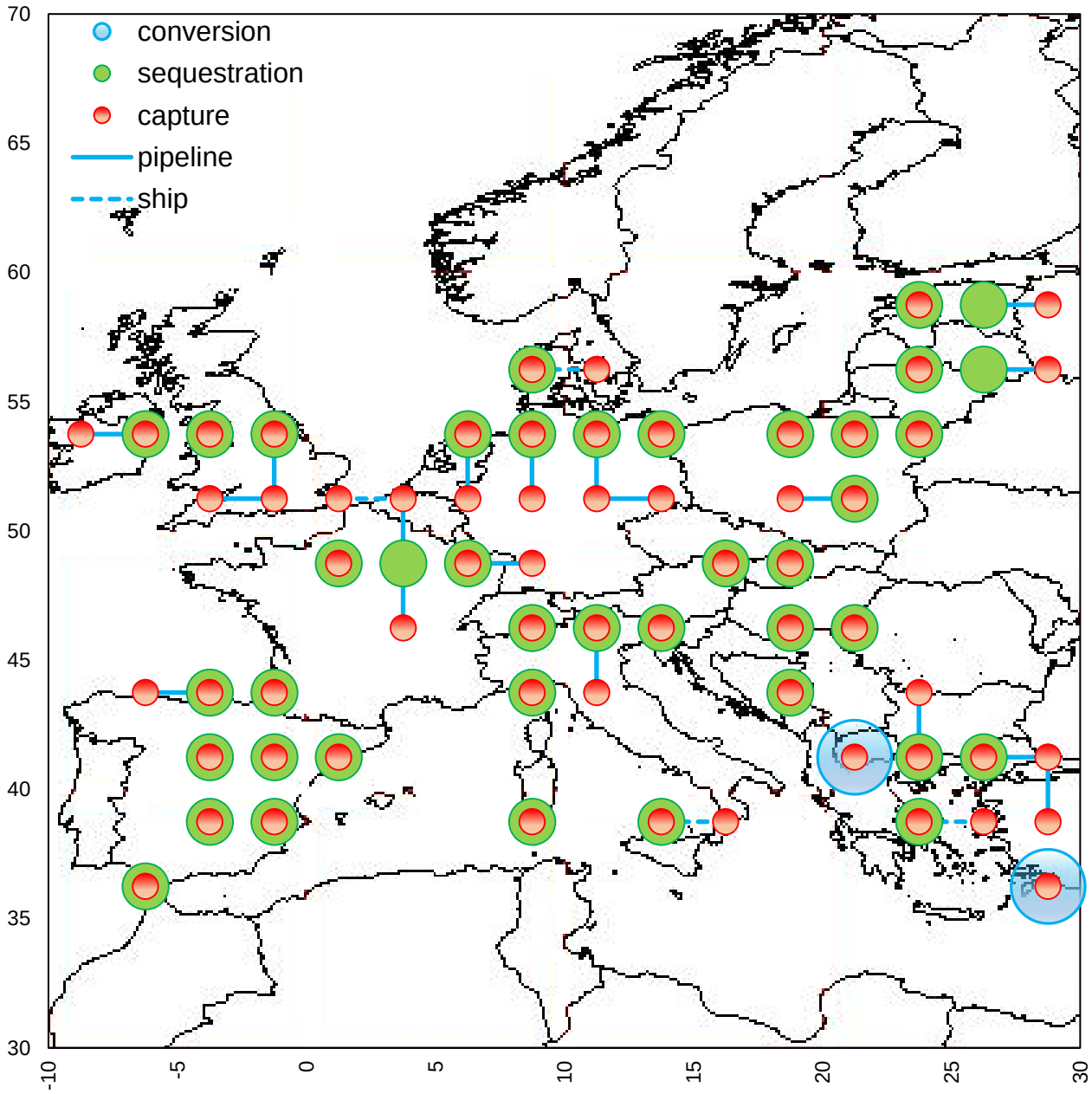

Figure 4.1 *Final spatially explicit representation for α = 43%.*

Figure 4.1 depicts the final SC configuration where α is imposed equal to 43% and the production rate of each chemical *c* is set equal to the current European production.

Compared to Figure 3.2, that shows the final SC arrangement of the CCS model, it can be observed that the transport infrastructure almost does not change, as it does the capture areas. Such configuration again confirms the fact that the presence of systems that convert CO_2 into chemicals does not modify in a substantial way the SC of CCS model. In general it can be noted that it is attempted to capture CO_2 near where inshore geological storage sites are already present.

With regard to the transport, the use of inshore pipelines ($l = \{inshore\ pipeline\}$) is maximized which represent the most economical method of transport. The only point where ship transport is used ($l = \{ship\}$) is at $g = \{35\}$, where CO_2 is captured with the pre-combustion technique ($k =$

$\{pre^{comb}\}$) which is the most economical and therefore justifies a more expensive transport methodology, ending to $g = \{34\}$: however since only 1 million of tons of CO_2 is transported, the cost results cheaper than offshore pipeline ($l = \{offshore\ pipeline\ \}$) because of the scaling factor described in Chapter 3 (Table 3.2).

About the set k the potential of net CO_2 processing and the technologies utilized are shown in Figure 4.2.

It may be noted that the only two technologies k chosen by the model are:

- the pre-combustion ($k = \{pre^{comb}\}$), which is used only by those that go with natural gas, is the most economical technique but the suitable plants are to a lesser extent (Eurostat, 2016b): in particular it is captured the 74% of the entire CO_2 available with this technology (i.e. 0.155 billion of tons of CO_2 that represents the 25.8% of the CO_2 processed at net of the respective efficiency);
- the post-combustion from coal power plants ($k = \{post_{coal}^{comb}\}$), as it is the second most economical technique, captures the 74% of the whole CO_2 available (i.e. 0.346 billion of tons of CO_2), which justifies the goodness of the solution reported by the solver.

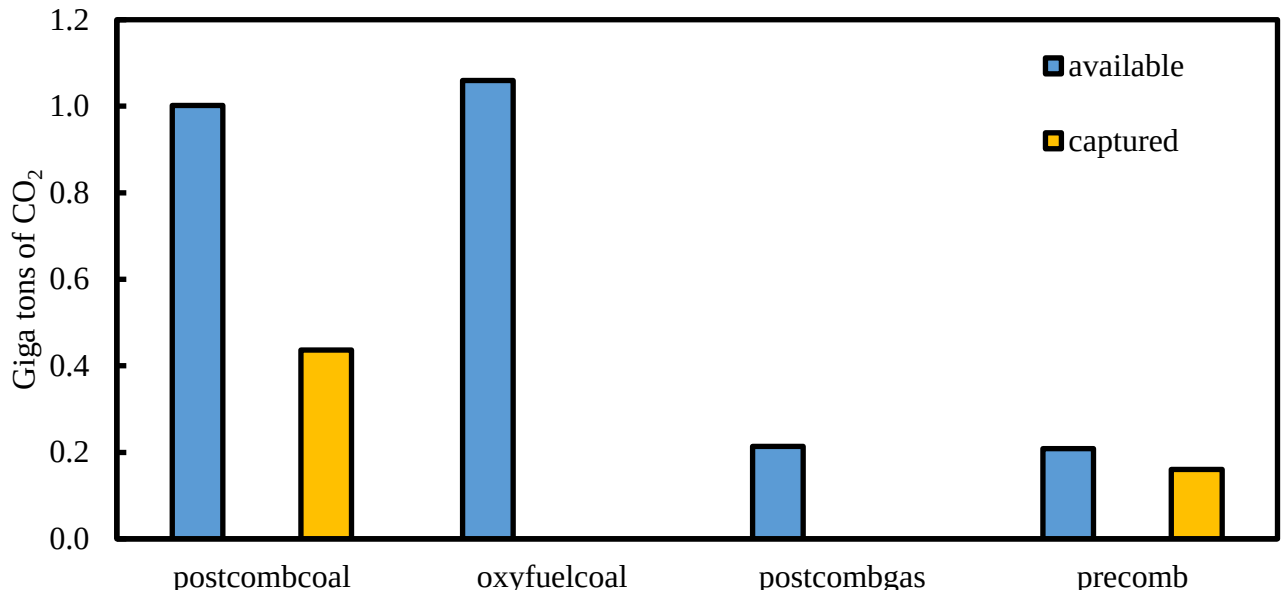

Figure 4.2. *Comparison between the net amount of CO_2 available for processing from power plants (blue) and the one captured (orange).*

4.1.2 Spatially-explicit results

The solution of the generic model for utilisation leads to the choice of a specific region g for a certain chemical, as it is shown in Figure 4.1. Therefore, the reasons behind these choices have been analysed, and the result is that the causes are to be found in the following aspects: corporate tax rate, cost of materials, energy price and labour costs.

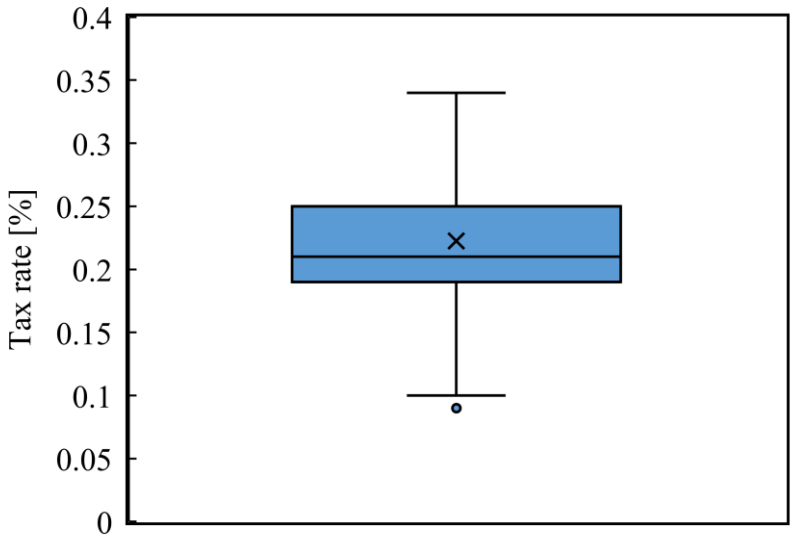

Figure 4.3. *Boxplot of corporate tax rate (KPMG, 2018).*

Regarding the corporate tax rate, it is possible to notice the large variability across the European Country. In fact it varies from a minimum of 9% up to a maximum of 34% (Figure 4.3): respectively they correspond to Hungary ($g = \{65\}$) and Belgium ($g = \{36\}$): indeed no plants of chemical c are built in region $g = \{36\}$. Then, it is observed that the tax rate of Macedonia ($g = \{95\}$) differs for 1% from the one of Hungary, while the one of Turkey ($g = \{98,110,111,124\}$) is close to the average (i.e. 20%) .

In fact, while the construction of the plant in Hungary and Macedonia is justified by the above mentioned value, the reason why it is built in Turkey has to be found in Figure 4.4: this shows the boxplot of the cost of raw materials (a) and the price of the utility (b) for each chemical product c that affect the variable manufacturing cost ($COM_{c,g}$ [€]) in the Eq. (3.25) through the tables $raw_{c,g}$ [€ / tons of c] and $util_{c,g}$ [€ / tons of c].

In particular, the cost of the raw materials for the production of PPP is not a function of a generic region g, since it is determined by market prices, and therefore considered constant according to the method explained in Chapter 2, while for methanol this is not valid as the feedstock to produce it are water , CO_2 and natural gas, which varies from state to state and is therefore function of each region g (Figure 4.4a).

The cost of natural gas, as well as the price of electricity, is important for each chemical c in order to determine the energy costs and therefore the geographic choice. In fact for what concerns the natural gas, the lowest price is found in Turkey at 0.0187 €/kWh (g = {*98,110,111,124*}), while the highest are in Finland (g = {1,..,7,9,10,11}) and Albania (g = {95}) respectively at 0.0441 €/kWh and at 0.0578 €/kWh. Compared to these regions g, both Hungary ($g = \{65\}$) and Macedonia ($g = \{95\}$) have higher prices, in particular close to the European average which is at 0.03 € / kWh (Figure 4.4*b*).

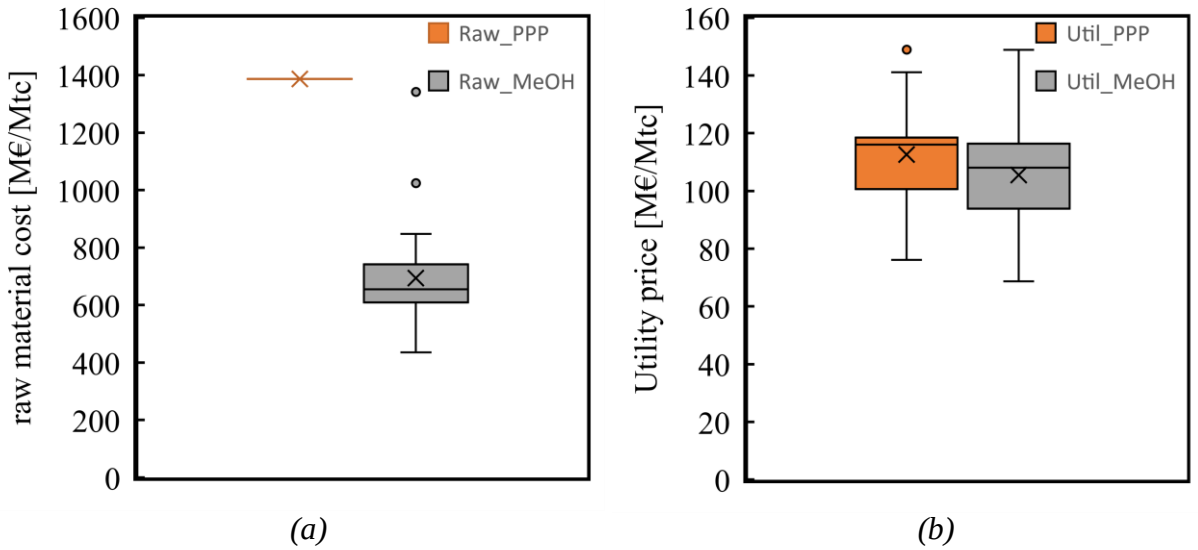

Figure 4.4. *Boxplots of raw material cost (a) and of utility price (b) expressed in euro per ton of c (for raw material MeOH values have been multiplied by 4, while for utility cost the PPP values have been multiplied by a factor of 45 in order to be readable).*

Whereas, with respect to the electricity price, the lowest cost is € 39.3 / MWh for Ukraine (g = {45.46.56, 57,58}) and it is 57.8 € / MWh for Moldova (g = {95}), while the countries that reach the highest cost are Germany (g = {24, .., 27.37, .., 40.50 , 51) up to € 151.9 / MWh and Italy (g = {75.76.77, 90, .., 93, 105.106, 107.119.120}) up to € 147.7 / MWh (Eurostat, 2017b). In fact the most energy intensive productions is *c* = {MeOH}, while for *c* = {PPP} the relative contribution is negligible (Figure 4.4*b*). Therefore, based on the values shown in Figure 4.4, the presence of plants of *c* = {MeOH} in Turkey is justifiable.

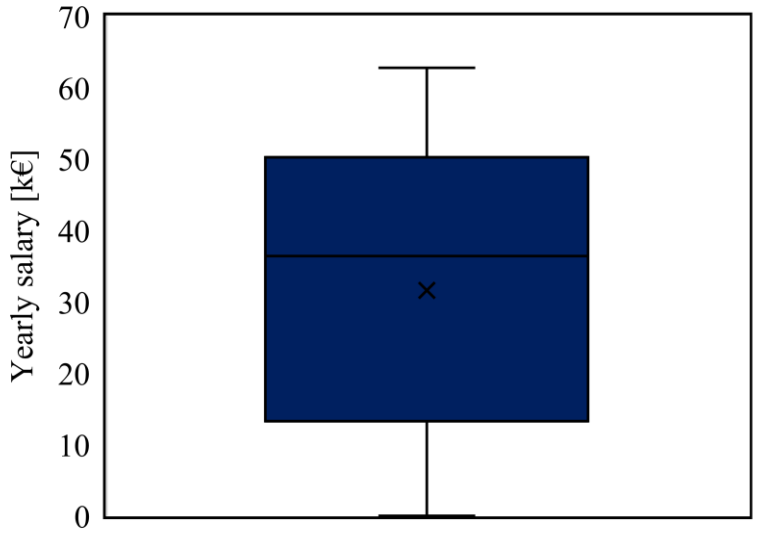

Figure 4.5. *Boxplot of yearly salary expressed in thousands of euros (Eurostat, 2017c).*

Figure 4.5 shows the boxplot of labour costs which affects the variable manufacturing cost ($COM_{c,g}$ [€]) via the parameter $lab_{c,g}$ [€] through the Eq. (3.25) (Eurostat, 2017c). In more detail, it can be observed that the nation with the highest salary is Denmark (g = {8,14,15}) which has it up to € 62,756 per year, meanwhile the one with the lowest wage is Ukraine (g = {45,46.56, 57,58}) up to

3,352 € per year. Hungary (g = {65}) and Turkey (g = {98,110,111,124}) have a value four times higher than the one of Ukraine and Moldova (g = {95}) two time higher.
Therefore, it is possible to notice that the choice of locating the plant in a given region g does not depend so heavily on the cost of labour, which nevertheless remains in the area below the lower quartile, since otherwise all the plants would have been located in Ukraine.
Summarizing, by only considering the data of the energy balances described in Chapter 2 the presence of plants of chemicals $c = \{PPP\}$ in the region $g = \{65\}$ or $g = \{95\}$ is caused mainly by the low taxation, since this process is consuming less energy than all. Regarding the production of PPP, the steam consumption it is about 100 times less than that of DMC and 50 times less than that of methanol (expressed as tons of steam per ton of c), meanwhile for what concerns the consumption of electric energy it is 4 times less than the one of DMC and 40 times less than that of methanol (expressed as kWh per ton of c).
As for the production of chemical c = {MeOH}, the location of the plants is equal for USAGE^{MINLP} and CCUS models because the natural gas has impacts on energy consumption and on the cost of raw materials.

4.2 Sensitivity analysis

The sensitivity analysis was carried out by analysing the variation of the objective function and its most significant variables, as the following aspects changed:

- Percentage of production of each chemical c among the world share (section 4.2.1) (scenario CCUS^{HQ});
- Possibility to store CO_2 only in certain regions g (section 4.2.2) (scenario CCUS^{REG});
- Different calculation of variables $FCI_{c,g}$ [€] and $lab_{c,g}$ [€] (section 4.2.3) (scenario CCUS^{FCI});
- possibility to utilise CO_2 in the DMC production according to the hypothesis done in Chapter 1.

4.2.1 Scenario CCUS^{HQ}

The focus is to investigate how the cost of CO_2 capture and the saturation of wells varies if it is increased the production of chemicals from the base case to 1.5 and 2 times the current European production.
When comparing the results of *CCUS^{HQ}* and CCUS model, it is possible to observe that overproduction affect the cost reduction of the whole SC as it is shown in Figure 4.6. In fact, the total cost (TC [€]) decreases by 8.9% and by 11.9% depending on whether the chosen quota is at 1.5 and 2. Moreover, the variable TC [€] is zeroed only when the production is 16.8 times the current

European production, as it is noted that there is a linear dependence between the production quota and the ration of the two total cost variables (i.e. $TC_{CCUS}{}^{HQ}/TC_{CCUS}$).

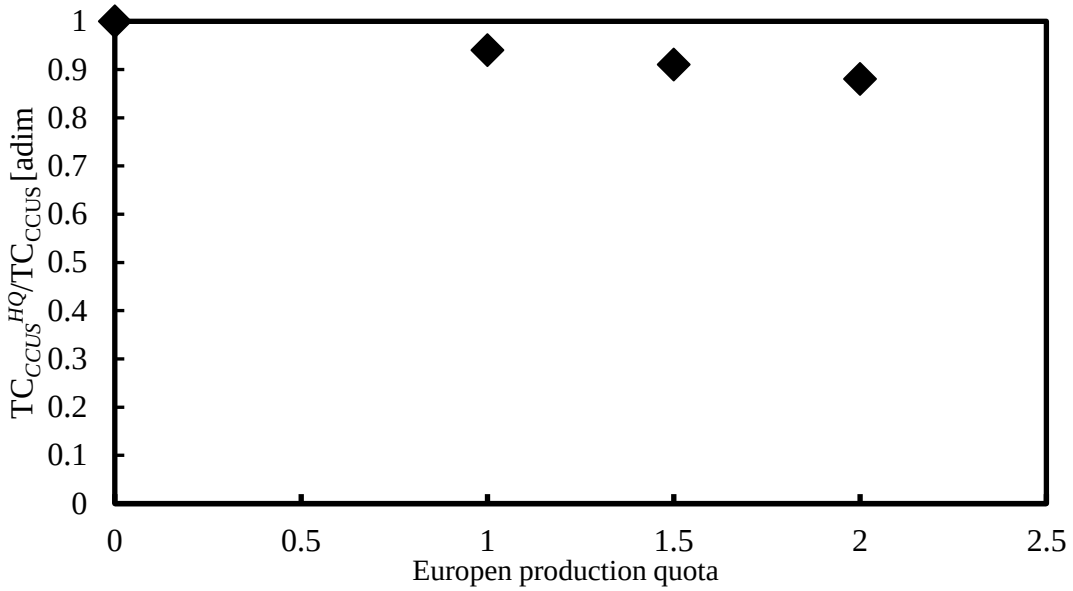

Figure 4.6. *Change in the total cost of the entire SC compared to the variation in the current European production. In abscissa 1 is exactly the European production, while 1.5 and 2 represent the number by which the quota has been multiplied.*

Instead, for what concerns the variation of the exploitation of the geological inshore storage, it can be observed that, while the base case reduces the exploitation by 1.44%, the overproduction leads to a reduction of 2.16% and 2.88%.So, the amount of *c* that should be produced in order to avoid CO_2 sequestration completely is 714% of world production, since, as above, the dependence between the variables in the ordinate and in the abscissa of Figure 4.7 is linear.

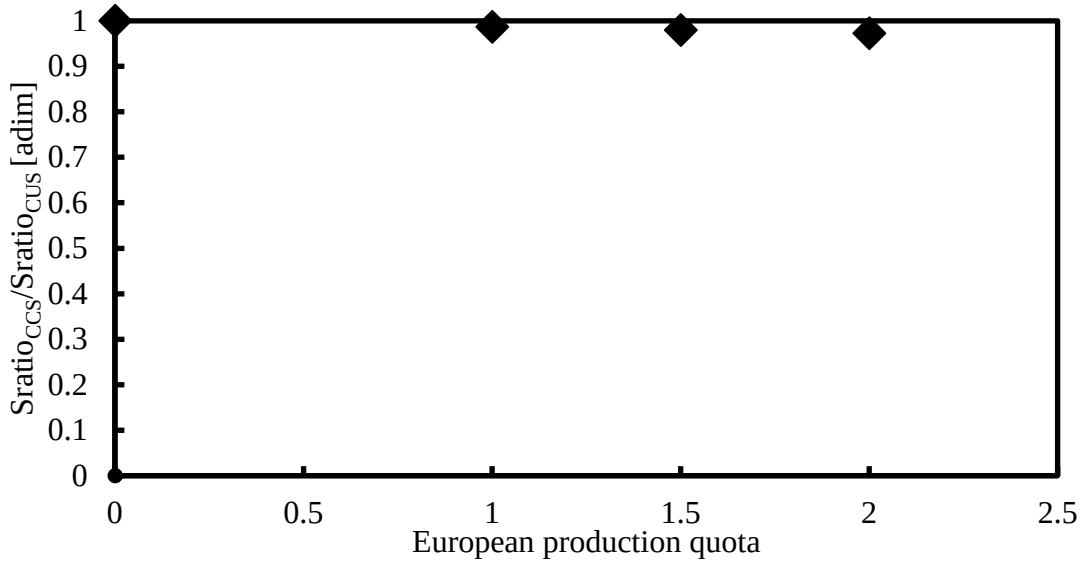

Figure 4.7. *Ratio of the exploitation potential ($S^{ratio}[\%]$) of the CCU model over the CCUS model. In abscissa 1 is exactly the European production, while 1.5 and 2 represent the number by which the quota has been multiplied.*

Therefore, it appears that the use of CO_2 does not significantly affect the exploitation of geological deposits, but affects the total cost of the entire infrastructure.
As for the aspects previously analysed in Figure 4.6 and 4.6, the first thing that is noted is regarding the computational time.
The base case is solved in 15 seconds, with the addition of the utilization of CO_2 the time becomes exponentially greater, since the variable $profit$ [€] has an order of magnitude less than the total cost (TC [€]) and this creates problems of scaling to achieve the economic optimum point. Although the percentage of CO_2 conversion and therefore the variable profit ($profit$ [B€]) increases, this is not sufficiently large to have an order of magnitude comparable with the objective function of the CCUS model and therefore there is no decrease in CPU time (Table 4.3).

Table 4.3. *Summary of the results of the variations in production ceilings.*

Scenario	TC [B€]	S^{ratio} [%]	L^{trans}[km]	Execution time [s]	Optimality gap
Base case	20.044	0.695	4409.64	15.711	0.0 %
10%	18.857	0.686	4843.34	56 962	0.381%
15%	18.257	0.681	4843.34	78 180	0.392%
20%	17.657	0.676	4479.65	7 217	0.726%

Finally the fact that the infrastructural dimension of transport is equal for scenario at 10% and 15%, proves that CO_2 utilization does not affect the SC.

4.2.2 Scenario CCUS^{REG}

Directive 2009/31 / EC on the storage of CO_2, has the task of determining a legal framework. The aim is to outline the conditions for which the geological sequestration is environmentally safe and risk-free for health, transport and storage infrastructure.
For this reason, some states restrict (Czech Republic, Germany, Sweden, Holland and UK) or do not allow (Austria, Croatia, Estonia, Ireland, Latvia, Finland and Belgium) the onshore CO_2 sequestration, while others (UK, Poland and Holland) are in the process of being authorized (European Commission, 2017).
In particular, the Czech Republic will authorize storage in natural geological formations before 2020, Germany has imposed an annual limit of 4Mt CO_2 and 1.3Mt2 of CO_2 for each storage (except for those located in Lower Saxony, Scheleswig-Holstein, Mecklenburg-Western Pomerania, Saxony-Anhalt and Bremen). Now Sweden, UK and the Netherlands only allow the offshore exploitation, while at the moment Poland agrees only on demonstration sites. For these reasons, prudently, it was decided to exclude, in addition to the aforementioned states, also Sweden, UK, the

Netherlands, Poland and Germany as the five Länder that issued this provision are also the only regions that have storage capacity (European Commission, 2017).

Therefore, by eliminating from the $Stotg$ [tons of CO2] parameter the regions g where storage is not permitted, it is proceeded with the resolution of the model, which in this case is called CCS^{REG} and $CCUS^{REG}$, if CO_2 is also converted into chemicals as well geologically stored.

In the following Table 4.4 the main features of the model are summarized.

It can be shown that the variable of total cost (TC [B€]) changes not significantly (about 2% more expensive), while the variables S^{ratio} [%], L^{trans}[km] and TTC [B€] increase respectively by 74%, 66% and 34%.

Table 4.4. *Comparison of the most significant variables of the CCS, CCS^{REG}, CCUS and $CCUS^{REG}$ models.*

	TC [B€]	$TC/Stot^{CO2}$ [€/ton of CO_2]	S^{ratio} [%]	L^{trans}[km]	TTC [B€]
CCS	20.044	33.41	0.695	4409.64	1.177
CCS^{REG}	20.467	34.11	1.210	7326.84	1.612
CCUS	18.571	30.95	0.686	4843.34	1.180
$CCUS^{REG}$	19.276	31.65	1.193	7048.77	1.553

Thus, increasing the size (L^{trans}[km]) and cost of transport infrastructure (TTC [€]), these do not affect the costs. However, the choice that some countries of the European Community have undertaken, weighs heavily on the storage capacity of CO_2. The saturation of inshore fields in fact drops from 87 years to 50.

Moreover by comparing the scenario CCS^{REG} and $CCUS^{REG}$ in which the sequestration is not currently permitted, the use of CO_2 allows a one-year increase in the exploitation potential. Ultimately the incidence of the usage has proportionally equal effects regarding those caused in the scenario in which there are no restrictions in the sequestration of CO_2: the total cost of the entire SC (TC [€]) falls by 7%, while the variables L^{trans}([km]) and TTC ([€]) decrease by 3.5%. Therefore also in this scenario, the chemical conversion of CO_2 does not significantly impact on the entire SC.

First, it may be noted that, in accordance to what has been hypothesized the model did not choose to sequestrate CO_2 where it is prohibited by law, as it is shown in the final SC configuration (Figure 4.8).

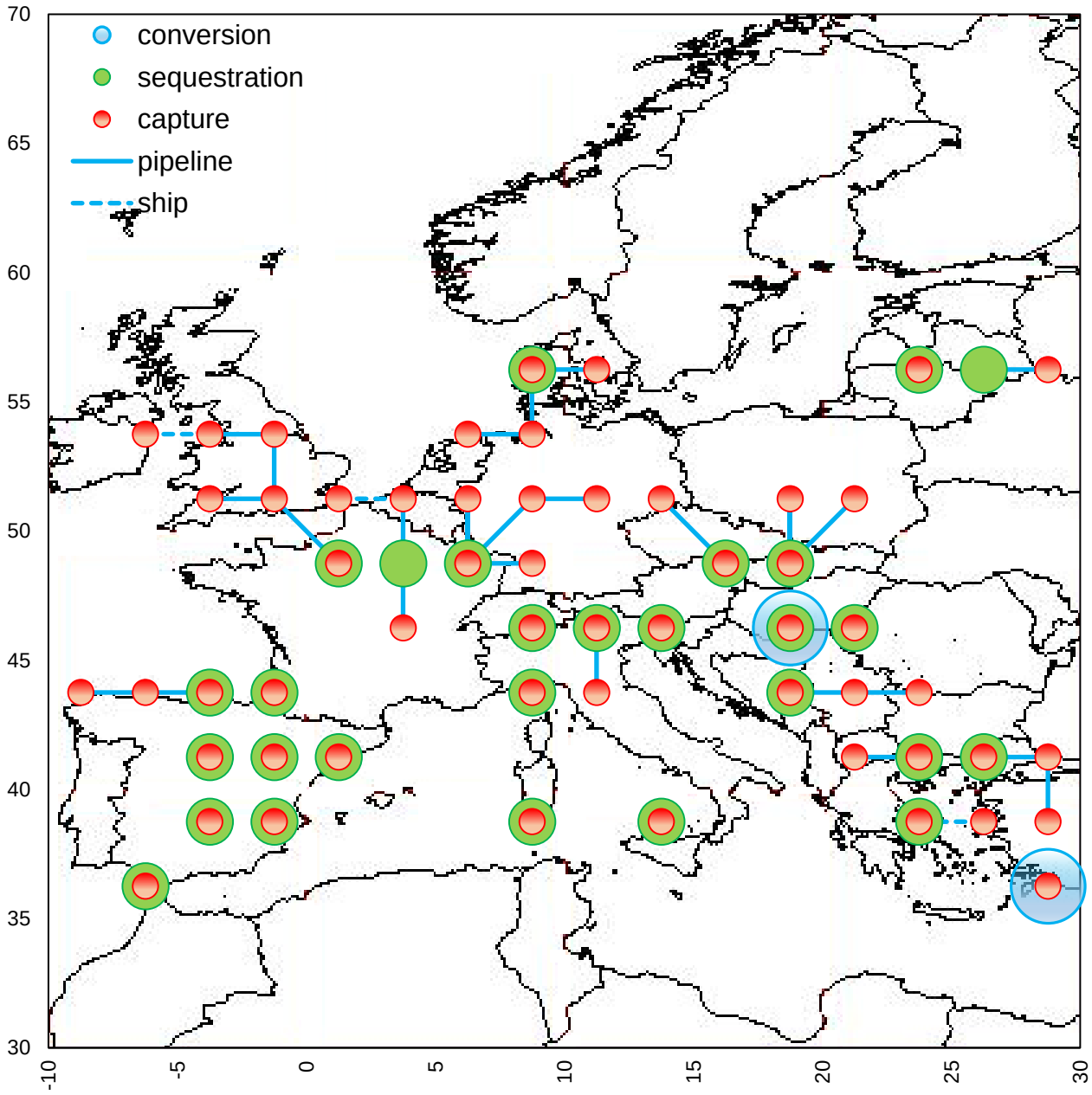

Figure 4.8. *Final SC configuration for CCUS^{REG} scenario α = 43%.*

It appears that the infrastructural network is more complex, which is an obvious consequence of the lower presence of inshore storage. The method of transport by ship ($l = \{ship\}$) has increased by two locations compared to the base case scenario, going from 174 km to 555 km, as for the offshore pipelines ($l = \{offshore\ pipeline\}$) it has gone from 0 km to 330 km (from $g = \{34\}$ to $g = \{37\}$). In this case the CO_2 transported is equal to 30 million of tons, which justifies the choice of this set l since the unitary transport cost ($UTC_{p,l}$ [€/ton of CO_2/km]) is lower (Table 3.2).

The region g of chemical conversion is different with reference to the base case: for $c = \{PPP\}$ the production shifts from $g = \{95\}$ to $g = \{65\}$.

4.2.3 Scenario CCUS^{FCI}

The last topic that has been analysed is how the variable $profit$ [€] changes with the variation of the formulation of the model. In particular, as described in Chapter 3, it was decided to consider the plant size constant and equal to that of the reference articles (Fernández-Dacosta et al., 2017; Souza et al., 2014; Wiesberg et al., 2016).

Since there no plants that have a commercial maturity, here it is wanted to check how the profitability due to the sale of chemicals and to the total cost (TC [€]) of the entire SC change in the worst scenario, which is represented by the impossibility of using the scaling factor, which allows to save on the fixed capital cost ($FCI_{c,g}$[€]) and on the labour cost.

First of all, the comparison between the USAGE^{MILP} and USAGE^{MIP} models has been performed, as shown in Table 4.5.

Table 4.5. *Comparison between USAGE^{MILP} e USAGE^{MIP} of model statistics, economic results and location of plants .*

Description	Unit	Scenario USAGE^{MILP}	Scenario USAGE^{MIP}
Model statistics			
Solution time	[s]	0.257	0.247
Optimality gap	[%]	0	0
Economic results			
$Profit$	[B€]	1.006	0.403
FCI_{PPP}	[M€]	106.11	189
FCI_{MeOH}	[M€]	1 187.52	0
Labour cost of PPP	[M€]	2.76	6.15
Labour cost of MeOH	[M€]	2.01	0
COM_{PPP}	[B€]	4.132	3.908
COM_{MeOH}	[B€]	2.953	0
CF_{PPP}	[M€]	458.34	402.65
CF_{MeOH}	[M€]	547.55	0
Plant location			
$c = \{PPP\}$		$g = \{65\}$	$g = \{95\}$
$c = \{MeOH\}$		$g = \{98\}$	

From a computational speed point of view the two models behave in a very similar way since on one hand they are well formulated under a scaling perspective, on the other hand the problem has few variables compared to the CCS or CCUS model: precisely for this last reason the execution

time is not affected by the lack of binary variables which typically slows down the resolution of the model.

Regarding the economic data it is possible to notice that the results change significantly; in fact, the lack of the scaling factor leads to a reduction in the profitability of 60%. This is mainly caused by the fact that bi-reforming plants are not capable to produce anymore profit for the 250 kton/y size. While for what concerns the production of polyols, despite the labour cost the fixed capital cost are respectively increased by 123% and by 78%, the cash flow (CF_{PPP} [€]) decreases only by 12%.

Table 4.6. *Comparison between CCUS and CCUS^{FCI} of model statistics and economic results.*

Description	Unit	CCUS	CCUS^{FCI}
Model statistics			
Solution time	[s]	56 903	9047
Optimality gap	[%]	0.38	0.35
Number of variables		1 020 192	1 020 192
Economic results			
TC	[B€]	18.857	19.493
TCC	[B€]	18.402	18.420
TTC	[B€]	1.180	1.165
TSC	[B€]	0.277	0.277
$profit$	[B€]	1.002	0.367
Plant location			
$c = \{PPP\}$		$g = \{95\}$	$g = \{95\}$
$c = \{MeOH\}$		$g = \{124\}$	$g = \{124,110\}$

Whereas, regarding CCUS and CCUS^{FCI} scenarios, there are two main differences. The first is about the computational time: the zeroing of the binary variables leads to a decrease of 84% of the solution time despite having the same number of variables and equations (Table 4.6).

The second concerns the fact that despite Table 4.5 shows that producing methanol does not generate more profit, it is anyway produced even though it makes losses since it is still cheaper than capture CO_2. In fact, the total cost of capture (TCC [€]) drops only by 0.1%, and this can be motivated by the fact that 140 kton/y less of MeOH and 150 kton/y less of PPP are produces, and, producing methanol, the $profit$ [€] generated by chemical conversion activities drops by 8.9%.

Then with respect to the base case, as it shown in Figure 4.9, the final SC configuration does not change much: the location of the plants is identical ($g = \{110\}$ and g = {124} are always the same country), the total transport cost (TTC [€]) is almost the same (the variation is only of 1.2%) and

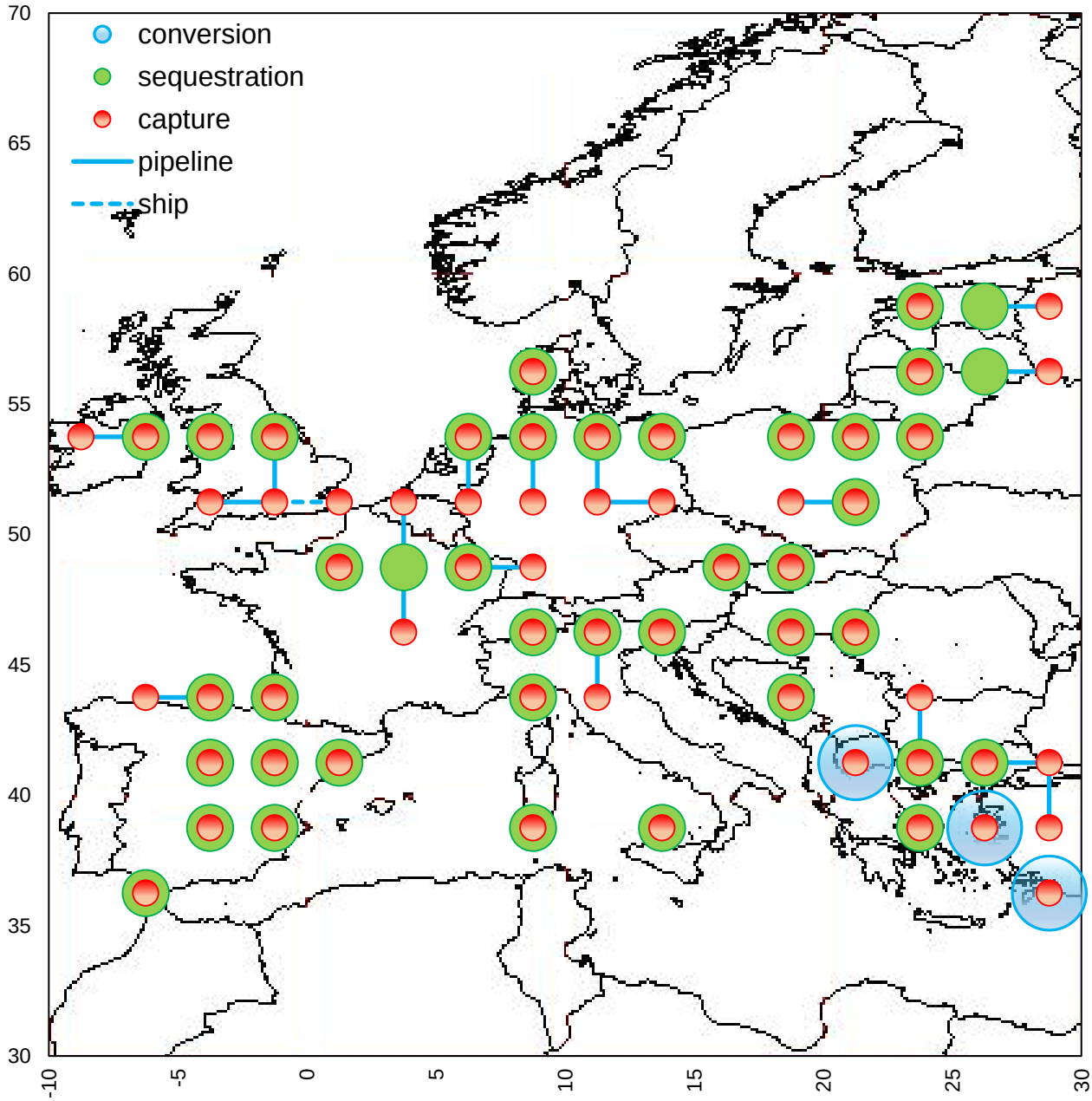

Figure 4.9. *Final SC configuration for CCUS^{FCI} scenario.*

total sequestration cost (TSC [€]) does not vary: therefore the change is negligible.

4.2.4 Scenario CCUS^{DMC}

The goal of conducting the simulation of the CCUS^{DMC} scenario is to observe how the $TC/Stot^{CO2}$ *[€/ton of* CO_2*]*, L^{trans}*[km*], Net^{CO2} *[%]* and S^{ratio} *[%]* variables change if it is decided to utilise the DMC in all those sectors where there is potential for use. Currently, its use is reserved for niche

processes (e.g. green production of PC, methylating agent, solvent..), however, if DMC replace phosgene in PC production and MTBE, the demand in Europe would reach 1.4 Mton/y. Table 4.7 shows the differences between the results of the base case and of the CCUS^{DMC} scenario.

Table 4.7. *Comparison between CCUS e CCUS^{DMC}*

	Optimality gap [%]	$TC/Stot^{CO2}$ [€/ton of CO_2]	S^{ratio} [%]	L^{trans}[km]	Net^{CO2} [%]
CCUS	0.381	31.39	0.686	4843.34	0.584
CCUS^{DMC}	0.382	30.52	0.685	4626.49	0.621

Using CO_2 in the DMC production process, the total cost of capture drops by 2.8%. The most significant change is in the variable Net^{CO2} [%], which represents the net share of CO_2 chemically sequestered: this is increased by 6.2%.

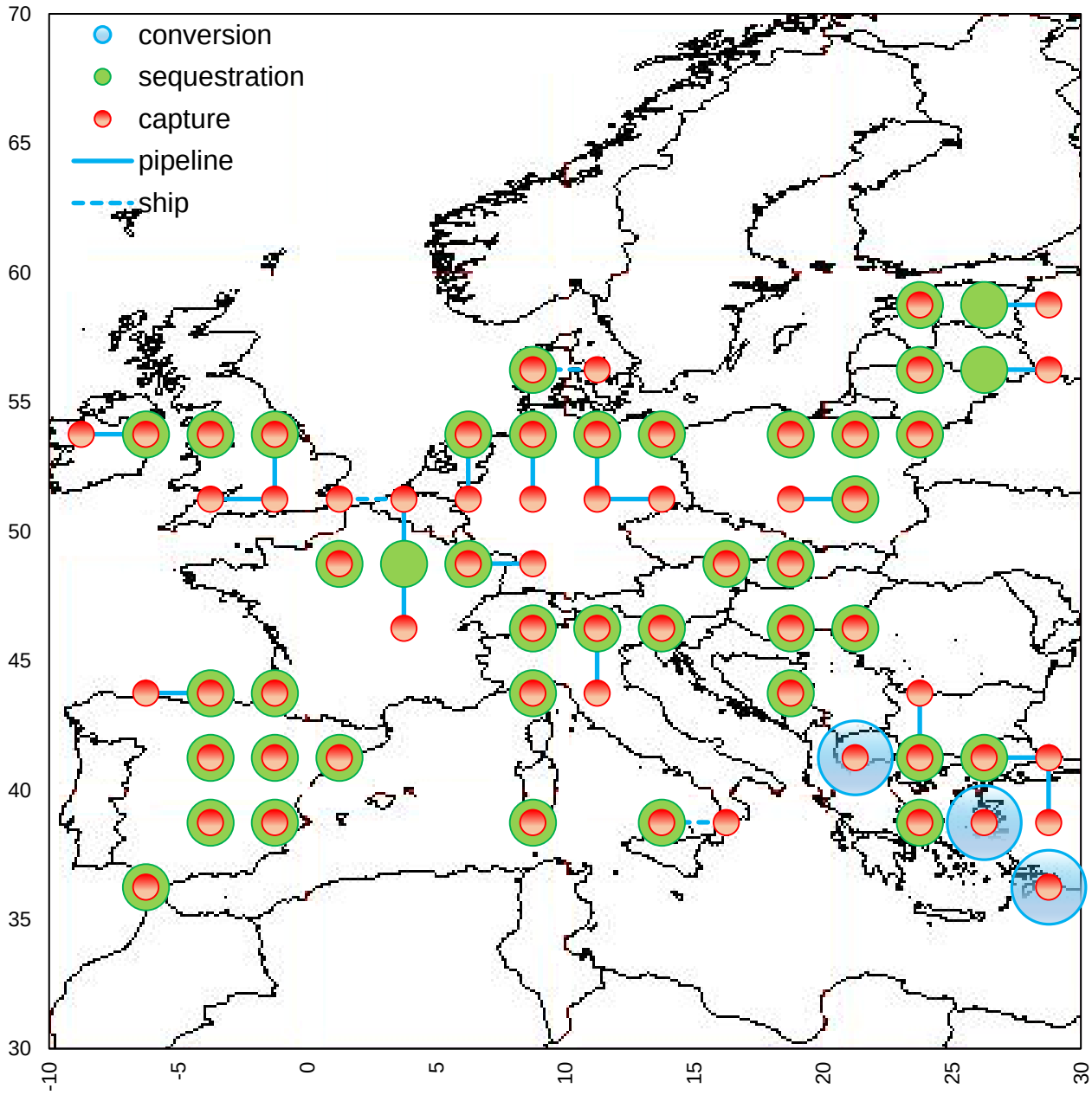

Figure 4.10. *Final SC configuration for CCUS^{DMC} scenario.*

This is caused by the fact that every tons of DMC produced, 0.37 tons of CO_2 are utilised, which is more than twice that of polyols (i.e. 0.15 tons of CO_2 per tonne of PPP) and about half compared to methanol (i.e. 0.65 tons of CO_2 per tonne of MeOH).
Then Figure 4.10 shows the final SC configuration of the $CCUS^{DMC}$ model. It is noticed that the configuration is almost the same compared with the base case, with except that the presence of DMC systems allows to reduce the transport infrastructure as it is necessary to reduce the number of ships (i.e. from $g = \{109\}$ to $g = \{110\}$).
Lastly, for what concerns the exploitation of the inshore geological storage, the reduction is almost insignificant, as it decreases by 0.15%.

4.3 Final remarks

The model described in Chapter 3 is here optimised to provide the minimum cost of an entire CCUS SC.
The results obtained from the optimisation show that the total cost of the European CCUS SC is equal to € 31.40/ton of CO_2 and that thanks to its utilisation, it is possible to chemically sequester about 0.6% of the whole CO_2 emitted by large combustion. In particular, through the simulation of four scenarios, it was possible to take a wider look following different developments: however the variations are not substantial and confirm the estimates obtained with the base case model, namely that the conversion is not an alternative to the geological sequestration, but rather an adjuvant.
More details are contained in the conclusions

Conclusions

In this Master Thesis the problem of developing a MILP model has been addressed, with the purpose of optimising the total cost of the European SC for CCUS, considering to sequester 43% of all the CO_2 emitted by large combustion plants in order to comply with the European target of 2030. Through the development of a basic case and four scenarios, aiming to show at best the current situation.

Firstly, the main cost is represented by the capture, which is always at least 90% of the total cost for the entire infrastructure, while the one for the geological inshore sequestration is constantly around 1%.

As for the total cost of the entire SC, if the CO_2 is not chemically converted, the cost varies between 33.41 €/ton of CO_2 and 34.11 €/ton of CO_2 depending whether all or only some countries allow the inshore geological storage of CO_2. While if the carbon is utilised for the production of chemicals the total cost of the whole SC will vary between 29.39 €/ton of CO_2, if it is permitted to overproduce twice as much as the current European production, and 32.45 €/ton of CO_2 , if the plant size is constant. This last scenario is interesting especially for the reason that the model anyway chooses to produce MeOH, although it does not make profit, since the loss generated is lower than the cost of capture. On the contrary, both for the base case and for the scenario in which the production of DMC is allowed, the total cost is closer to the minimum (i.e. respectively 31.39 €/ton of CO_2 and 30.52 €/ton of CO_2), whereas whether constraints are applied to the inshore geological sequestration the total cost reaches 31.36 €/ton of CO_2. Therefore, the chemical conversion of CO_2 allows to reduce costs up to 14% compared to CCS SC, which is a significant amount.

On the other hand, the performance in terms of reducing GHG does not seem to be as effective as in the case of the total cost. In fact, at best (i.e. overproduction two times higher than the current European production) it is possible to chemically sequester 1.168% of all the CO_2 emitted by large combustion plants. This percentage drops to 0.584% and to 0.621% respectively in the base case and in the scenario in which the conversion of CO_2 into DMC is allowed.

Another important aspect to consider is the saturation time of the inshore storage. Even in this case the use of CO_2 does not affect the increase in its duration, which instead is dramatically influenced by the current decision of some countries to allow or not the sequestration: in fact, it drops from 87 years to 50. In this context, the inshore geological storages allow a medium-term solution, which is hoped that it will be integrated both with the progressive increase of renewable energy quota and with an increase in energy efficiency in the industrial and residential sectors.

So, on the basis of economic and environmental considerations, the chemical conversion of CO_2 in the climate mitigation is not effective for the reduction of GHG, but rather it is useful in reducing the entire cost of the SC.

Given the current immobility of the European Community in deciding whether and how many funds to allocate for this purpose, it was decided to conclude by seeing how much the CO_2 reduction of 43% could impact on the electricity bill. Considering that, in the European regions dealt with by this Master Thesis, currently 550 Mtons of equivalent oil from fossil fuel power plants are produced (European Community, 2017), which corresponds to 6.4 Tera kWh (IEA, 2018), the electricity bill should be increased by 0.00295 € /kWh for the base case. In percentage terms it means having to increase by 4.5% and 4.8% the bill of the two countries that have the lowest cost of electricity for the residential and industrial sectors (i.e. respectively Serbia and Bosnia Herzegovina); while considering the European average cost of electricity, the increase is lowered to 1.4% and 2.5% for the residential and industrial sectors respectively.

Based on these last considerations, if the European Community decides to allocate a fund that allows the construction of the entire infrastructure for the reduction of 43% of the GHG, the increase in the cost of electricity paid by the consumers would still be low. Therefore both economic and environmental sustainability are respected.

In conclusion, the future developments of this Master Thesis may be the transition from a static model to a multi-period one and the analysis of the uncertainty given by the price fluctuations of raw materials through a stochastic model. Finally it could be interesting to estimate the positive implications in indirect economic terms that can cause the SC of the CCUS (e.g. labour,..).

Appendix

Dataset

The following tables show the values of the tables used in the model implemented in GAMS® for the part linked to utilisation, indicating for each value the region *g* and the corresponding country.

Table A1. Labour cost in each country *g* for each chemical *c* [M€] (Eurostat, 2017c)

g		Lab_{DMC}	Lab_{PPP}	Lab_{MeOH}	g		Lab_{DMC}	Lab_{PPP}	Lab_{MeOH}	g		Lab_{DMC}	Lab_{PPP}	Lab_{MeOH}
1	**FIN**	0.71	3.88	2.67	**43**	**PL**	0.19	1.02	0.70	**85**	**ESP**	0.51	2.80	1.93
2	**FIN**	0.71	3.88	2.67	**44**	**PL**	0.19	1.02	0.70	**86**	**ESP**	0.51	2.80	1.93
3	**FIN**	0.71	3.88	2.67	**45**	**UKR**	0.05	0.26	0.18	**87**	**ESP**	0.51	2.80	1.93
4	**FIN**	0.71	3.88	2.67	**46**	**UKR**	0.05	0.26	0.18	**88**	**ESP**	0.51	2.80	1.93
5	**FIN**	0.71	3.88	2.67	**47**	**FR**	0.75	4.11	2.83	**89**	**ESP**	0.51	2.80	1.93
6	**FIN**	0.71	3.88	2.67	**48**	**FR**	0.75	4.11	2.83	**90**	**ITA**	0.61	3.37	2.32
7	**FIN**	0.71	3.88	2.67	**49**	**FR**	0.75	4.11	2.83	**91**	**ITA**	0.61	3.37	2.32
8	**DK**	0.88	4.83	3.33	**50**	**DE**	0.73	3.99	2.75	**92**	**ITA**	0.61	3.37	2.32
9	**FIN**	0.71	3.88	2.67	**51**	**DE**	0.73	3.99	2.75	**93**	**ITA**	0.61	3.37	2.32
10	**FIN**	0.71	3.88	2.67	**52**	**CZ**	0.24	1.35	0.93	**94**	**ALB**	0.06	0.36	0.25
11	**FIN**	0.71	3.88	2.67	**53**	**CZ**	0.24	1.35	0.93	**95**	**MKD**	0.09	0.51	0.35
12	**UK**	0.66	3.62	2.49	**54**	**SVK**	0.21	1.17	0.81	**96**	**GR**	0.39	2.17	1.49
13	**UK**	0.66	3.62	2.49	**55**	**SVK**	0.21	1.17	0.81	**97**	**GR**	0.39	2.17	1.49
14	**DK**	0.88	4.83	3.33	**56**	**UKR**	0.05	0.26	0.18	**98**	**TUR**	0.19	1.07	0.74
15	**DK**	0.88	4.83	3.33	**57**	**UKR**	0.05	0.26	0.18	**99**	**PT**	0.31	1.72	1.18
16	**LTU**	0.14	0.79	0.54	**58**	**UKR**	0.05	0.26	0.18	**100**	**ESP**	0.51	2.80	1.93
17	**LTU**	0.14	0.79	0.54	**59**	**FR**	0.75	4.11	2.83	**101**	**ESP**	0.51	2.80	1.93
18	**LTU**	0.14	0.79	0.54	**60**	**FR**	0.75	4.11	2.83	**102**	**ESP**	0.51	2.80	1.93
19	**IRL**	0.70	3.82	2.63	**61**	**ITA**	0.61	3.37	2.32	**103**	**ESP**	0.51	2.80	1.93
20	**IRL**	0.70	3.82	2.63	**62**	**ITA**	0.61	3.37	2.32	**104**	**ESP**	0.51	2.80	1.93
21	**UK**	0.66	3.62	2.49	**63**	**ITA**	0.61	3.37	2.32	**105**	**ITA**	0.61	3.37	2.32
22	**UK**	0.66	3.62	2.49	**64**	**HRV**	0.23	1.28	0.88	**106**	**ITA**	0.61	3.37	2.32
23	**NL**	0.79	4.32	2.97	**65**	**HUN**	0.18	1.01	0.70	**107**	**ITA**	0.61	3.37	2.32
24	**DE**	0.73	3.99	2.75	**66**	**RO**	0.11	0.59	0.41	**108**	**GR**	0.39	2.17	1.49
25	**DE**	0.73	3.99	2.75	**67**	**RO**	0.11	0.59	0.41	**109**	**GR**	0.39	2.17	1.49
26	**DE**	0.73	3.99	2.75	**68**	**RO**	0.11	0.59	0.41	**110**	**TUR**	0.19	1.07	0.74
27	**DE**	0.73	3.99	2.75	**69**	**MDA**	0.11	0.59	0.41	**111**	**TUR**	0.19	1.07	0.74
28	**PL**	0.19	1.02	0.70	**70**	**PT**	0.31	1.72	1.18	**112**	**ESP**	0.51	2.80	1.93
29	**PL**	0.19	1.02	0.70	**71**	**ESP**	0.51	2.80	1.93	**113**	**NA**	-	-	-
30	**PL**	0.19	1.02	0.70	**72**	**ESP**	0.51	2.80	1.93	**114**	**NA**	-	-	-
31	**PL**	0.19	1.02	0.70	**73**	**ESP**	0.51	2.80	1.93	**115**	**NA**	-	-	-
32	**PL**	0.19	1.02	0.70	**74**	**FR**	0.75	4.11	2.83	**116**	**NA**	-	-	-
33	**UK**	0.66	3.62	2.49	**75**	**ITA**	0.61	3.37	2.32	**117**	**NA**	-	-	-
34	**UK**	0.66	3.62	2.49	**76**	**ITA**	0.61	3.37	2.32	**118**	**NA**	-	-	-
35	**UK**	0.66	3.62	2.49	**77**	**ITA**	0.61	3.37	2.32	**119**	**ITA**	0.61	3.37	2.32
36	**BE**	0.78	4.29	2.95	**78**	**BA**	0.14	0.75	0.51	**120**	**ITA**	0.61	3.37	2.32
37	**DE**	0.73	3.99	2.75	**79**	**BA**	0.14	0.75	0.51	**121**	**GR**	0.39	2.17	1.49
38	**DE**	0.73	3.99	2.75	**80**	**SRB**	0.12	0.65	0.45	**122**	**GR**	0.39	2.17	1.49
39	**DE**	0.73	3.99	2.75	**81**	**RO**	0.11	0.59	0.41	**123**	**GR**	0.39	2.17	1.49
40	**DE**	0.73	3.99	2.75	**82**	**RO**	0.11	0.59	0.41	**124**	**TUR**	0.19	1.07	0.74
41	**PL**	0.19	1.02	0.70	**83**	**RO**	0.11	0.59	0.41					
42	**PL**	0.19	1.02	0.70	**84**	**PT**	0.31	1.72	1.18					

Table A2. Raw material cost in each country *g* for each chemical *c* [M€/Mtons$_C$]b

g		Raw_{DMC}	Raw_{PPP}	Raw_{MeOH}	g		Raw_{DMC}	Raw_{PPP}	Raw_{MeOH}	g		Raw_{DMC}	Raw_{PPP}	Raw_{MeOH}
1	**FIN**	778.8	1386.6	326.9	**43**	**PL**	778.8	1386.6	195.1	**85**	**ESP**	778.8	1386.6	210.1
2	**FIN**	778.8	1386.6	326.9	**44**	**PL**	778.8	1386.6	195.1	**86**	**ESP**	778.8	1386.6	210.1
3	**FIN**	778.8	1386.6	326.9	**45**	**UKR**	778.8	1386.6	169.6	**87**	**ESP**	778.8	1386.6	210.1
4	**FIN**	778.8	1386.6	326.9	**46**	**UKR**	778.8	1386.6	169.6	**88**	**ESP**	778.8	1386.6	210.1
5	**FIN**	778.8	1386.6	326.9	**47**	**FR**	778.8	1386.6	222.9	**89**	**ESP**	778.8	1386.6	210.1
6	**FIN**	778.8	1386.6	326.9	**48**	**FR**	778.8	1386.6	222.9	**90**	**ITA**	778.8	1386.6	176.0
7	**FIN**	778.8	1386.6	326.9	**49**	**FR**	778.8	1386.6	222.9	**91**	**ITA**	778.8	1386.6	176.0
8	**DK**	778.8	1386.6	381.1	**50**	**DE**	778.8	1386.6	219.4	**92**	**ITA**	778.8	1386.6	176.0
9	**FIN**	778.8	1386.6	326.9	**51**	**DE**	778.8	1386.6	219.4	**93**	**ITA**	778.8	1386.6	176.0
10	**FIN**	778.8	1386.6	326.9	**52**	**CZ**	778.8	1386.6	166.7	**94**	**ALB**	778.8	1386.6	290.1
11	**FIN**	778.8	1386.6	326.9	**53**	**CZ**	778.8	1386.6	166.7	**95**	**MKD**	778.8	1386.6	198.6
12	**UK**	778.8	1386.6	170.2	**54**	**SVK**	778.8	1386.6	170.2	**96**	**GR**	778.8	1386.6	185.8
13	**UK**	778.8	1386.6	170.2	**55**	**SVK**	778.8	1386.6	170.2	**97**	**GR**	778.8	1386.6	185.8
14	**DK**	778.8	1386.6	381.1	**56**	**UKR**	778.8	1386.6	169.6	**98**	**TUR**	778.8	1386.6	127.9
15	**DK**	778.8	1386.6	381.1	**57**	**UKR**	778.8	1386.6	169.6	**99**	**PT**	778.8	1386.6	199.1
16	**LTU**	778.8	1386.6	196.8	**58**	**UKR**	778.8	1386.6	169.6	**100**	**ESP**	778.8	1386.6	210.1
17	**LTU**	778.8	1386.6	196.8	**59**	**FR**	778.8	1386.6	222.9	**101**	**ESP**	778.8	1386.6	210.1
18	**LTU**	778.8	1386.6	196.8	**60**	**FR**	778.8	1386.6	222.9	**102**	**ESP**	778.8	1386.6	210.1
19	**IRL**	778.8	1386.6	213.1	**61**	**ITA**	778.8	1386.6	176.0	**103**	**ESP**	778.8	1386.6	210.1
20	**IRL**	778.8	1386.6	213.1	**62**	**ITA**	778.8	1386.6	176.0	**104**	**ESP**	778.8	1386.6	210.1
21	**UK**	778.8	1386.6	170.2	**63**	**ITA**	778.8	1386.6	176.0	**105**	**ITA**	778.8	1386.6	176.0
22	**UK**	778.8	1386.6	170.2	**64**	**HRV**	778.8	1386.6	178.3	**106**	**ITA**	778.8	1386.6	176.0
23	**NL**	778.8	1386.6	256.5	**65**	**HUN**	778.8	1386.6	192.2	**107**	**ITA**	778.8	1386.6	176.0
24	**DE**	778.8	1386.6	219.4	**66**	**RO**	778.8	1386.6	184.1	**108**	**GR**	778.8	1386.6	185.8
25	**DE**	778.8	1386.6	219.4	**67**	**RO**	778.8	1386.6	184.1	**109**	**GR**	778.8	1386.6	185.8
26	**DE**	778.8	1386.6	219.4	**68**	**RO**	778.8	1386.6	184.1	**110**	**TUR**	778.8	1386.6	127.9
27	**DE**	778.8	1386.6	219.4	**69**	**MDA**	778.8	1386.6	165.0	**111**	**TUR**	778.8	1386.6	127.9
28	**PL**	778.8	1386.6	195.1	**70**	**PT**	778.8	1386.6	199.1	**112**	**ESP**	778.8	1386.6	210.1
29	**PL**	778.8	1386.6	195.1	**71**	**ESP**	778.8	1386.6	195.1	**113**	**NA**	-	-	-
30	**PL**	778.8	1386.6	195.1	**72**	**ESP**	778.8	1386.6	195.1	**114**	**NA**	-	-	-
31	**PL**	778.8	1386.6	195.1	**73**	**ESP**	778.8	1386.6	195.1	**115**	**NA**	-	-	-
32	**PL**	778.8	1386.6	195.1	**74**	**FR**	778.8	1386.6	222.9	**116**	**NA**	-	-	-
33	**UK**	778.8	1386.6	170.2	**75**	**ITA**	778.8	1386.6	176.0	**117**	**NA**	-	-	-
34	**UK**	778.8	1386.6	170.2	**76**	**ITA**	778.8	1386.6	176.0	**118**	**NA**	-	-	-
35	**UK**	778.8	1386.6	170.2	**77**	**ITA**	778.8	1386.6	176.0	**119**	**ITA**	778.8	1386.6	176.0
36	**BE**	778.8	1386.6	169.6	**78**	**BA**	778.8	1386.6	233.3	**120**	**ITA**	778.8	1386.6	176.0
37	**DE**	778.8	1386.6	219.4	**79**	**BA**	778.8	1386.6	233.3	**121**	**GR**	778.8	1386.6	185.8
38	**DE**	778.8	1386.6	219.4	**80**	**SRB**	778.8	1386.6	197.4	**122**	**GR**	778.8	1386.6	185.8
39	**DE**	778.8	1386.6	219.4	**81**	**RO**	778.8	1386.6	184.1	**123**	**GR**	778.8	1386.6	185.8
40	**DE**	778.8	1386.6	219.4	**82**	**RO**	778.8	1386.6	184.1	**124**	**TUR**	778.8	1386.6	127.9
41	**PL**	778.8	1386.6	195.1	**83**	**RO**	778.8	1386.6	184.1					
42	**PL**	778.8	1386.6	195.1	**84**	**PT**	778.8	1386.6	199.1					

Table A3. Utility cost in each region *g* for each chemical *c* [M€/Mtons$_c$]

g		Uti_{DMC}	Uti_{PPP}	Uti_{MeOH}	g		Uti_{DMC}	Uti_{PPP}	Uti_{MeOH}	g		Uti_{DMC}	Uti_{PPP}	Uti_{MeOH}
1	**FIN**	223.6	3.24	145.4	**43**	**PL**	146.9	3.08	130.1	**85**	**ESP**	152.6	3.01	128.3
2	**FIN**	223.6	3.24	145.4	**44**	**PL**	146.9	3.08	130.1	**86**	**ESP**	152.6	3.01	128.3
3	**FIN**	223.6	3.24	145.4	**45**	**UKR**	117.2	1.92	82.1	**87**	**ESP**	152.6	3.01	128.3
4	**FIN**	223.6	3.24	145.4	**46**	**UKR**	117.2	1.92	82.1	**88**	**ESP**	152.6	3.01	128.3
5	**FIN**	223.6	3.24	145.4	**47**	**FR**	159.1	2.92	125.4	**89**	**ESP**	152.6	3.01	128.3
6	**FIN**	223.6	3.24	145.4	**48**	**FR**	159.1	2.92	125.4	**90**	**ITA**	135.2	3.26	135.8
7	**FIN**	223.6	3.24	145.4	**49**	**FR**	159.1	2.92	125.4	**91**	**ITA**	135.2	3.26	135.8
8	**DK**	278.9	5.43	236.4	**50**	**DE**	166.2	3.77	159.3	**92**	**ITA**	135.2	3.26	135.8
9	**FIN**	223.6	3.24	145.4	**51**	**DE**	166.2	3.77	159.3	**93**	**ITA**	135.2	3.26	135.8
10	**FIN**	223.6	3.24	145.4	**52**	**CZ**	119.1	2.26	95.4	**94**	**ALB**	104.7	10.03	393.9
11	**FIN**	223.6	3.24	145.4	**53**	**CZ**	119.1	2.26	95.4	**95**	**MKD**	137.9	2.27	98.1
12	**UK**	129.1	3.01	125.5	**54**	**SVK**	145.0	3.03	128.1	**96**	**GR**	135.9	2.79	117.7
13	**UK**	129.1	3.01	125.5	**55**	**SVK**	145.0	3.03	128.1	**97**	**GR**	135.9	2.79	117.7
14	**DK**	278.9	5.43	236.4	**56**	**UKR**	117.2	1.92	82.1	**98**	**TUR**	92.7	1.93	79.6
15	**DK**	278.9	5.43	236.4	**57**	**UKR**	117.2	1.92	82.1	**99**	**PT**	146.9	3.08	130.1
16	**LTU**	140.9	2.65	113.0	**58**	**UKR**	117.2	1.92	82.1	**100**	**ESP**	152.6	3.01	128.3
17	**LTU**	140.9	2.65	113.0	**59**	**FR**	159.1	2.92	125.4	**101**	**ESP**	152.6	3.01	128.3
18	**LTU**	140.9	2.65	113.0	**60**	**FR**	159.1	2.92	125.4	**102**	**ESP**	152.6	3.01	128.3
19	**IRL**	155.8	3.14	133.8	**61**	**ITA**	135.2	3.26	135.8	**103**	**ESP**	152.6	3.01	128.3
20	**IRL**	155.8	3.14	133.8	**62**	**ITA**	135.2	3.26	135.8	**104**	**ESP**	152.6	3.01	128.3
21	**UK**	129.1	3.01	125.5	**63**	**ITA**	135.2	3.26	135.8	**105**	**ITA**	135.2	3.26	135.8
22	**UK**	129.1	3.01	125.5	**64**	**HRV**	128.4	2.50	105.6	**106**	**ITA**	135.2	3.26	135.8
23	**NL**	179.6	2.99	130.5	**65**	**HUN**	136.8	2.51	107.2	**107**	**ITA**	135.2	3.26	135.8
24	**DE**	166.2	3.77	159.3	**66**	**RO**	131.4	2.46	104.4	**108**	**GR**	135.9	2.79	117.7
25	**DE**	166.2	3.77	159.3	**67**	**RO**	131.4	2.46	104.4	**109**	**GR**	135.9	2.79	117.7
26	**DE**	166.2	3.77	159.3	**68**	**RO**	131.4	2.46	104.4	**110**	**TUR**	92.7	1.93	79.6
27	**DE**	166.2	3.77	159.3	**69**	**MDA**	118.8	2.33	98.0	**111**	**TUR**	92.7	1.93	79.6
28	**PL**	146.9	3.08	130.1	**70**	**PT**	146.9	3.08	130.1	**112**	**ESP**	152.6	3.01	128.3
29	**PL**	146.9	3.08	130.1	**71**	**ESP**	152.6	3.01	128.3	**113**	**NA**	-	-	-
30	**PL**	146.9	3.08	130.1	**72**	**ESP**	152.6	3.01	128.3	**114**	**NA**	-	-	-
31	**PL**	146.9	3.08	130.1	**73**	**ESP**	152.6	3.01	128.3	**115**	**NA**	-	-	-
32	**PL**	146.9	3.08	130.1	**74**	**FR**	159.1	2.92	125.4	**116**	**NA**	-	-	-
33	**UK**	129.1	3.01	125.5	**75**	**ITA**	135.2	3.26	135.8	**117**	**NA**	-	-	-
34	**UK**	129.1	3.01	125.5	**76**	**ITA**	135.2	3.26	135.8	**118**	**NA**	-	-	-
35	**UK**	129.1	3.01	125.5	**77**	**ITA**	135.2	3.26	135.8	**119**	**ITA**	135.2	3.26	135.8
36	**BE**	126.6	2.81	117.4	**78**	**BA**	161.0	2.52	110.4	**120**	**ITA**	135.2	3.26	135.8
37	**DE**	166.2	3.77	159.3	**79**	**BA**	161.0	2.52	110.4	**121**	**GR**	135.9	2.79	117.7
38	**DE**	166.2	3.77	159.3	**80**	**SRB**	137.9	2.34	100.6	**122**	**GR**	135.9	2.79	117.7
39	**DE**	166.2	3.77	159.3	**81**	**RO**	131.4	2.46	104.4	**123**	**GR**	135.9	2.79	117.7
40	**DE**	166.2	3.77	159.3	**82**	**RO**	131.4	2.46	104.4	**124**	**TUR**	92.7	1.93	79.6
41	**PL**	146.9	3.08	130.1	**83**	**RO**	131.4	2.46	104.4					
42	**PL**	146.9	3.08	130.1	**84**	**PT**	120.1	2.58	107.9					

References

Alper, E., Yuksel Orhan, O., 2017. CO 2 utilization: Developments in conversion processes. *Petroleum* 3, 109-126

Aresta, M., Dibenedetto, A., Angelini, A., 2013. The changing paradigm in *CO2 utilization. J. CO2* Util. 3–4, 65–73.

Aresta, M., Wiley InterScience (Online service), 2010. Carbon dioxide as chemical feedstock. *Wiley-VCH*.

Arnette, A.N., 2017. Renewable energy and carbon capture and sequestration for a reduced carbon energy plan: An optimization model. *Renew. Sustain. Energy Rev.* 70, 254–265.

Bakken, B.H., von Streng Velken, I., 2008. Linear models for optimization of infrastructure for CO2 capture and storage. *IEEE Trans. Energy Conver*s. 23, 824–833.

Barlow, J., Sims, R.C., Quinn, J.C., 2016. Techno-economic and life-cycle assessment of an attached growth algal biorefinery. *Bioresour. Technol*. 220, 360–368.

Beamon, B.M., Beamon, B.M., 1998. Supply Chain Design and Analysis: Models and Methods. *Int. J. Prod. Econ*. 55, 281--294.

Becker, W.L., Braun, R.J., Penev, M., Melaina, M., 2012. Production of Fischer-Tropsch liquid fuels from high temperature solid oxide co-electrolysis units. *Energy* 47, 99–115.

Bellotti, D., Rivarolo, M., Magistri, L., Massardo, A.F., 2017. Feasibility study of methanol production plant from hydrogen and captured carbon dioxide. *J. CO2 Util.* 21, 132–138.

Bezzo, F., 2017. Bioethanol : Second generation, teaching material from course "Biofuels and sustainable industrial processes".

Bezzo, F., 2016. Economic analysis of chemical processes, teaching material from course " Process Design".

Birol, F., 2008.IEA, World Energy Outlook 2008.

Bodénan, F., Bourgeois, F., Petiot, C., Augé, T., Bonfils, B., Julcour-Lebigue, C., Guyot, F., Boukary, A., Tremosa, J., Lassin, A., Gaucher, E.C., Chiquet, P., 2014. Ex situ mineral carbonation for CO2 mitigation: Evaluation of mining waste resources, aqueous carbonation processability and life cycle assessment (Carmex project). *Miner. Eng*. 59, 52–63.

Borowitzka, M.A., 1997. Microalgae for aquaculture: Opportunities and constraints. *J. Appl. Phycol.* 9, 393–401.

Brennan, L., Owende, P., 2010. Biofuels from microalgae-A review of technologies for production, processing, and extractions of biofuels and co-products. *Renew. Sustain. Energy Rev*. 14, 557–577.

Brentrup, F., Pallière, C., n.d. Energy efficiency and greenhouse gas emissions in European nitrogen fertilizer production and use 20–21, "technical report".

Breyer, C., Tsupari, E., Tikka, V., Vainikka, P., 2015. Power-to-gas as an emerging profitable

business through creating an integrated value chain. *Energy Procedia* 73, 182–189.

Bridgewater, A.V., 1979. International construction cost location factors. *Chem. Eng. J*,86(24)-119.

Buchholz, O.S., Van Der Ham, A.G.J., Veneman, R., Brilman, D.W.F., Kersten, S.R.A., 2014. Power-to-Gas: Storing surplus electrical energy a design study. *Energy Procedia* 63, 7993–8009.

Cairns, H., 2016. Global trends in Syngas,"technical report", *Stratas Advisors*.

Campbell, P.K., Beer, T., Batten, D., 2011. Life cycle assessment of biodiesel production from microalgae in ponds. *Bioresour. Technol*. 102, 50–56.

Chang, E.E., Pan, S.Y., Chen, Y.H., Chu, H.W., Wang, C.F., Chiang, P.C., 2011. CO2 sequestration by carbonation of steelmaking slags in an autoclave reactor. *J. Hazard. Mater*. 195, 107–114.

Chiang, J.H., Hopper, J.R., 1983. Kinetics of the hydrogenation of carbon dioxide over supported nickel. *Ind. Eng. Chem. Prod. Res. Dev*. 22, 225–228.

Chisti, Y., Yan, J., 2011. Energy from algae: Current status and future trends. Algal biofuels - A status report. *Appl. Energy* 88, 3277–3279.

Ciriminna, R., Pina, C. Della, Rossi, M., Pagliaro, M., 2014. Understanding the glycerol market. *Eur. J. Lipid Sci. Technol*. 116, 1432–1439.

Covestro, 2017. Investor Presentation "technical report".

D'Amore, F., Bezzo, F., 2017. Economic optimisation of European supply chains for CO2capture, transport and sequestration. *Int. J. Greenh. Gas Control* 65, 99–116.

Davis, R., Aden, A., Pienkos, P.T., 2011. Techno-economic analysis of autotrophic microalgae for fuel production. *Appl. Energy* 88, 3524–3531.

Davis, R., Kinchin, C., Markham, J., Tan, E., Laurens, L., Sexton, D., Knorr, D., Schoen, P., Lukas, J., 2014a. Process Design and Economics for the Conversion of Algal Biomass to Biofuels: Algal Biomass Fractionation to Lipid- and Carbohydrate-Derived Fuel Products, "*National Renewable Energy Laboratory*".

Davis, R., Kinchin, C., Markham, J., Tan, E.C.D., Laurens, L.M.L., 2014b. Process Design and Economics for the Conversion of Algal Biomass to Biofuels : Algal Biomass Fractionation to Lipid- Products Process Design and Economics for the Conversion of Algal Biomass to Biofuels : Algal Biomass Fractionation to Lipid- and Carbohyd, *NREL/TP-5100-62368*.

de Freitas Silva, T., Dias, J.A.C., Maciel, C.G., Assaf, J.M., 2013. Ni/Al_2O_3 catalysts: effects of the promoters Ce, La and Zr on the methane steam and oxidative reforming reactions. *Catal. Sci. Technol.* 3, 635–643.

De Groot, F.F.T., Lammerink, R.R.G.J., Heidemann, C., Van Der Werff, M.P.M., Garcia, T.C., Van Der Ham, L.A.G.J., Van Den Berg, H., 2014a. The industrial production of dimethyl carbonate from methanol and carbon dioxide. *Chem. Eng. Trans*. 39, 1561–1566.

Dietrich, R.-U., Albrecht, F.G., Maier, S., König, D.H., Estelmann, S., Adelung, S., Bealu, Z., Seitz, A., 2017. Cost calculations for three different approaches of biofuel production using biomass, electricity and CO2. *Biomass and Bioenergy* 1–9.

Dixit, S., 2016. Optimization and Fuel Properties of Water Degummed Linseed Biodiesel from Transesterification *Process. Chem. Sci. J*.7:131

Dobrée, J., 2016. Carbon Capture Utilisation and Storage 43–45,"technical report", *European*

Commission.

Domenicali, G., 2013. Analisi economica di un impianto industriale per la produzione autotrofa di olio da microalghe 2012–2013, Tesi di Laurea in Ingegneria Chimica, DIPIC, Università di Padova.

Edrisi, A., Mansoori, Z., Dabir, B., 2016. Urea synthesis using chemical looping process - Techno-economic evaluation of a novel plant configuration for a green production. *Int. J. Greenh. Gas Control* 44, 42–51.

Elahi, N., Shah, N., Korre, A., Durucan, S., 2014. Multi-period least cost optimisation model of an integrated carbon dioxide capture transportation and storage infrastructure in the UK. *Energy Procedia* 63, 2655–2662.

European CCS Demonstration Project Network, 2015. 2015 Situation Report on the European Large Scale Demonstration Projects Network : Public Summary.

European Commission, 2017. Implementation of Directive 2009/31/EC on the Geological Storage of Carbon Dioxide. Brussels COM 1. available at :https://ec.europa.eu/commission/sites/beta-political/files/report-carbon-capture-storage_en.pdf

European Commission, 2015a. EU ETS Handbook. DG Clim. Action 138., avaliable at: ttp://ec.europa.eu/clima/publications/docs/ets_handbook_en.pdf

European Commission, 2014. Quadro per le politiche dell'energia e del clima per il periodo dal 2020 al 2030 1–21.

Fernández-Dacosta, C., Van Der Spek, M., Hung, C.R., Oregionni, G.D., Skagestad, R., Parihar, P., Gokak, D.T., Strømman, A.H., Ramirez, A., 2017a. Prospective techno-economic and environmental assessment of carbon capture at a refinery and CO2 utilisation in polyol synthesis. *J. CO2 Util.* 21, 405–422.

Feron, P.H.., Jansen, A.., 1997. The production of carbon dioxide from flue gas by membrane gas absorption. Energy Convers. Manag. 38, S93–S98.

Forstmeier, M., 2017. Carbon and Energy Storage with Biological Methanation, "technical report"

Fu, Q., Mabilat, C., Zahid, M., Brisse, A., Gautier, L., 2010. Syngas production via high-temperature steam/CO2 co-electrolysis: an economic assessment. *Energy Environ. Sci*. 3, 1382.

Fujita, S. ichiro, Terunuma, H., Nakamura, M., Takezawa, N., 1991. Mechanisms of Methanation of CO and CO2 over Ni. *Ind. Eng. Chem. Res*. 30, 1146–1151.

Fukuoka, S., Fukawa, I., Tojo, M., Oonishi, K., Hachiya, H., Aminaka, M., Hasegawa, K., Komiya, K., 2010. A Novel Non-Phosgene Process for Polycarbonate Production from CO2: Green and Sustainable Chemistry in Practice. *Catal. Surv. from Asia* 14, 146–163.

Garcia-Herrero, I., Cueílar-Franca, R.M., Enríquez-Gutierez, M., Alvarez-Guerra, M., Irabien, A., Azapagic, A., 2016. Environmental Assessment of Dimethyl Carbonate Production: Comparison of a Novel Electrosynthesis Route Utilizing CO 2 with a Commercial Oxidative Carbonylation Process, *ACS Sust. Chem.Eng* 2088-2097

Geske, J., Berghout, N., van den Broek, M., 2014. Cost-effective balance between CO2vessel and pipeline transport: Part II - Design of multimodal CO2transport: The case of the West Mediterranean region. *Int. J. Greenh. Gas Control* 33, 122–134.

Gong, J., You, F., 2015. Value-added chemicals from microalgae: Greener, more economical, or

both *ACS Sustain. Chem. Eng.* 82-96

Götz, M., Lefebvre, J., Mörs, F., McDaniel Koch, A., Graf, F., Bajohr, S., Reimert, R., Kolb, T., 2016. Renewable Power-to-Gas: A technological and economic review. *Renew. Energy* 85, 1371–1390.

Graves, C., Ebbesen, S.D., Mogensen, M., Lackner, K.S., 2011. Sustainable hydrocarbon fuels by recycling CO2 and H 2O with renewable or nuclear energy. *Renew. Sustain. Energy Rev*. 15, 1–23.

Haba, O., Itakura, I., Ueda, M., Kuze, S., 1999. Synthesis of polycarbonate from dimethyl carbonate and bisphenol-A through a non-phosgene process. *J. Polym. Sci. Part A Polym. Chem*. 37, 2087–2093.

Han, J., Lee, I., 2012. Multiperiod Stochastic Optimization Model for Carbon Capture and Storage Infrastructure under Uncertainty in CO 2 Emissions , Product Prices , and Operating Costs *I&EC Research* 11445-11457

Hasan, M.M.F., First, E.L., Boukouvala, F., Floudas, C.A., 2015a. A multi-scale framework for CO2 capture, utilization, and sequestration: CCUS and CCU. *Comput. Chem. Eng*. 81, 2–21.

Heffer, P., Prud'homme, M., 2016. 84th IFA Annual Conference, Moscow, 30 May-1 June 2016, in: Fertilizer Outlook 2016-2020. *International Fertilizer Industry Association (IFA)*, Moscow.

Herzog, H., Golomb, D., Zemba, S., 1991. Feasibility, modeling and economics of sequestering power plant CO2 emissions in the deep ocean. Environ. Prog. 10, 64–74.

Huijgen, W.J.J., Comans, R.N.J., 2003. Carbon dioxide sequestration by mineral carbonation, Environmental science & technology, "technical report".

Iizuka, A., Fujii, M., Yamasaki, A., Yanagisawa, Y., 2004. Development of a New CO2 Sequestration Process Utilizing the Carbonation of Waste Cement. *Ind. Eng. Chem. Res*. 43, 7880–7887.

International Gas Union, 2014. World LNG Report -2014 Edition, "technical report".

IPCC, 2014. Climate Change-Synthesis Report, Climate Change 2014: Synthesis Report. Contribution of Working Groups I, II and III to the Fifth Assessment Report of the Intergovernmental Panel on Climate Change.

IPCC, 2007. Climate Change 2007 Synthesis Report, Intergovernmental Panel on Climate Change [Core Writing Team IPCC.

Joo, O.S., Jung, K.D., Moon, I., Rozovskii, a Y., Lin, G.I., Han, S.H., Uhm, S.J., 1999. Carbon dioxide hydrogenation to form methanol via a reverse-water-gas-shift reaction (the CAMERE process). *Ind. Eng. Chem. Res*. 38, 1808–1812.

Kallrath, J., 2012. Algebraic Modeling Systems. *Springer-Verlag* Berlin Heidelberg.

Kalyanarengan Ravi, N., Van Sint Annaland, M., Fransoo, J.C., Grievink, J., Zondervan, E., 2017. Development and implementation of supply chain optimization framework for CO2 capture and storage in the Netherlands. *Comput. Chem. Eng.* 102, 40–51.

Keller, N., Rebmann, G., Keller, V., 2010. Catalysts, mechanisms and industrial processes for the dimethylcarbonate synthesis. J. Mol. *Catal. A Chem*. 317, 1–18.

Kempka, T., Plötz, M.L., Schlüter, R., Hamann, J., Deowan, S.A., Azzam, R., 2011. Carbon dioxide utilisation for carbamide production by application of the coupled UCG-Urea process. *Energy*

Procedia 4, 2200–2205.

Kiehl, J.T., Trenberth, K.E., Kiehl, J.T., Trenberth, K.E., 1997. Earth's Annual Global Mean Energy Budget. *Bull. Am. Meteorol. Soc*. 78, 197–208.

Kongpanna, P., Pavarajarn, V., Gani, R., Assabumrungrat, S., 2015. Techno-economic evaluation of different CO2-based processes for dimethyl carbonate production. *Chem. Eng. Res. Des*. 93, 496–510.

König, D.H., Baucks, N., Kraaij, G.J., Wörner, A., 2014. Entwicklung und Bewertung eines Verfahrenskonzeptes zur Herstellung flüssiger Kohlenwasserstoffe unter Nutzung von CO 2 Inhalt 1–18.

König, D.H., Freiberg, M., Dietrich, R.U., Wörner, A., 2015. Techno-economic study of the storage of fluctuating renewable energy in liquid hydrocarbons. *Fuel* 159, 289–297.

Kuenen, H.J., Mengers, H.J., Nijmeijer, D.C., van der Ham, A.G.J., Kiss, A.A., 2016. Techno-economic evaluation of the direct conversion of CO2 to dimethyl carbonate using catalytic membrane reactors. *Comput. Chem. Eng*. 86, 136–147.

Kwak, D.-H., Kim, J.-K., 2017a. Techno-economic evaluation of CO2 enhanced oil recovery (EOR) with the optimization of CO2 supply. *Int. J. Greenh. Gas Control* 58, 169–184.

Lackner, K.S., Wendt, C.H., Butt, D.P., Joyce, E.L., Sharp, D.H., 1995. Carbon dioxide disposal in carbonate minerals. *Energy* 20, 1153–1170.

Langanke, J., Wolf, A., Hofmann, J., Böhm, K., Subhani, M.A., Müller, T.E., Leitner, W., Gürtler, C., 2014. Carbon dioxide (CO_2) as sustainable feedstock for polyurethane production. *Green Chem*. 16, 1865–1870.

Leckel, D., Liwanga-Ehumbu, M., 2006. Diesel-selective hydrocracking of an iron-based Fischer-Tropsch wax fraction (C15-C45) using a MoO3-modified noble metal catalyst. Energy and *Fuels* 20, 2330–2336.

Lee, R., 2014. Polyurethanes & Intermediates, "technical report".

Li, X., Anderson, P., Jhong, H.-R.M., Paster, M., Stubbins, J.F., Kenis, P.J.A., 2016. Greenhouse Gas Emissions, Energy Efficiency, and Cost of Synthetic Fuel Production Using Electrochemical CO_2 Conversion and the Fischer–Tropsch Process. *Energy & Fuels* 30, 5980–5989.

Lu, X., Leung, D.Y.C., Wang, H., Leung, M.K.H., Xuan, J., 2014. Electrochemical Reduction of Carbon Dioxide to Formic Acid. *ChemElectroChem* 1, 836–849.

Mata, T.M., Martins, A.A., Caetano, N.S., 2010. Microalgae for biodiesel production and other applications: A review. Renew. S*ustain. Energy Rev*. 14, 217–232.

Mazzotti, M., Carlos, J., Allam, R., Lackner, K.S., Meunier, F., Rubin, E.M., Sanchez, J.C., Yogo, K., Zevenhoven, R., 2005. Mineral carbonation and industrial uses of carbon dioxide. IPCC Spec. Rep. Carbon dioxide Capture Storage 319–338.

Meindl, B., Templ, M., 2012. Analysis of commercial and free and open source solvers for linear optimization problems. ESSnet commom tools *Harmon. Methodol*. SDC ESS 1, 1–14.

Methanol Institute, 2016. DME: an emerging global fuel, "technical report".

Metz, B., Davidson, O., de Coninck, H., Loos, M., Meyer, L., 2005. IPCC. Cambridge University Press, Cambridge, United Kingdom and New York,NY,USA.

Meylan, F.D., Piguet, F.P., Erkman, S., 2017. Power-to-gas through CO2 methanation: Assessment of the carbon balance regarding EU directives. J. *Energy Storage* 11, 16–24.

Middleton, R.S., Kuby, M.J., Wei, R., Keating, G.N., Pawar, R.J., 2012. A dynamic model for optimally phasing in CO2capture and storage infrastructure. *Environ. Model. Softw*. 37, 193–205.

Modesti, M., 2011. FISCHER-TROPSCH PROCESS, teaching material from course "Processi industriali 2"

Mondal, K., Sasmal, S., Badgandi, S., Chowdhury, D.R., Nair, V., 2016. Dry reforming of methane to syngas: a potential alternative process for value added chemicals—a techno-economic perspective. *Environ. Sci. Pollut. Res*. 23, 22267–22273.

Müller, T.E., Gürtler, C., Wohak, M., Hofmann, J., Subhani, M.A., Walter Leitner, Ilja Peckermann, A.W., n.d. Polyether carbonate polyol production method. US 9273183 B2.

Newall, Clarke, Haywood, Scholes, Clarke, King, Barley, 2000. CO2 STORAGE AS CARBONATE MINERALS Report Number PH3 / 17.

O'Connor, W., Dahlin, D., Rush, G., Gerdemann, S., Penner, L.R., Nilsen, D., 2005. Aqueous Mineral Carbonation. *Doe/Arc-Tr-04-002*.

OGDEN, J., 2003. Modeling Infrastructure for a Fossil Hydrogen Energy System with CO2 Sequestration, in: Greenhouse Gas Control Technologies - 6th International Conference. Elsevier

Park, J.N., McFarland, E.W., 2009. A highly dispersed Pd-Mg/SiO2 catalyst active for methanation of CO2. *J. Catal*. 266, 92–97.

Parra, D., Patel, M.K., 2016. Erratum: Techno-economic implications of the electrolyser technology and size for power-to-gas systems (International Journal of Hydrogen Energy (2016) 41 (3748-3761. *Int. J. Hydrogen Energy* 41, 7527–7528.

Parra, D., Zhang, X., Bauer, C., Patel, M.K., 2017. An integrated techno-economic and life cycle environmental assessment of power-to-gas systems. *Appl. Energy* 193, 440–454.

Passell, H., Dhaliwal, H., Reno, M., Wu, B., Ben Amotz, A., Ivry, E., Gay, M., Czartoski, T., Laurin, L., Ayer, N., 2013. Algae biodiesel life cycle assessment using current commercial data. J. *Environ. Manage*. 129, 103–111.

Peeters, A., Valvekens, P., Ameloot, R., Sankar, G., Kirschhock, C.E.A., De Vos, D.E., 2013. Zn–Co Double Metal Cyanides as Heterogeneous Catalysts for Hydroamination: A Structure–Activity Relationship. *ACS Catal*. 3, 597–607.

Pérez-Fortes, M., Schöneberger, J.C., Boulamanti, A., Harrison, G., Tzimas, E., 2016a. Formic acid synthesis using CO2 as raw material: Techno-economic and environmental evaluation and market potential. *Int. J. Hydrogen Energy* 41, 16444–16462.

Peterson, A.A., Abild-Pedersen, F., Studt, F., Rossmeisl, J., Nørskov, J.K., 2010. How copper catalyzes the electroreduction of carbon dioxide into hydrocarbon fuels. *Energy Environ. Sci*. 3, 1311.

plastic information europe, 2016. POM,"technical report",*PIE*.

Reddy, S., Bhakt, M., Gilmartin, J., Yonkoski, J., 2014. Cost effective CO2 capture from flue gas for increasing methanol plant production. *Energy Procedia* 63, 1407–1414.

Rivera-Tinoco, R., Farran, M., Bouallou, C., Auprêtre, F., Valentin, S., Millet, P., Ngameni, J.R., 2016. Investigation of power-to-methanol processes coupling electrolytic hydrogen production and catalytic CO2 reduction. *Int. J. Hydrogen Energy* 41, 4546–4559.

Roh, K., Frauzem, R., Gani, R., Lee, J.H., 2016a. Process systems engineering issues and applications towards reducing carbon dioxide emissions through conversion technologies. *Chem. Eng. Res. Des*. 116, 27–47.

Rubin, E.S., Davison, J.E., Herzog, H.J., 2015. The cost of CO2 capture and storage. *Int. J. Greenh. Gas Control* 40, 378–400.

Sakakura, T., Kohno, K., 2009. The synthesis of organic carbonates from carbon dioxide. *Chem. Commun*. 11,1312-1336.

Samantha McCulloch, Simon Keeling, Raimund Malischek, Tristan Stanley, IEA, 2016. 20 Years of Carbon Capture and Storage. *Accel. Futur. Deploy.* 115-142.

Schiebahn, S., Grube, T., Robinius, M., Tietze, V., Kumar, B., Stolten, D., 2015. Power to gas: Technological overview, systems analysis and economic assessment for a case study in Germany. *Int. J. Hydrogen Energy* 40, 4285–4294.

Schmidt, P., Weindorf, W., Roth, A., Batteiger, V., Riegel, F., 2016a. Power-to-Liquids Potentials and Perspectives for the Future Supply of Renewable Aviation Fuel 32, "technical report"

Schmidt, P., Zittel, W., Weindorf, W., Raksha, T., 2016b. Chancen und Potenziale alternativer Kraftstoffe Results from the FVV scenario study «Renewables in Transport 2050», "technical report"

Sinnot, R., Towler, G., 2009. Chemical Engineering Design, 5th ed.,*Elsevier*,Burlington, USA

Sioshansi, R., Conejo, J. antonio, 2017. Optimization in Engineering,1st ed.. *Springer optimization and its applications*,Cham, Switzerland.

Slade, R., Bauen, A., 2013. Micro-algae cultivation for biofuels: Cost, energy balance, environmental impacts and future prospects. *Biomass and Bioenergy* 53, 29–38.

Soratana, K., Landis, A.E., 2011. Evaluating industrial symbiosis and algae cultivation from a life cycle perspective. *Bioresour. Techno*l. 102, 6892–6901.

Souza, L.F.S., Ferreira, P.R.R., De Medeiros, J.L., Alves, R.M.B., Araújo, O.Q.F., 2014a. Production of DMC from CO2 via indirect route: Technical-economical-environmental assessment and analysis. *ACS Sustain. Chem. Eng*. 2, 62–69.

Souza, L.F.S., Ferreira, P.R.R., Medeiros, J.L. De, Alves, R.M.B., Arau, Q.F., 2014b. Production of DMC from CO 2 via Indirect Route: Technical − Economical − Environmental Assessment and Analysis. *ACS Sustain. Chem. Eng*. 2, 1–7.

Sterner, M., 2009. Bioenergy and renewable power methane in integrated 100% renewable energy systems. Limiting global warming by transforming energy systems, Kassel University press..

Stolaroff, J.K., Lowry, G. V., Keith, D.W., 2005. Using CaO- and MgO-rich industrial waste streams for carbon sequestration. *Energy Convers. Manag*. 46, 687–699. 9

Sun, A., Davis, R., Starbuck, M., Ben-Amotz, A., Pate, R., Pienkos, P.T., 2011. Comparative cost analysis of algal oil production for biofuels. *Energy* 36, 5169–5179.

Tapia, J.F.D., Lee, J.Y., Ooi, R.E.H., Foo, D.C.Y., Tan, R.R., 2016. Planning and scheduling of CO2capture, utilization and storage (CCUS) operations as a strip packing problem. *Process*

Saf. Environ. Prot. 104, 358–372.

Thomas, S., Fries, donata maria, Paciello, R., Mohl, K., Schafer, M., Rittinger, S., Schneider, D., 2014. Process for preparing formic acid by reaction of carbon dioxide with hydrogen. US8791297 B2.

Tremel, A., Wasserscheid, P., Baldauf, M., Hammer, T., 2015. Techno-economic analysis for the synthesis of liquid and gaseous fuels based on hydrogen production via electrolysis. *Int. J. Hydrogen Energy* 40, 11457–11464.

Treut, L., Somerville, R., Cubasch, U., Ding, Y., Mauritzen, C., Mokssit, a, Peterson, T., Prather, M., Qin, D., Manning, M., Chen, Z., Marquis, M., Averyt, K.B., Tignor, M., 2007. Historical Overview of Climate Change Science. *Earth Chapter* 1, 93–127.

Tundo, P., Selva, M., 2002. The chemistry of dimethyl carbonate. *Acc. Chem. Res*. 35, 706–716.

Turton, R., Baile, R.C., Whiting, W.B., Shaeiwitz, J.A., Bhattacharyya, D., 2015. Analysis, synthesis, and design of chemical processes, Fourth Edi. ed. Pearson Education, Inc.,New Jersey,USA

Tzimas, E., Georgakaki, A., 2005. Enhanced oil recovery using carbon dioxide in the European energy system, Report EUR.

Ullmann's Encyclopedia of Industrial Chemistry, 7th ed, 2000.

United Nations, 2015. Paris Agreement. 21st Conf. Parties.

Van-Dal, Bouallou, C., 2013. Design and simulation of a methanol production plant from CO2 hydrogenation. *J. Clean. Prod*. 57, 38–45.

Vanden Bussche, K.M., Froment, G.F., 1996. A Steady-State Kinetic Model for Methanol Synthesis and the Water Gas Shift Reaction on a Commercial Cu/ZnO/Al2O3Catalyst. *J. Catal*. 161, 1–10.

Vandewalle, J., Bruninx, K., D'Haeseleer, W., 2015. Effects of large-scale power to gas conversion on the power, gas and carbon sectors and their interactions. *Energy Convers.* Manag. 94, 28–39.

Vangkilde-Pedersen, T., Kirk, K., Vincke, O., Neele, F., Nindre, Y.-M. Le, 2008. Project no . SES6-518318 EU GeoCapacity Assessing European Capacity for Geological Storage of Carbon Dioxide 63.

von der Assen, N., Bardow, A., 2014a. Life cycle assessment of polyols for polyurethane production using CO_2 as feedstock: insights from an industrial case study. *Green Chem*. 16, 3272–3280.

von der Assen, N., Bardow, A., 2014b. Life cycle assessment of polyols for polyurethane production using CO2as feedstock: insights from an industrial case study. *Green Chem*. 16, 3272–3280.

Wang, M., Wang, H., Zhao, N., Sun, Y., 2007. High-Yield Synthesis of Dimethyl Carbonate from Urea and Methanol Using a Catalytic Distillation Process. *Ind. Eng. Chem. Res*. 46, 2683–2687.

Wang, M., Zhao, N., Wei, W., Sun, Y., 2005. Synthesis of dimethyl carbonate from urea and methanol over ZnO. *Ind. Eng. Chem. Res.* 44, 7596–7599.

Wang, S., Lu, G.Q. (Max), Millar, G.J., 1996. Carbon Dioxide Reforming of Methane To Produce

Synthesis Gas over Metal-Supported Catalysts: State of the Art. *Energy & Fuels* 10, 896–904.

Wankat, P.C., 2017. Separation Process Engineering Includes Mass Transfer Analysis, 4th ed., Prentice Hall, USA

Weatherbee, G.D., Bartholomew, C.H., 1982. Hydrogenation of CO2 on group VIII metals. II. Kinetics and mechanism of CO2 hydrogenation on nickel. *J. Catal*. 77, 460–472.

Whipple, D.T., Kenis, P.J.A., 2010. Prospects of CO2 utilization via direct heterogeneous electrochemical reduction. *J. Phys. Chem. Lett*. 1, 3451–3458.

Wiesberg, I.L., de Medeiros, J.L., Alves, R.M.B., Coutinho, P.L.A., Araújo, O.Q.F., 2016. Carbon dioxide management by chemical conversion to methanol: HYDROGENATION and BI-REFORMING. *Energy Convers. Manag.* 125, 320–335.

Yanagisawa, Y., 2001. A new CO2 disposal process via artificial weathering of calcium silicate accelerated by acetic acid. *Energy* 26, 341–354.

ZEP, 2011. Post-demonstration CCS in the EU The Costs of CO 2 Capture, Transport and Storage European Technology Platform for Zero Emission Fossil Fuel Power Plants. Eur. Technol. Platf. Zero Emiss. Foss. Fuel Power Plants,"technical report".

Website

http://www.adnkronos.com/sostenibilita/world-in-progress/2017/10/16/alghe-luce-solare-cosi-eniprodurra-bio-carburante_hSsZXKEPzPRO5AWTiHB0lO.html (last access 3.29.18).

http://secure.alacra.com/acm/2084_sample.pdf (last access 3.29.18).

https://www.alibaba.com/showroom/price-of-dimethyl-carbonate.html (last access 3.24.18)

www.argusmedia.com/~/media/files/pdfs/petchems/mtbe-2015-annual-flyer.pdf?la=en (last access 2.27.17)

http://www.bp.com/content/dam/bp/en/corporate/pdf/energy-economics/statistical-review-2017/bp-statistical-review-of-world-energy-2017-full-report.pdf (last access 3.24.18)

https://www.clal.it/en/?section=concimi (last access 3.29.18).

https://cen.acs.org/articles/90/i17/Dimethyl-Carbonate-PlantSetChina.html?type=paidArticleContent (last access 10.25.17).

http://www.consilium.europa.eu/uedocs/cms_data/docs/pressdata/en/ec/145397.pdf (last access 3.12.18)

http://edition.cnn.com/travel/article/boeing-biofuel/index.html (last access 3.29.18).

http://press.covestro.com/news.nsf/id/aazc7k-premiere-for-new-raw-material

http://ec.europa.eu/eurostat/statistics-explained/index.php/Natural_gas_price_statistics (last access 11.27.17).

http://eurlex.europa.eu/legalcontent/EN/TXT/PDF/?uri=CELEX:52011DC0885&from=EN%0Ahttp://ec.europa.eu/energy/en/topics/energy-strategy/2020-energy-strategy (last access 11.27.17).

http://ec.europa.eu/eurostat/statistics-explained/index.php/Energy_price_statistics (last access 11.27.17).

http://ec.europa.eu/eurostat/web/labour-market/labour-costs/database (last access 11.27.17).

http://ec.europa.eu/eurostat/web/ (last access 3.13.18).

https://ec.europa.eu/clima/policies/strategies/2030_en (last access 2.27.17)

https://ec.europa.eu/clima/policies/strategies/2050_en (last access 3.29.18)

http://www.fertilizerseurope.com/fileadmin/user_upload/publications/statistics_publications/Stat_website.pdf (last access 3.29.18).

http://www.globalccsinstitute.com/projects (last access 3.29.18)

http://www.infomercatiesteri.it/paesi.php (last access 3.23.18).

https://www.icis.com/resources/news/2013/04/13/9658385/chemical-profile-europe-ethylene-oxide/ (last access 3.29.18).

http://www.icis.com/resources/news/2006/07/26/2015258/chemical-profile-formic-acid/ (last access 12.15.17).

https://www.icis.com/resources/news/2017/01/05/10060192/outlook-17-stable-to-softer-for-us-polyether-polyols/ (last access 3.29.18).

https://www.icis.com/resources/news/2016/01/11/9959149/outlook-16-asia-glycerine-outlook-hinges-on-biodiesel-policies/ (last access 11.27.17).

https://www.icis.com/resources/news/2014/08/18/9811842/icis-value-chain-propylene-oxide/ (last access 11.27.17).

https://www.icis.com/resources/news/2012/10/26/9607632/european-chemical-profile-polyols/ (last access 3.29.18).

https://www.icis.com/resources/news/2011/11/21/9509807/chemical-profile-propylene-oxide/ (last access 11.27.17).

https://www.icis.com/resources/news/2007/11/06/9076442/propylene-glycol-pg-prices-and-pricing-information/ (last access 3.29.18).

http://www.iea-amf.org/content/fuel_information/ethanol/ethers (last access 3.26.18).

https://www.ihs.com/products/chemical-technology-pep-reviews-ethylene-carbonate-from-ethylene-2003.html (last access 11.27.17).

https://www.ihs.com/products/chemical-technology-pep-reviews-ethylene-carbonate-from-ethylene-2003.html (last access 3.29.18).

https://ihsmarkit.com/products/chemical-technology-pep-dimethyl-carbonate.html (last access 3.26.18).

http://www.ilsole24ore.com/art/finanza-e-mercati/2018-03-22/piu-fossili-e-meno-efficienza-record-le emissioni-co2-2017-183607.shtml?uuid=AEpA1qLE&refresh_ce=1 (last access 4.1.18)

http://www.indexmundi.com/commodities/?commodity=urea (last access 10.26.17).

https://www.indexmundi.com/energy/?product=fuel-oil&graph=production (last access 3.26.18).

https://www.intratec.us/chemical-markets/ethylene-oxide-price (last access 11.27.17).

https://www.intratec.us/chemical-markets/propylene-oxide-price (last access 11.27.17).

https://www.intratec.us/chemical-markets/demineralized-water-price (last access 11.27.17)

https://home.kpmg.com/xx/en/home/services/tax/tax-tools-and-resources/tax-rates-online/corporate-tax-rates-table.html (last access 2.2.18).

https://www.linkedin.com/pulse/propylene-glycol-market-q3-2017-increased-prices-echemi-technology (last access 11.27.17)

https://mcgroup.co.uk/news/20140627/formaldehyde-production-exceed-52-mln-tonnes.html (last access 3.25.18).

http://www.methanol.org/wp-content/uploads/2016/07/Marc-Alvarado-Global-Methanol-February-2016-IMPCA-for-upload-to-website.pdf (last access 3.5.18).

https://www.methanex.com/sites/default/files/methanol-price/MxAvgPrice_Oct 27, 2017.pdf (last access 11.27.17).

https://www.mintecglobal.com/2014/08/flexible-polyols-price-rises-amid-tight-supply/ (last access 3.29.18).

http://www.molbase.com/en/cas-96-49-1.html (last access 3.29.18).

https://www.platts.com/latest-news/agriculture/london/world-biodiesel-productionconsumption-torise-26485632 (last access 10.25.17).

https://www.statista.com/statistics/650304/polycarbonate-global-production-capacity-by-country/ (last access 3.25.18).

https://www.statista.com/statistics/270007/capacity-of-ethylene-by-region/ (last access 3.26.18).

http://www.topsoe.com/sites/default/files/topsoe_large_scale_methanol_prod_paper.ashx_.pdf (last access 3.29.18)

http://utech-polyurethane.com/news/juyuan-starts-up-polyether-polyol-plant/ (last access 12.15.17).

https://valueinvestingfund.wordpress.com/tag/ethylene-glycol/ (last access 3.29.18).

https://en.wikipedia.org/wiki/List_of_oil_refineries (last access 3.5.18).

Ringraziamenti

In primo luogo ringrazio il Prof. Fabrizio Bezzo che mi ha concesso questa incredibile opportunità di Tesi, facendomi crescere moltissimo.
Desidero ringraziare inoltre l' Ing. Federico d’Amore per la sua disponibilità ed i preziosi consigli ricevuti, nonostante la distanza dell'ultimo periodo.
Ringrazio poi tutti gli amici del CAPE-Lab con i quali ho condiviso questo percorso.
Un immenso grazie va ai miei genitori Ellen e Vittorio per avermi sostenuto durante questo percorso.
Infine ringrazio di cuore Alexandra per avermi supportato (e sopportato) in ogni momento.